Supramolecular redox-responsive ferrocene hydrogels and microgels

Xiong Liu, Li Zhao, Fangfei Liu, Didier Astruc, Haibin Gu

Supramolecular Redox-Responsive Ferrocene Hydrogels and Microgels

Xiong Liu[a], Li Zhao[a], Fangfei Liu[a], Didier Astruc[b,*], Haibin Gu[a,*]

[a]Key Laboratory of Leather Chemistry and Engineering of Ministry of Education, Sichuan University, Chengdu 610065, China. E-mail: guhaibinkong@126.com

[b]ISM, UMR CNRS N° 5255, Univ. Bordeaux, 351 Cours de la Liberation, 33405 Talence Cedex, France. E-mail: didier.astruc@u-bordeaux.fr

Abstract: Stimuli-responsive hydrogels have lately attracted a lot of attention in the chemistry and material fields because of the "smart" change of their properties under outside stimuli including light, temperature, electric or magnetic field, pH, chemicals, shear stress, and redox reagents. Ferrocenyl (Fc) is often employed as a redox-responsive building unit due to its properties of chemical and electrochemical redox reversibility. This property involves reversible change between hydrophobicity and hydrophilicity, which endows hydrogels with unexpected features. Also, Fc derivatives are used as guest molecules featuring host–guest interactions with macrocyclic host molecules, mainly including cyclodextrins and pillararenes, commonly leading to the formation of supramolecular hydrogels with shape-memory, self-healing and sol-gel transition performances. This review focuses on the fabrication of various kinds of Fc-containing hydrogels and describes their gelling mechanisms, characteristic structures and properties, as well as functional applications.

The review is divided into covalently cross-linked hydrogels and supramolecular cross-linked hydrogels. Furthermore, Fc-containing microgels constructed by chemically cross-linked three-dimensional polymer networks that are related to traditional hydrogels are also discussed. Fc-containing hydrogels and microgels are becoming more and more important as advanced functional materials, especially biomedical, shape-memory and self-healing materials.

Keywords: ferrocene, hydrogels, covalent cross-linking, supramolecular, host–guest interaction, microgels

Abbreviations: AAm, acrylamide; Ad, adamantane; Ada, adamantane amine; AdCANa, adamantane carboxylic acid sodium salt; AES, atomic emission spectrometry; AFM, atomic force microscope; AgNPs, silver nanoparticles; Alg-β-CD, β-cyclodextrin grafted alginate; APS, ammonium peroxodisulfate; Au EQCM, gold electrochemical-quartz-crystal-microbalance electrode; AuNPs, gold nanoparticles; CNTs, carbon nanotubes; α-CD, α-cyclodextrin; β-CD, β-cyclodextrin; β-CD-AAm, mono-6-acrylamido-β-CD; β-CD-CS, β-CD modified chitosan; β-$CDNH_2$, 6-deoxy-6-amino-β-cyclodextrin; CAD, Computer Added Design; CAN, ceric ammonium nitrate; 6-CD-EDA, mono-6-deoxy-6-ethylenediamine-β-CD; CD@QD, β-CD modified CdS quantum dot; CS6, calix[6]arene hexasulfonic acid sodium salt; CV, cyclic voltammetry; 2D, two-dimensional; 3D, three-dimensional; DASS, *N*,*N*'-bis(acryloyl)cystine; DCC, dicyclohexylcarbodiimide; DCSH, dually cross-linked supramolecular hydrogel; DFO, metal chelating deferoxamine; DFT, density functional theory; DMA, dynamic thermomechanical analysis; DMAP, 4-(dimethylamino) pyridine; DMAPMA, *N*-[3-(dimethylamino)propyl] methacrylamide; DMIEA, 2-(dimethylmaleimido)-*N*-ethylamine; DMSO, dimethyl sulfoxide; DS, degree of substitution; DSC, differential scanning calorimetry; *E. coli, Escherichia coli*; EDC, 1-ethyl-3-(3'-dimethylaminopropyl)carbodiimide; EDX, energy dispersive X-ray spectroscopy; EGDGE, ethylene glycol diglycidyl ether; EGP6, ethylene glycol chain-modified pillar[6]arene; EIS, electrochemical impedance spectra; FBI, *N*,*N*'-bis(ferrocenyl-methylene) diaminobutane; F127-Fc, ferrocenyl-terminated pluronic F127; Fc, ferrocenyl; Fc^+, substituted ferricenium; Fc-AAm, Fc-modified acrylamide; FcBA, ferroceneboronic acid; Fc-COCl, ferrocenylcarboxyl chloride; FcCS, ferrocene-modified chitosan; Fc-CTA, Fc-modified chain-transfer agent; Fc-F, ferrocenoyl phenylalanine; Fc–FF, Fc–diphenylalanine; FcMeOH, ferrocenylmethanol; Fc-M, 2-acryloyloxyethyl ferrocenylcarboxylate; GA, glutaraldehyde; GCE, glass carbon electrode; GOD, Glucose oxidase; GSH, glutathione; $HAuCl_4$, tetrachloroauric acid; HRTEM, high resolution TEM; IS, ionic strength; ITO, indium tin oxide; LBL, layer-by-layer; LCST, lower critical solution temperature; MAA, methylacrylicacid; MBAAm, *N*,*N*'-methylenebisacrylamide; MNPs, metal nanoparticles; MSCL, macromolecular supramolecular cross-linker; MWNTs, multiwalled carbon nanotubes; NHS, *N*-hydroxysuccinimide; NIPAM, *N*-isopropylacrylamide; oxNG–DFO, oxidation-sensitive iron chelating nanogels; pAA, poly(acrylic

acid); PAA-Fc, Fc-modified poly(acrylic acid); PAs, pillar[n]arenes; PBS, phosphate-buffered saline; PBu_3, tri-*n*-butylphosphine; P-CD, cyclodextrin polymer; P(DMA-*r*-GMA-CD), poly(*N*,*N*-dimethylacrylamide-*r*-glycidol methacrylate-β-CD); P(DMA-*r*-HEMA-Fc), poly (*N*,*N*-dimethylacrylamide-*r*-2-hydroxyethylmethacrylate-Fc); PdNPs, palladium nanoparticles; PEI, poly-(ethylenimine); PEO, polyethylene oxide; PFS, poly(ferrocenylsilane); PFS-AO, poly(ferrocenyl(3-acryloyloxypropyl)methylsilane); PFS-Br, poly(ferrocenyl(3-bromopropyl)methylsilane); PFS-I, poly(ferrocenyl(3-iodopropyl)-methylsilane); PILs, poly(ionic liquid)s; PMDETA, *N*,*N*,*N*',*N*'',*N*''-pentamethyldiethylenetriamine; PMVF, Poly(2-methacryloyloxyethyl phosphorylcholine-*co*-*p*-vinylphenylboronic acid-*co*-vinylferrocene); PNIPAM, poly(*N*-isopropylacrylamide); PPO, poly(propylene oxide); PSA, prostate specific antigen; PVA, poly(vinyl alcohol); QDs, quantum dots; RAFT, reversible addition fragmentation chain-transfer polymerization; ROP, ring-opening polymerization; SCE, saturated calomel electrode; SMP, shape-memory polymer; SPR, surface plasmon resonance; SPR-OWS, SPR combined with optical waveguide spectroscopy; SWNTs, single-walled carbon nanotubes; SSNa, styrenesulfonic acid sodium salt; TEM, transmission electron microscope; TEMED, *N*,*N*,*N*',*N*'-tetramethylethylenediamine; TGA, thermogravimetric analysis; THF, tetrahydrofuran; UV-LED, ultraviolet light-emitting diode; VA-044, 2,2'-azobis[2-(2-imidazolin-2-yl)-propane] dihydrochloride; VDMA, 2-vinyl-4,4-dimethylazlactone; XRD, X-ray diffraction.

Contents

1. Introduction

Hydrogels, formed by 3D polymeric networks with chemical or physical crosslinkings, have the ability to swell by absorbing a good deal of water while maintaining their original structures. Due to their soft, rubbery and highly swelling properties, hydrogels have presented many kinds of promising applications in drug delivery[1-5], catalysis[6], self-healing[7,8], tissue engineering[9-11] and actuation[12,13]. Stimuli-responsive hydrogels are regarded as the most promising hydrogels. Indeed they have attracted eye-catching attention from chemistry and material fields owing to the "smart" changes in their performances triggered by external stimuli, including light[14], temperature[15], electric or magnetic fields[16], pH[17,18], chemicals[19], shear stress[20-22], and redox reagents[23,24]. The imbedding of metal centers into hydrogels leads to the formation of a new class of inorganic/organometallic hydrogels that exhibit numerous particular characteristics. For example, (i) the metal centers act as architectural templates during the fabrication of the organic functional subunits; (ii) the metal centers serve as redox-responsive or paramagnetic centers generating active species for charge transfer; (iii) the metal centers alter the

electronic and optical activities of organic π-systems; (iv) all kinds of macromolecular frameworks are built by changing the coordination number, geometry and valence state of metal ions[25-34]. As a result, the formed metal-containing hydrogels commonly exhibit unique stimuli-sensitive behaviors on account of the changes in electric or magnetic field[35,36], pH[37], chemicals[38], shear stress[39], redox reagents[40-42], etc.

Precise control over the structure and function of metal complexes embedded in hydrogels has been pursued for the preparation of metal-containing hydrogels with regulable performances for ultimate applications. Ferrocene is a remarkable organometallic complex with d^6 Fe(II) 18-electron sandwich structure, and it exhibits redox properties and satisfactory stability[43-48]. The hydrophobic neutral ferrocene form with orange color may be oxidized to the 17-electron hydrophilic cationic ferricenium with purple color by using electrochemical oxidation or various chemical oxidants (e.g. $FeCl_3$, NaClO, $AgNO_3$, $HAu^{III}Cl_4$, iodine, H_2O_2, $KMnO_4$, etc.), and the resulting ferricenium cation may be then reversibly changed back to the initial ferrocene form by using electrochemical reduction or reducing agents (e.g. $TiCl_3$, thiosulfate, decamethylferrocene, ascorbic acid, glutathione (GSH), etc.) [49-51]. Notably, during the redox transformation, the sandwich structure is not broken, and the change in the length of the Fe-C bonds is very small[57-62]. The combination of Fc into hydrogels is benifical for the formation of smart hydrogels with reversiblly redox-responsive activities, and especially the reversible hydrophobicity-hydrophilicity change, which is caused by the redox action of the Fc units, could endow hydrogels with some unexpected features. In some very early work (1990s), Fc-based gels typically focused on fabrication of redox sensors [63-66]. In recent studies, it was found that the change in electrochemical or chemical conditions can result in macroscopically swelling and shrinking of Fc-

based hydrogels [67]. More interestingly, Fc derivatives have been used as guest molecules to be enveloped through host-guest interactions into the hydrophobic interior of macrocyclic host molecules such as β-cyclodextrin (β-CD) and pillar[n]arenes (PAs) [68-72]. The introduction of these host–guest interactions is commonly helpful for the formation of supramolecular hydrogels exhibiting self-healing and shape-memory functions[73]. Thus, intensive focus has been paid on the fabrication of Fc-containing hydrogels and their functional applications in various fields such as drug delivery[74], electrical actuation[75], biosensing[76], self-healing[77] and shape-memory materials[78].

In several earlier reviews[79-85], Fc-containing organogels and hydrogels have been mentioned. Fc-containing hydrogels provide dramatical advantages according to green chemistry compared to the corresponding organogels, and exhibit various exciting and valuable applications in many fileds incuding biomedicine and materials science. Herien, this review discusses the preparation of various types of Fc-containing hydrogels and their gelling mechanisms, structural features, properties and functional applications. The following description is mainly composed of two parts, namely covalently cross-linking Fc-containing hydrogels and supramolecular ones. In the first part, the main-chain and side-chain Fc-containing polymers are adopted, respectively, to fabricate the covalently cross-linking Fc-containing hydrogels. In the second part, the focus is paid on the supramolecular Fc-containing hydrogels that were mainly prepared by the β-CD/Fc and PA/Fc host–guest interactions, the self-assembly of Fc-containing peptides, and other Fc-containing supramolecular systems. Emphasis is brought on the β-CD/Fc supramolecular system. Figure 1a-c shows the schematic structures of representative guest and host molecules for the construction of Fc-containing hydrogels. Figure 1D-E involves typical networks of covalently cross-linking and

supramolecular Fc-containing hydrogels. Fc-containing microgels are also introduced, because they are composed of chemically cross-linking 3D polymeric networks that are similar to conventional hydrogels.

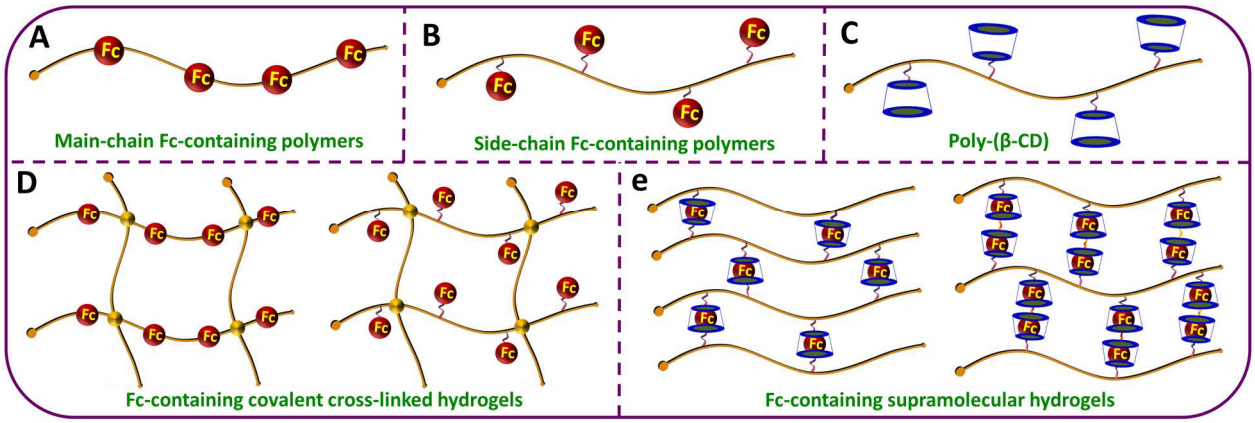

Figure 1. Schematic structures of representative guest (A,B) and host (C) molecules, and covalently cross-linked (D) and supramolecular (E) Fc-containing hydrogels.

2. Covalently cross-linked Fc-containing hydrogels

Covalently cross-linked hydrogels usually have the tridimensional networks constructed by nonreversible covalent bonds among polymeric chains. Typically, these hydrogels are generated by mixing two polymers (or one polymer and one small molecular cross-linker) containing complementary reactive groups, which results in the formation of covalent bonds. Besides, this type of hydrogels is also formed by the polymerization reactions of as-prepared monomers or polymers with polymerizable groups. The resulting hydrogels commonly possess satisfactory mechanical or physical strength and high stability. When the cross-linked hydrogels are used as drug delivery matrixes, they present the feature of retarding or stopping premature disassembly even in low polymeric concentration[86-88].

2.1. Main-chain Fc-containing polymer hydrogels

Hydrogels prepared from main-chain Fc-containing polymers have recently rapidly developed, especially as a new type of stimuli-responsive soft materials. Owing to the high-density distribution of Fc units in the polymeric skeleton, the main-chain Fc-containing polymer hydrogels normally exhibit dramatic response to the outside redox change. Polyferrocenylsilanes (PFSs) show robust covalent Fe–cyclopentadienyl bonds and are the most often investigated type of main-chain Fc-containing polymers to prepare the corresponding hydrogels. Normally, PFS polymers are fabricated by ring-opening polymerization (ROP) of strained [1] or [2]-ferrocenophane monomers[89-94]. At present, the PFS-based hydrogels are mainly formed upon covalent cross-linking of PFS chains. In general, PFS-based hydrogels are prepared according to two strategies. The first one consists in introducing polymerizable groups into the side-chain of PFSs, followed by radical polymerization to form typical network structures. The second one involves the incorporation of reactive groups into the side-chain of PFSs, followed by their reactions with as-prepared crosslinkers, leading to the formation of PFS hydrogels.

For example, Vancso's group [93] reported the synthesis of a new class of PFS-based poly(ionic liquid)s (PILs) (Figure 2). These PILs were redox-sensitive and water-soluble, and more importantly, they featured self-crosslinkable ability. At low concentrations, the formation of nanogels was observed, whereas at higher concentrations macroscopic hydrogels were generated by them. The PIL of PFS-Vim was synthesized by the route shown in Figure 2. Its polymerizable vinylimidazolium groups were located in the side chains, and its connection was accomplished by the modification reaction of poly(ferrocenyl(3-iodopropyl)-methylsilane) (PFS-I) by using 1-

vinylimidazole, followed by dialysis treatment in NaCl aqueous solution to obtain Cl^- counterions for a better water solubility of the salt. The PFS-VIm aqueous solution (0.5 mg/mL) was irradiated under UV light (365 nm) in the presence of a photoinitiator, and its photopolymerization reaction led to the formation of a stable, translucent dispersion of nanogels (Figure 2A). Figure 2B shows the TEM image evidencing the formation of nanogels with diameters of 20–50 nm. When the concentration of PFS-VIm was increased to 60 mg/mL, its photopolymerization reaction resulted in the formation of a transparent amber-colored hydrogel (Figure 2C). The honeycomb-like pore structure of the obtained hydrogel was confirmed by the SEM image shown in Figure 2D.

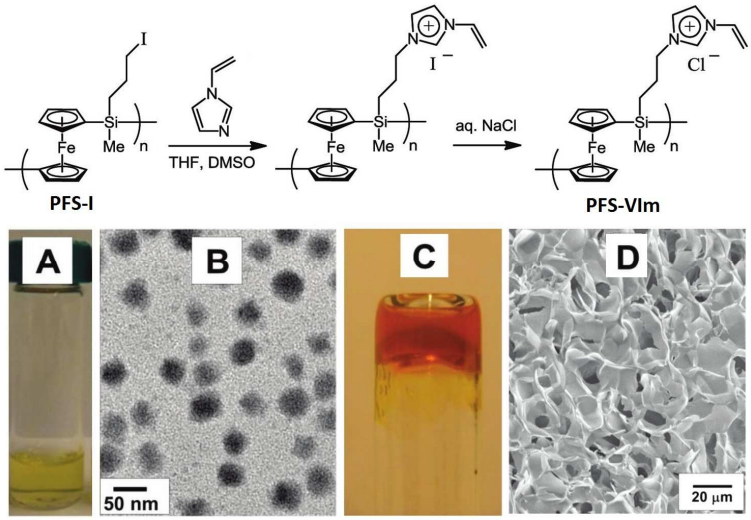

Figure 2. Synthesis route to PFS-PIL and its nanogel and hydrogel. (A) Picture of PFS-PIL nanogel; (B) TEM image of PFS-PIL nanogel; (C) Picture of PFS-PIL hydrogel; (D) SEM image of PFS-PIL hydrogel.[93] Reproduced with permission from Ref. [93]. Copyright 2017 American Chemical Society.

Vancso et al.[94] also reported a new, redox- and thermo-responsive PFS-based PIL and the corresponding smart hydrogels exhibiting hysteretic volume-phase transformations with bi-stable states. The new PIL, abbreviated as PFS-DMAPMA-PBu_3, also exhibited cross-linkable property,

and its molecular structure is shown in Figure 3A. Similarly, PFS-I was adopted as the starting polymer, and its quaternization reaction with tri-*n*-butylphosphine (PBu_3) led to the incorporation of tetraalkylphosphonium sulfonate groups into the side chains of PFS backbone. Then the anion exchange reactions followed to give Cl^- or alkyl sulfonate counterions. The reactive vinyl groups were further introduced via the modification reaction of PFS-I by *N*-[3-(dimethylamino)propyl] methacrylamide (DMAPMA). The resulting PFS-DMAPMA-PBu_3 was used to prepare hydrogels by mixing it with a 4-arm polyethylene glycol (PEG)-thiol cross-linker containing a pentaerythritol core. The thiol-Michael addition reactions between them led to the formation of the targeted Fc-containing hydrogels (Figure 3B,C) with adjustable degrees of crosslinking (x) and DMAPMA/PBu_3 ratio ((x + y):z). The formed hydrogels exhibited a LCST-type thermo-sensitive property, and the transformation temperature was regulated in a wide range by carefully changing the degrees of crosslinking and the type of anion groups. As expected, the macroscopic properties of these hydrogels were also reversibly adjusted by changing their chemical or electrochemical situation. The volume of these hydrogels was finely tuned by varying the environmental temperature and the redox state of Fc units. Interestingly, as shown in Figure 3D and 3E, the as-formed hydrogels displayed a unique, obviously hysteretic volume-phase change and long-lived bi-stable states at a "coercivity" temperature of about 20 ^oC. This hysteretic behavior was expected to be usable for the design and fabrication of memory devices. Furthermore, by utilizing the powerful dispersing abilities of PFS-DMAPMA-PBu_3, the authors further successfully fabricated the hybrid conductive composite hydrogels containing carbon nanotubes (CNTs). These composite hydrogels exhibited bi-stable states and adjustable resistance during the heating–cooling treatments. This new class of PIL and PIL-based organometallic hydrogels may find a variety of fascinating

and valuable functional applications in smart soft materials and devices.

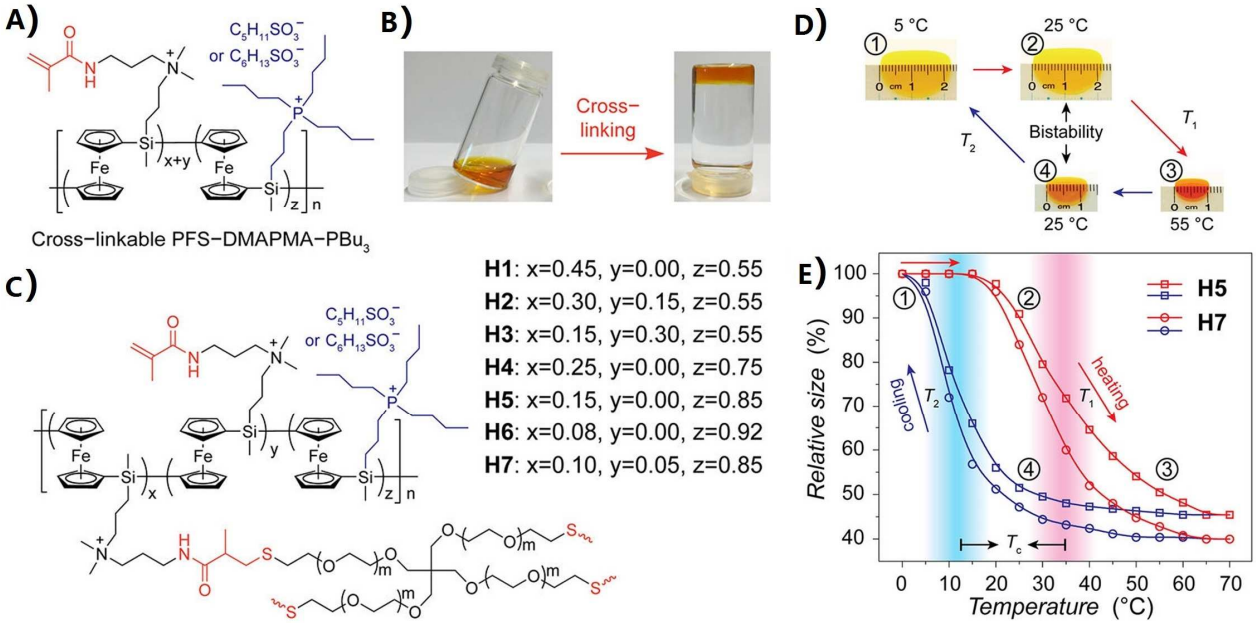

Figure 3. (A) Molecular structure of PFS-DMAPMA-PBu$_3$. (B) Pictures showing the formation of PFS-DMAPMA-PBu$_3$ hydrogels. (C) Schematic cross-linking of PFS-DMAPMA-PBu$_3$ hydrogel and its composition (**H1–H7**). (D) Pictures of the shrinking-swelling behaviors of the hydrogel (**H7**). (E) Hysteresis loops of the hydrogels (**H5**, **H7**). Reproduced with permission from Ref. [94]. Copyright 2017 American Chemical Society.

Fc derivatives have been used as reductants to prepare metal nanoparticles (MNPs) due to their reducing properties [95-100]. So, Fc-containing hydrogels have the potential advantage to *in-situ* synthesize MNPs, resulting in the formation of MNPs-containing composite hydrogels. For example, Hempenius et al.[101] prepared main-chain Fc-containing polymer hydrogels that were used to *in-situ* generate silver nanoparticles (AgNPs) for antimicrobial applications. As shown in Figure 4, using PFS-I as the starting polymer, its reaction with sodium acrylate resulted in the

formation of polymerizable poly(ferrocenyl(3-acryloyloxypropyl)methylsilane) (PFS-AO). The obtained PFS-AO was then copolymerized with *N*-isopropylacrylamide (NIPAM) and *N*,*N*'-methylenebisacrylamide (MBAAm) with the aid of a photoinitiator (Irgacure 651). The reaction was carried out in tetrahydrofuran (THF) under UV-emitting diode irradiation (365 nm). A gel state was reached quickly, then THF was removed, and soaking in water led to the formation of hydrogel. Obviously, these hydrogels show both thermo- and redox- responsiveness owing to the presence of PNIPAM and PFS segments. It was found that the used amounts of both MEA and PFS-AO affected the crosslink density of these hydrogels. As shown in Figure 4A-C, these hydrogels possess a homogeneous, porous structure, and the pore size decreases along with the increase of the PFS content. The analysis of differential scanning calorimetry (DSC) indicated that the addition of PFS into PNIPAM hydrogels merely led to a slight increase of the transformation temperature (about 2 ^{o}C) after being oxidized. The *in-situ* formation of AgNPs was further achieved by soaking these PFS hydrogels into the aqueous solution of silver nitrate, and the formed AgNPs were absorbed and located in the hydrogel matrix, which led to the preparation of PFS-PNIPAM-Ag composite hydrogels. As shown in Figure 4D, the formed AgNPs were uniformly distributed within the hydrogel network, which was attributed to the homogenous distribution of PFS chains inside the network. The co-existence of Ag and Fe elements was undisputedly proved by energy dispersive X-ray spectroscopy (EDX), as shown in Figure 4E. The formed AgNPs-hydrogel composites exhibited strong inhibitory effect against *Escherichia coli* (*E. coli*) while maintaining a high biocompatibility with cells.

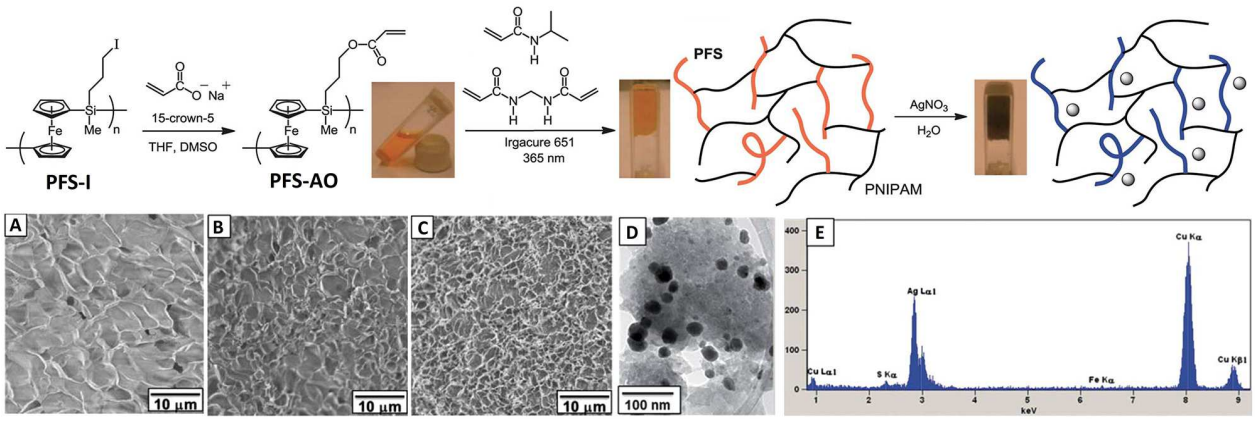

Figure 4. Schematic synthesis route to PNIPAM–PFS hydrogel and its AgNP composite. SEM images of PNIPAM hydrogels with different ratio of PFS (A) 1% PFS, (B) 2% PFS and (C) 5% PFS. (D) TEM image of AgNPs inside the hydrogel and (E) EDX result of the composite hydrogel. Reproduced with permission from Ref. [101]. Copyright 2013 Royal Society of Chemistry.

Zoetebier and coworkers[67] reported a new class of Fc-containing hydrogels constructed using redox-sensitive PFS and PEG segments and their utilization in the *in-situ* preparation of palladium nanoparticles (PdNPs). Figure 5 shows the synthetic route to the PFS polyanion PFS-N_3-*s*-PFS-SO_3Na bearing an adjustable amount of reactive azide units and water-soluble alkane sulfonate functional groups in the side chains. The corresponding hydrogel was fabricated by mixing the obtained PFS-N_3-*s*-PFS-SO_3Na and the four-arm star PEG with bicyclononyne terminals (BCN-4-PEG) in methanol, followed by dialysis treatment in water. The crosslinking was triggered by the copper-free azide–alkyne Huisgen cycloaddition "click" reactions between the bicyclononyne units of BCN-4-PEG and the side-chain azide groups of PFS-N_3-*s*-PFS-SO_3Na. As shown in Figure 5A, the formed anionic PFS hydrogel was an amber elastic hydrogel. This PFS-based hydrogel exhibited reversible redox behavior under chemical or electrochemical stimuli. The color of this hydrogel varied from original amber to blue-green after oxidation by a Fe(III) salt, and the visible

shrinkage of the hydrogel was also observed (Figure 5B). This shrinkage is attributed to electrostatic attraction between the resulting positive Fc^+ groups in the main chains and the negative sulfonate groups in the side chains. As expected, the subsequent addition of sodium ascorbate as a reducing agent recovered the swelling state and elastic property of the hydrogel (Figure 5C). The PFS hydrogel was further used as a reducing matrix to fabricate a PdNP-containing hydrogel composite. As shown in Figure 5D, the TEM image indicates well-dispersed, unaggregated PdNPs with a size of 8.2 ± 2.2 nm located in the hydrogel matrix, and the chemical nature of the obtained PdNPs was confirmed by the EDX result (Figure 5E).

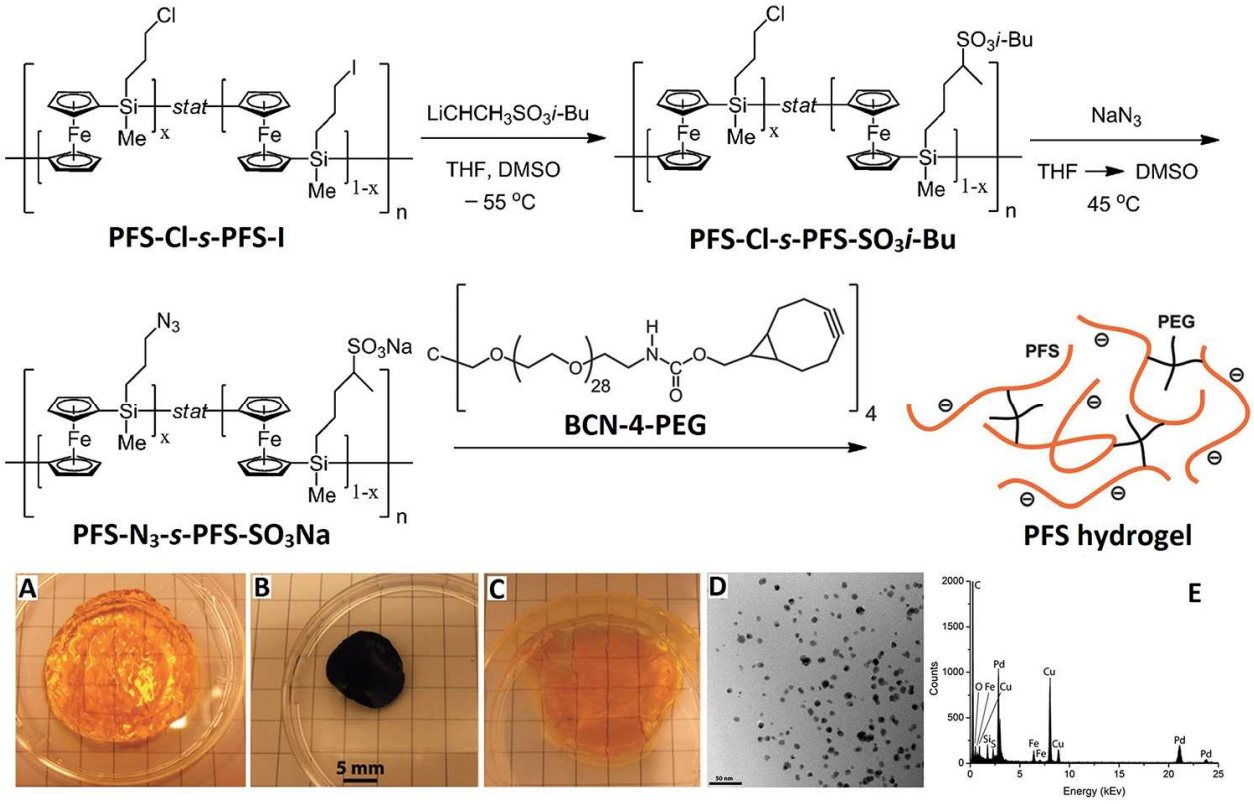

Figure 5. Synthesis route of the PFS-N_3-*s*-PFS-SO_3Na-based hydrogel and the *in-situ* reduced PdNPs. A-C) Reversible redox behavior of hydrogel. TEM (D) and EDX (E) results of PdNPs. Reproduced with permission from Ref. [67]. Copyright 2015 Royal Society of Chemistry.

According to the reports of Feng and coworkers[102], the PFS-based redox-responsive hydrogel thin film provided a reducing surface for the *in-situ* preparation of PdNPs that was used in the electrochemical oxidation of ethanol. The hydrogel network was formed by the cross-linking quaternization reaction between poly(ferrocenyl(3-bromopropyl)methylsilane) (PFS-Br) and *N*,*N*,*N*',*N*'',*N*''-pentamethyldiethylenetriamine (PMDETA). PFS-Br and PMDETA were mixed directly in THF/dimethylsulfoxide (DMSO, 2:1, v/v), as shown in Figure 6. The hydrogel thin films were then prepared by spin-coating the mixture solution on the silicon or indium tin oxide (ITO) substrate. In the present work, the thickness of the formed film was in the range of 0.728 -2.15 μm, and these films were successfully peeled off from the substrates. As expected, the resulting hydrogel films showed reversible redox behavior when treated by electrochemical stimuli or chemical reagents, and this redox property was further utilized to *in-situ* fabricate PdNPs. Specifically, the hydrogel-PdNP composite was synthesized through soaking the modified ITO substrate into K_2PdCl_4 aqueous solution, and its structure and component were well characterized by AFM, TEM, high-resolution TEM (HRTEM) and EDX measurements. Results of catalytic experiments confirmed that the PdNP-hydrogel films had the highly efficient and stable catalytic activity and were used to catalyze the oxidation of ethanol.

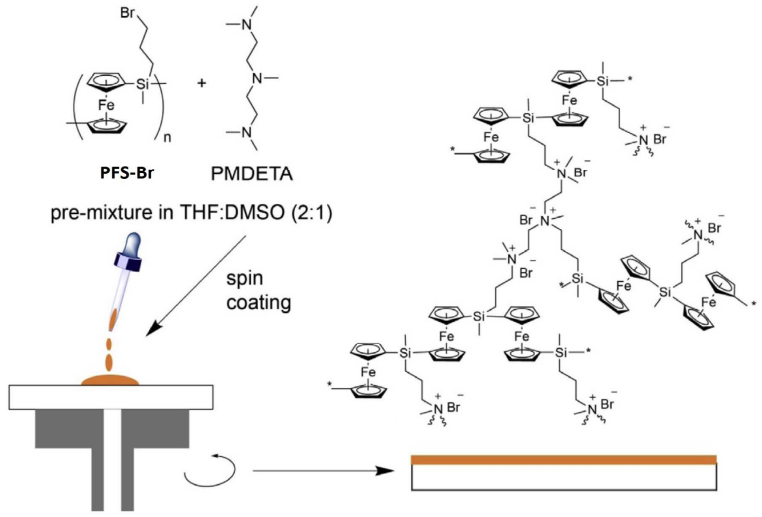

Figure 6. Schematic fabrication diagram of PFS-Br/PMDETA films. Reproduced with permission from Ref. [102]. Copyright 2015 Elsevier Ltd.

PFS- and PNIPAM-based hydrogels with both redox- and thermo-responsiveness were also fabricated by Feng and co-workers[103], and the resulting Fc-containing hydrogels provided reducing microenvironments to prepare AuNP-containing hybrid hydrogels. As shown in Figure 7A, the photo-copolymerization of NIPAM and PFS-VIm was carried out in aqueous solution in the presence of the photoinitiator Irgacure 2959 under UV light (365 nm) irradiation. The formation of amber hydrogels was observed within 5 min of irradiation. The PFS-VIm served as a macromolecular crosslinker, and its dosage had intensive impact on the swelling ratio (Figure 7B), morphology (Figure 7C) and LCST of the hydrogels formed. The hydrogels exhibited representative uniform and porous structures (Figure 7C). When the ratio PFS block was increased, the resulting hydrogel showed reduced swelling ratios and pore sizes. The swelling ratio of the NIPAM/PFS-VIm hydrogels was tuned by changing the type of counterions, too. The authors further prepared an AuNP-hydrogel composite by directly immersing the NIPAM/PFS-VIm hydrogel into an aqueous tetrachloroauric acid ($HAuCl_4$) solution, in which the PFS segments

served as the *in-situ* reducing agents. The optical property of the AuNP-hydrogel composites was regulated by changing the volume-phase transition, and this hybrid hydrogel was expected to find possible applications as optoelectronics and sensors.

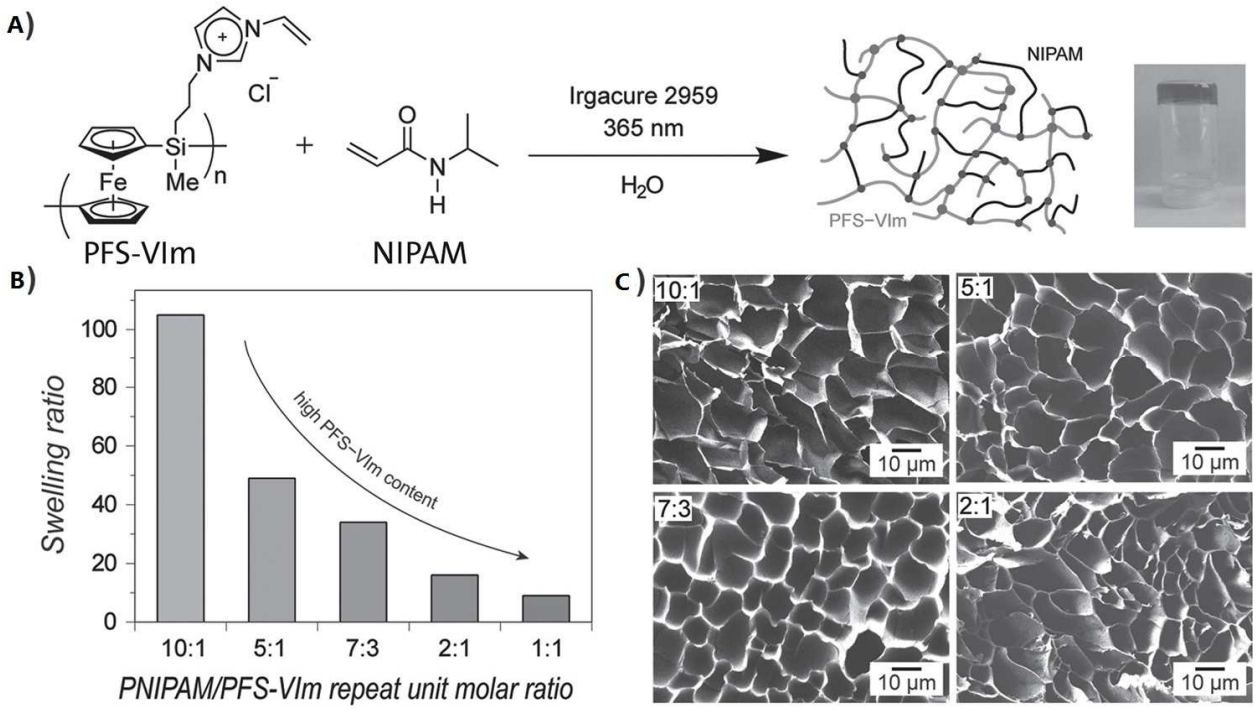

Figure 7. A) Schematic synthesis of redox- and thermo-responsive PFS hydrogels and their representative picture. B) Swelling ratios and C) SEM of hydrogels with different NIPAM/PFS-VIm ratios. Reproduced with permission from Ref. [103]. Copyright 2016 WILEY-VCH Verlag GmbH & Co. KGaA, Weinheim.

2.2. Side-chain Fc-containing polymer hydrogels

The side-chain Fc-containing polymer hydrogels are commonly fabricated by direct polymerization of Fc-containing monomers or by post-modification of as-prepared polymer chains with reactive

Fc-containing groups[104-106]. This type of hydrogels has received increasing attention owing to the easy availability of raw materials, moderate synthetic conditions and flexible designability for the performances. The formed Fc-containing hydrogels normally exhibit obvious volume change under chemically or electrochemically redox stimuli.

For example, Karbarz et al.[107] reported the preparation of thermo-sensitive and electroactive Fc-containing hydrogels by using NIPAM and *N*,*N*'-bis(acryloyl)cystine (DASS) (Figure 8). To obtain NIPAM-ASS hydrogels, NIPAM, DASS, and MBAAm were copolymerized *via* free-radical polymerization. Then, the disulfide bonds in the resulting NIPAM-ASS hydrogels were reduced into thiol by using unitsdithiothreitol. Subsequently, ferrocenemethanol (FcMeOH) was used to modify the hydrogels to introduce the Fc units in the side chains, which led to the formation of Fc-containing hydrogels NIPAM-ASS-Fc. The invertible volume-phase transition performance of NIPAM-ASS-Fc hydrogels was investigated and confirmed by using $Ce(SO_4)_2$ as oxidizing agent and ascorbic acid as reducing agent. Especially, the NIPAM-ASS-Fc hydrogel containing 2% BISS exhibited macroscopical volume-phase transformation caused by variation of the redox state of the Fc units. The NIPAM-ASS-Fc hydrogels showed a comparatively wide temperature window of 35-40 ^{o}C, because the hydrogels showed sensibility towards the oxidation state of the Fc groups. The volume of the hydrogels was regulated over one order of magnitude only by altering the number of oxidized Fc units. The present Fc-containing hydrogels show the possibility of giant volume change at the body temperature and are anticipated to have extensive applications such as artificial muscle, drug delivery system, chemical valve and pump.

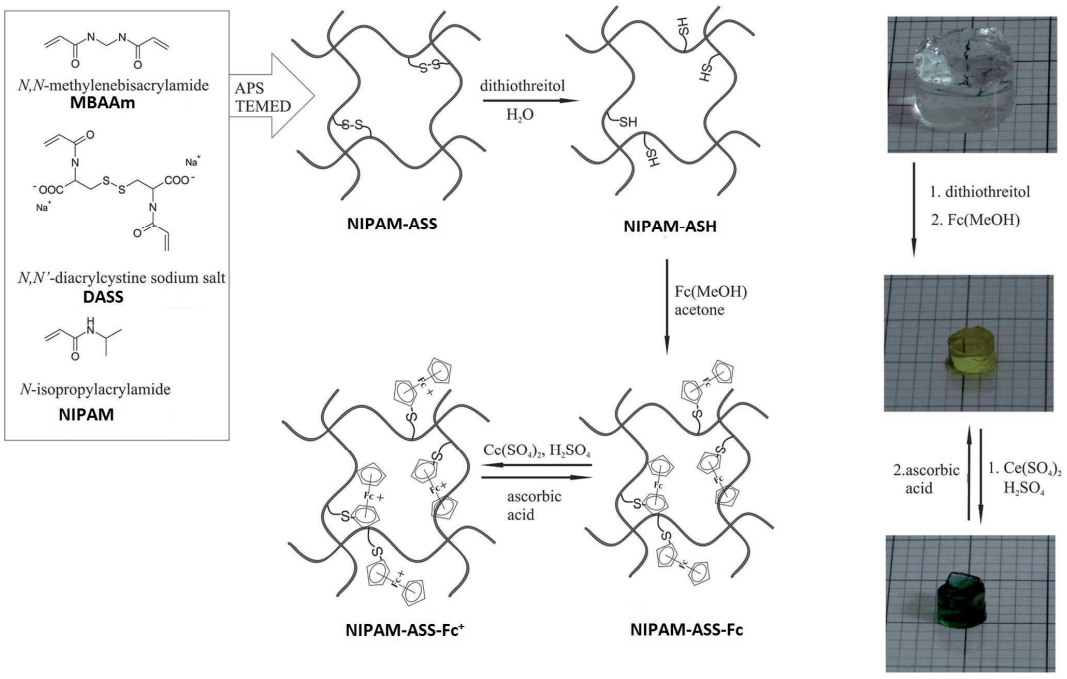

Figure 8. Synthesis route of NIPAM-ASS-Fc hydrogels and their redox-responsiveness. Reproduced with permission from Ref. [107]. Copyright 2013 Royal Society of Chemistry.

Recently, Gu and coworkers[108, 109] described the fabrication of gelatin hydrogels and their AgNP and AuNP composites using a new Fc- and aldehyde-containing tetrablock terpolymer [P(NCHO-*b*-NFc-*b*-NTEG-*b*-NCHO)] as the crosslinking agent (Figure 9). The tetrablock terpolymer was first precisely fabricated via ring-opening metathesis polymerization (ROMP) as a controlled method. The tetrablock terpolymer was then used to cross-link gelatin through Schiff-base reaction to generate the corresponding hydrogels. The fabrication conditions of gelatin hydrogels were optimized by changing the used amount of this crosslink agent and gelatin, and controlling block ratios in the tetrablock terpolymer, and the produced hydrogel HG was characterized by SEM (Figure 9), dynamic thermomechanical analysis (DMA), DSC and TG/DTG. Interestingly, the tetrablock terpolymer was adopted as a reductant of Au(III) and Ag(I) and a stabilizer of the generated AuNPs and AgNPs, which resulted from the reducing ability of the Fc

groups and the mild stabilization by triazole structures for MNPs. Based on these properties, the authors further successfully provided two facile methods to prepare three kinds of composite hydrogels bearing AgNPs or AuNPs. In the blending method, the tetrablock terpolymer, gelatin and $HAuCl_4$ (or $AgNO_3$) were blended together, and the Fc-based *in-situ* reduction of Au^{III} to Au^0 (or Ag^I to Ag^0) was synchronous with the gelling process. In the soaking route, the as-prepared HG hydrogel (Figure 9), which was cross-linked by the Fc-containing polymer, was adopted as a starting point for the *in-situ* fabrication of AuNPs or AgNPs in the hydrogel network, and the composite hydrogel was obtained through simply soaking HG hydrogel into the water solution of $HAuCl_4$ (or $AgNO_3$). Inhibition zone experiments indicated that the resulting AgNP hydrogel composites possessed antibacterial activities towards *Escherichia coli* and *Staphylococcal aureus*. In addition, the AuNP-hydrogel composites were also applied as recyclable catalysts for the reduction by $NaBH_4$ of 4-nitrophenol to 4-aminophenol. The present method is universal, feasible, effective and a clean route to prepare gelatin-based hydrogels and their MNPs composites by using the Fc-containing polymer. The formed hybrid composite hydrogels are expected to be potential candidates in the fields of drug delivery and catalysis.

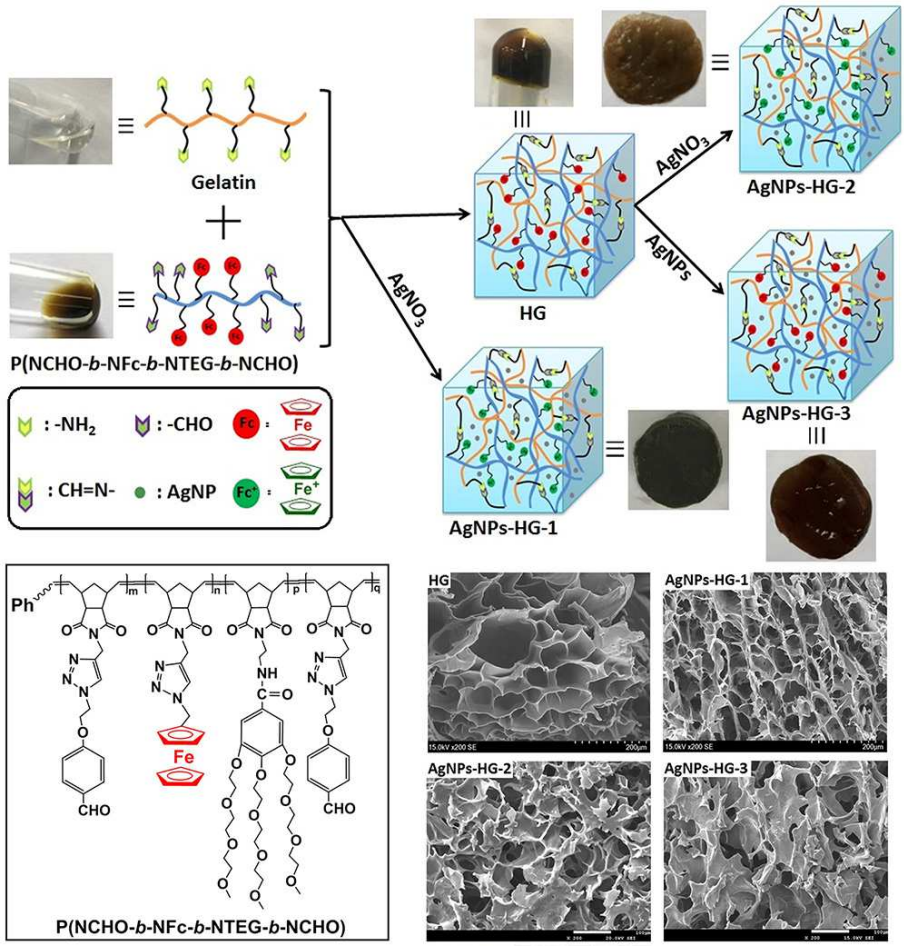

Figure 9. Fabrication routes to various gelatin hydrogels cross-linked by tetrablock terpolymer and their photographs and SEM images. Reproduced with permission from Ref. [108]. Copyright 2019 Elsevier Ltd.

Knoll et al.[110] reported the high-efficiency and fast fabrication of luminescent CdSe-ZnS QDs encapsulated through thermo- and redox-sensitive Fc-containing hydrogel that was prepared by the photo-cross-linking of PNIPAM copolymers. Figure 10A shows molecular structures of the adopted copolymers poly(NIPAM-*co*-MABP) and poly(NIPAM-*co*-VFc-*co*-MABP). The converting process is illustrated in Figures 10B and 10C. The CdSe-ZnS covered by oleic acid (OA) (or oleylamine, OAm) and one of the above copolymers were dissolved together in the solvent of CH_2Cl_2 under the action of ultrasound. After the equivalent volume of H_2O was mixed evenly with

the above mixture, it was found that the copolymer self-assembled rapidly into a large solid sphere that possesssed strong luminescence according to the photographs of fluorescence emission. This result suggested that OA (orOAm)-modified QDs could be encapsulated into the sphere. The resulting polymer sphere was dissolved in cold water (5 °C), and the formed aqueous solution of QDs was subsequently photo-cross-linked using UV light (λ = 365 nm) by benzophenone cross-linking upon the reaction with C-H bonds. The kinetics of the photo-crosslinking course could be monitored using UV-vis. absorption spectroscopy. When the Fc-containing poly(NIPAM-*co*-VFc-*co*-MABP) was used to encapsulate CdSe-ZnS QDs, the obtained luminescent hydrogel particles showed a controllable "on-off" behavior on the basis of external redox stimuli. Figure 10D shows the supposed mechanism for the solvent-driven phase separation behavior and the loading of QDs. The present strategy provides a promising example used to encapsulate hydrophobic chemicals into hydrogels for controlled release.

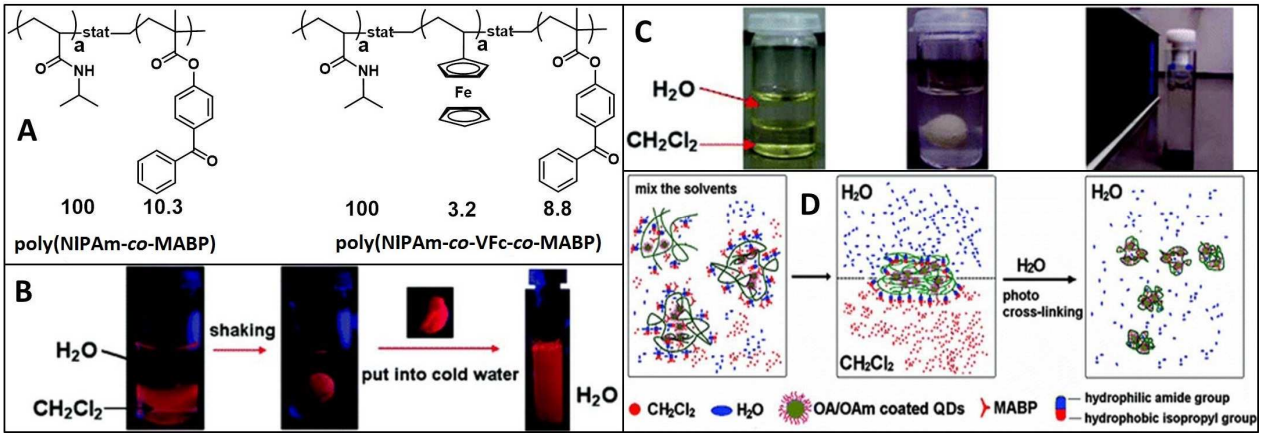

Figure 10. (A) Chemical structures of poly(NIPAM-*co*-MABP) and poly(NIPAM-*co*-VFc-*co*-MABP). (B) Fluorescence pictures and (C) the water-solubilization course of QDs. (D) The encapsulation of QDs into poly(NIPAM-*co*-MABP). Reproduced with permission from Ref. [110]. Copyright 2008 American Chemical Society.

Ishihara et al.[111] reported the fabrication of a Fc-containing phospholipid polymer hydrogel by using poly(vinyl alcohol) (PVA) and boron hydroxyl- and Fc-containing copolymer PMBVF (Figure 11) and the loading of an electron-generating bacteria (*Shewanella oneidensis* MR-1) in the prepared hydrogel. As shown in Figure 11, the gelling mechanism of PMBVF/PVA hydrogel was explained by the covalent crosslinking interaction between the OH groups in PVA and phenylboronic acid groups in PMBVF. The presence of Fc units has no obvious effect on the hydrogel formation. While the PVA solution was blended with the PMBVF solution containing *Shewanella*, the encapsulation of the bacteria was simultaneous with the formation of the hydrogel. The addition of *D*-sorbitol solution led to the dissociation of the hydrogel, and thus the analysis of loaded bacteria was easily conducted. The results of CV experiments demonstrated that the PMBVF/PVA composite hydrogels served as an electron transport mediator owing to the presence of Fc moieties. The Fc units in the hydrogel were believed to make a great contribution to electron transport from *Shewanella* to the surface of an electrode. The *Shewanella*-loaded composite hydrogels dramatically improved the quantity of current generated per unit of time. Thus, this Fc-containing hydrogel not only offered a biocompatible microenvironment for bacterias, but also enhanced electron transport efficiency. The present Fc-containing hydrogel/bacteria hybrid biomaterials are expected to find potential applications in developing various living cell-based electronic devices.

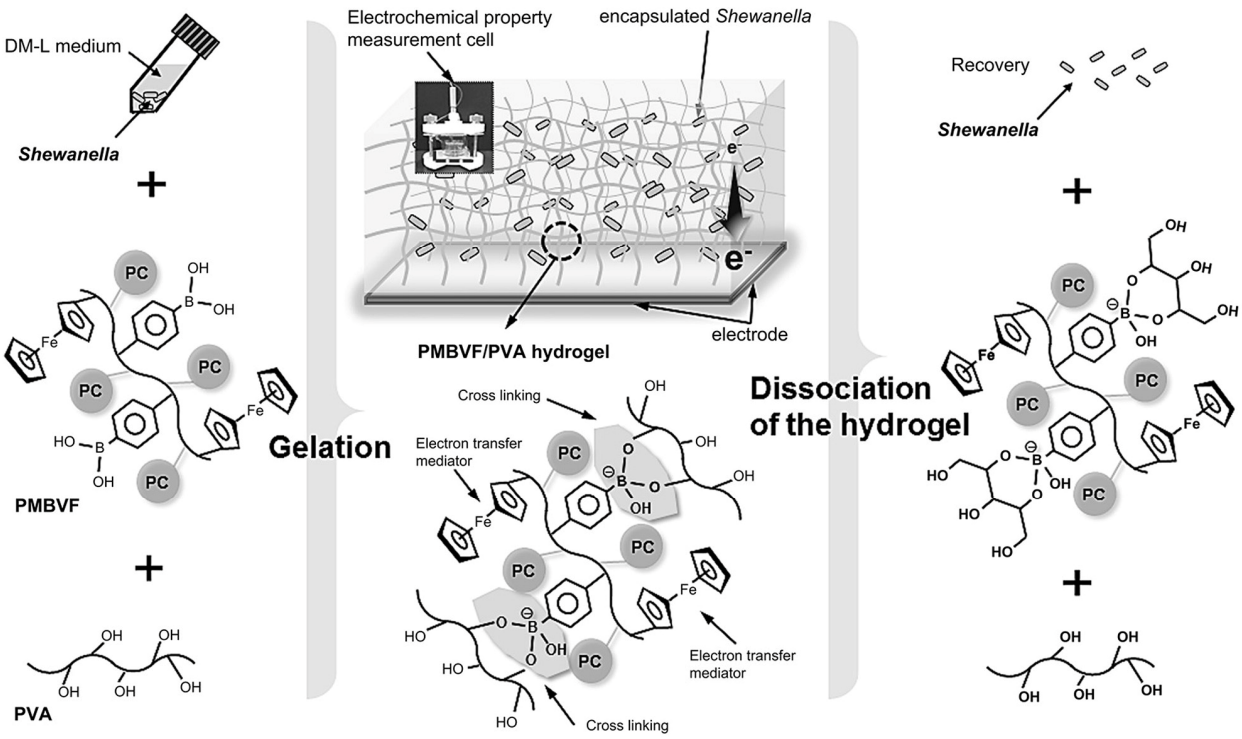

Figure 11. Schematic illustration of the PMBVF/PVA hydrogel as a matrix used to load electron-generating bacteria.[111] Reproduced with permission from Ref. [111]. Copyright 2012 Elsevier Ltd.

It is of significance to detect chemical and biological substances in biomedical and environmental applications[112,113]. Electrochemistry affords versatile and forceful analytical methods and techniques involving instrumental simplicity, appropriate cost and portability. Modern electrochemical approaches are commonly sensitive, selective, and fast in the biomedical field[114]. Electrochemical biosensors that are promising chemical sensors, possess low detection limit and relatively high specificity in the biological recognition field[115,116]. Fc derivatives are among the most frequently used compounds for the design and construction of various biosensors[117]. The remarkable electrochemical features (e.g. rapid electron transport rate, low oxidation potential, high stability of both reducing and oxidizing states, etc.) of Fc unit make its derivatives good

mediators[118-120]. Therefore, Fc-containing hydrogels also have great potentials in the field of redox-responsive biosensors.

For example, Schmidtke et al.[121] used Fc-functionalized linear and branched poly-(ethylenimine)(PEI), namely Fc-LPEI and Fc-BPEI (Figure 12A), to study the influence of various factors including pH, electrolytes and cross-linking on the charge transfer and swelling of hydrogel films. The hydrogel films from Fc-LPEI and Fc-BPEI were prepared using ethylene glycol diglycidyl ether (EGDGE) as a crosslinker. The redox behaviors of both Fc-LPEI and Fc-BPEI were determined by using cyclic voltammetry (CV) technique, and their electron diffusion coefficients were confirmed by electrochemical impedance spectroscopy. Interestingly, the Fc-LPEI hydrogel fully swelled at low pH of HCl solution (Figure 12B) and shrink with the ratio of around 55% after adding NaOH (pH = 11) (Figure 12C). Also, the full swelling of Fc-LPEI hydrogel was observed in water without any electrolyte (Figure 12D), but it cracked after adding 0.1 M perchlorate (Figure 12E). **Note of caution: perchlorates should be avoided or used with extreme caution, because they are hazardous, explosive compounds**. Glucose oxidase (GOD) was also incorporated into the hydrogel film, and the resulting glucose sensors possessed enzyme saturation current densities in the range of 240-480 $\mu A/cm^2$ under glucose stimuli, which relied on the environmental pH and supporting electrolyte used. The $FcMe_2$-LPEI and $FcMe_4$-LPEI hydrogel films were also applied to construct amperometric glucose sensors and biofuel cell materials[76,122,123]. Furthermore, the authors further investigated the effect of incorporating SWNTs or MWNTs into the composite hydrogel films using $FcMe_2$-LPEI polymer (Figure 12A) and GOD[124]. The fabrication course of the composite hydrogel films is shown in Figure 12F. CV and electrochemical impedance spectra (EIS) measurements indicated that the hydrogel films

bearing (7,6) SWNTs possessed much higher sensitivity towards glucose than those without SWNTs. In addition, (6,5) SWNTs (or MWNTs)-loading hydrogel films exhibited relatively lower response to glucose than the ones containing (7,6) SWNTs. After further optimizing the preparation condition of (7,6) SWNTs-loading hydrogel films, the optimal response to glucose was increased to 11.2 mA/cm^2. An enzymatic biofuel cell was further obtained by combining the optimized (7,6) SWNTs-loading hydrogel film with a Pt electrode, and exhibited the maximum power density output of 340 μW/cm^2. All these results showed that the nature of SWNTs has a great impact on the preparation and performance of the corresponding composite biosensors.

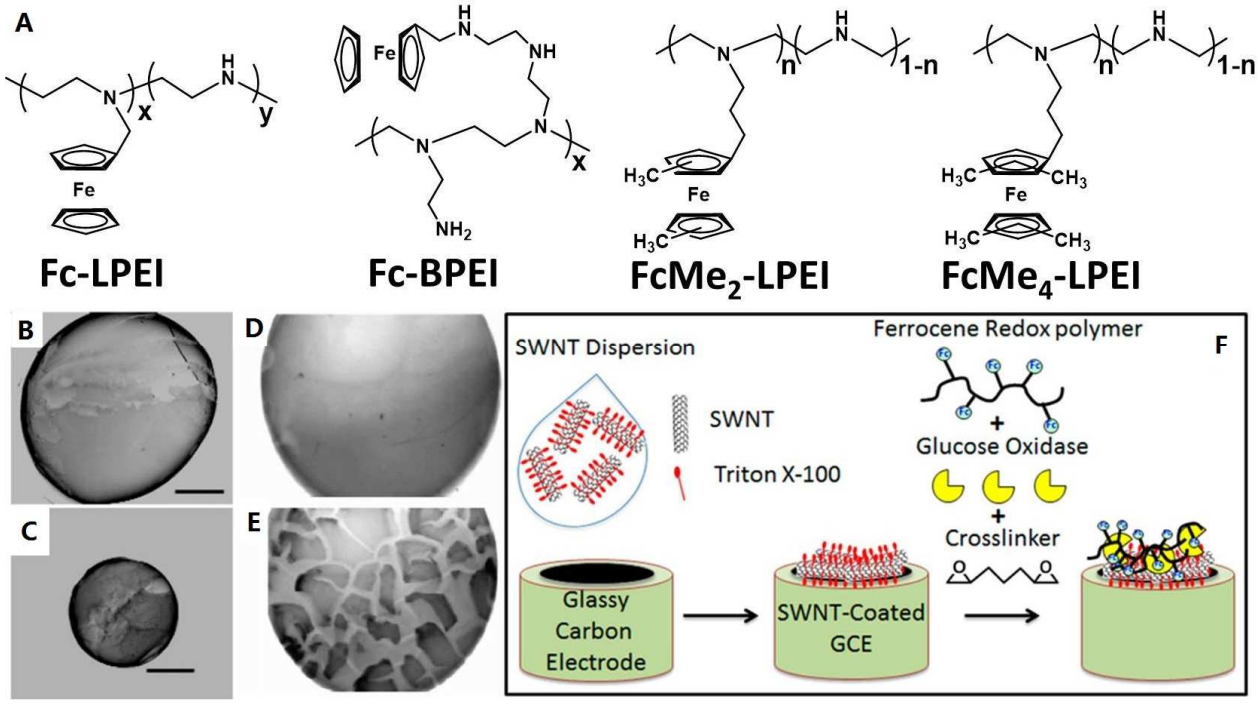

Figure 12. (A) Molecular structure of Fc-LPEI, Fc-BPEI, FcMe$_2$-LPEI and FcMe$_4$-LPEI. Optical images of Fc-LPEI hydrogel at pH = 1 (B) and pH = 11 (C). Optical images of Fc-LPEI hydrogel in H_2O (D) and (E) perchlorate with pH 5.0. Reproduced with permission from Ref. [121]. Copyright 2007 American Chemical Society. (F) The fabrication course of the modified electrodes. Reproduced with permission from Ref. [124]. Copyright 2017 American Chemical Society.

Ma et al.[125] reported the preparation of a conducting hydrogel with redox catalytic activity by using aniline and VFc as monomers and phytic acid as gelator. The resulting hydrogel exhibited great potential as an immunosensor to be used to ultrasensitively detect prostate specific antigen (PSA). The porous hydrogel (Figure 13A) was readily fabricated on the surface of a glassy carbon electrode (GCE), resulting in the improvement of its surface area and conductivity. When AuNPs was anchored to the hydrogel, the resulting AuNPs composite hydrogel presented a clear heterostructure (Figure 13B) after the treatment of electrochemical deposition, in which AuNPs had advantages in facilitating electron transfer and fixing PSA. Thereafter, the redox hydrogel/AuNPs composite was used to fabricate the label-free amperometric immunosensor as shown in Figure 13C. The electrochemical signal was clearly amplified, which was explained by the redox catalytic activity (outer mediation-type redox catalysis) of the Fc units towards the oxidation of ascorbic acid. PSA is an important pointer of prostate cancer and is detected as a cancer marker. The present immunosensor exhibited highly sensitive determination property for PSA at the optimized condition. In addition, this immunosensor was also used to detect PSA in human blood serum with a satisfactory outcome. This indicates that the redox-based hydrogels provided in this work have a great potential to detect cancer markers.

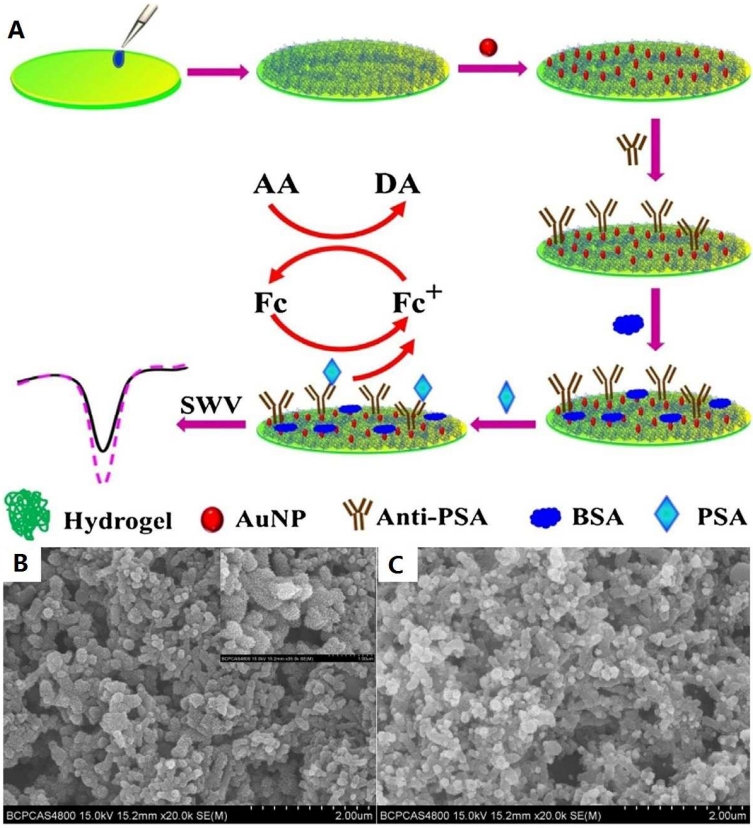

Figure 13. (A) Preparation of label-free immunosensor. SEM images of redox-based hydrogel (B) and redox hydrogel/AuNPs composite (C). Reproduced with permission from Ref. [125]. Copyright 2017 Elsevier B.V.

Ishihara et al.[126] adopted the layer-by-layer (LBL) strategy to fabricate a redox-based multilayer hydrogel on the Au electrode surface. The PVFc-based copolymer PMVF as shown in Figure 14 was prepared and employed as a redox-based adjuster. GOD was used as the model enzyme and was attached to the side chain of PVA under mild conditions. The crosslinked hydrogel structure was formed spontaneously via the reaction of the phenylboronic acid moieties of PMVF with hydroxyl moieties of PVA. The spin-coating method was adopted to prepare the hydrogel with multilayer structure. The electrochemical feature of the hydrogel-modified Au electrode was tested in the existence of glucose. It was found that the hydrogel multilayer was able to accomplish

intermolecular electron transport and allow the rapid diffusion of glucose. The LBL hydrogel multilayer prepared in this work showed potential applications in the development of bioelectronic devices with well-defined architectures and adjustable electrochemical activity.

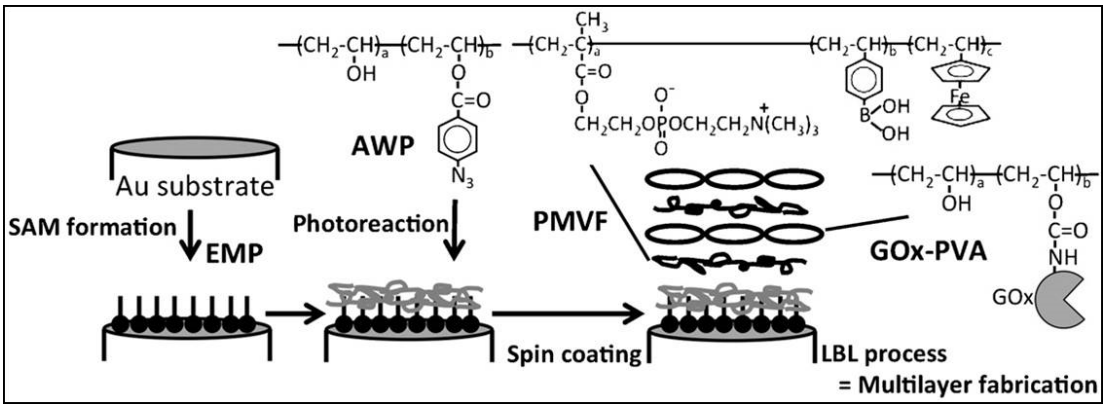

Figure 14. Fabrication of a multilayer hydrogel on Au electrode surface. Reproduced with permission from Ref. [126]. Copyright 2012 Elsevier B.V.

3. Supramolecular Fc-containing hydrogels

Supramolecular chemistry involves the astute design of invertible, precise, controllable and tailored molecular recognition moieties using dynamic noncovalent bonds, leading to the formation of organized systems across length-scales. Hydrogels constructed by supramolecular chemistry feature transient and invertible interactions (or bonds) among molecular chains, including H-bonds, electrovalent bonds, metal coordination, π–π stacking and host-guest inclusion interactions. Therefore, supramolecular hydrogels not only have various characteristics of conventional covalently cross-linked hydrogels, but also possess some particular performances including self-healing capability, degradability, and self-adaptation. Furthermore, supramolecular hydrogels generally have the capacity to simulate organisms and make a rapid response when environmental

factors change, which is attributed to their dynamic and invertible properties[127-136].

3.1. β-CD/Fc hydrogels

The supramolecular host-guest interactions between β-CD and Fc-containing compounds are well known, and the formed inclusion complexes disassemble upon applying a certain voltage or action of chemicals. Thus, Fc derivatives have been widely investigated for the fabrication of redox-active supramolecular hydrogels, because they show a response to the electrochemical or chemical redox stimuli, leading to large variations of the corresponding host–guest inclusion. The host–guest inclusion complexes between Fc derivatives and β-CD have already been intensively studied by researchers in the fields of chemistry, medicine and materials science. The neutral Fc group has a comparatively robust binding capacity to stoichiometrically bind β-CD with an equilibrium constant of 2.2×10^3 M^{-1} at 20 °C[137]. The obtained inclusion compounds are decomposed when the Fc moieties are changed into cationic hydrophilic Fc^+ under of electrochemical or chemical treatment[138]. Supramolecular hydrogels fabricated via β-CD/Fc host-guest interactions usually present self-healing and shape-memory performances as well as a sol-gel transition process. According to various types of host and guest molecules (Figure 15), β-CD/Fc hydrogels are divided into poly-(β-CD)/poly-(Fc), poly-(β-CD)/dual-(Fc), poly-(β-CD)/mono-(Fc), mono-(β-CD)/dual-(Fc) and mono-(β-CD)/mono-(Fc) hydrogels.

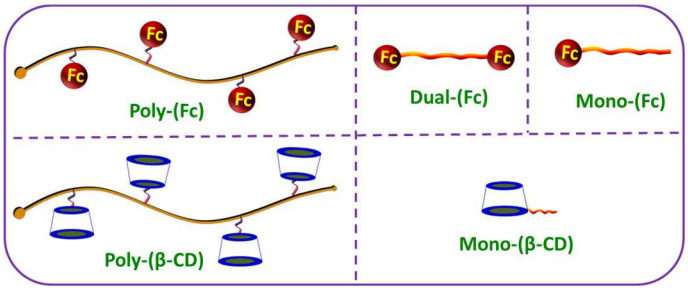

Figure 15. Schematic structures of representative guest and host molecules for the construction of β-CD/Fc hydrogels.

3.1.1. Poly-(β-CD)/Poly-(Fc) hydrogels

Side-chain β-CD-containing polymers and side-chain Fc-containing polymers are the most frequent starting materials that are used to fabricate supramolecular Fc-containing hydrogels through the host–guest dynamic binding between β-CD and the Fc moiety. This is because this system generates a large number of binding sites between Fc groups and β-CD units that form the effective construction of supramolecular hydrogels. Harada and co-workers[73,139] pioneered the fabrication of self-healing and redox-sensitive supramolecular hydrogels using poly(acrylic acid) (pAA) grafted by β-CD host groups in the side chain and pAA modified by pendent Fc guest moieties (Figure 16A). The host polymer pAA-6βCD was prepared via an amidation modification of pAA by using 6-amino-βCD, while the guest polymer pAA-Fc was fabricated by grafting aminoethylamido Fc to pAA. The degree of substitution is 4-5% for the former and 2.7% for the latter. A transparent supramolecular hydrogel was fabricated via directly mixing pAA-6βCD and pAA-Fc at 1:1 feed mole ratio. This solid supramolecular hydrogel changed into the fluent sol state in the presence of a competitive guest (e.g. adamantane carboxylic acid sodium salt, AdCANa) or host (e.g. β-CD) molecules in the environment. This reversible sol−gel transformation was also triggered in the presence of chemical and electrochemical redox stimuli. This is the result of the invertible change between hydrophobic Fc and hydrophilic Fc^+ moieties and the on-off control of complexation and dissociation of guest with β-CD (Figure 16B). For example, as shown in Figure 16C, NaClO was adopted as an oxidizing agent, and its treatment triggerred the transition of the

supramolecular hydrogel solid into the sol liquid. On the contrary, the treatment of glutathione (GSH) as a reducing agent led to the change of the resulting sol into the original hydrogel solid. This is a reversible cycle. Also, a similar change from solidified hydrogel to fluent sol was observed when the electrochemical oxidation was carried out using a potentiostat, and the reverse change happenned when the heating treatment of 50 ^{o}C was conducted (Figure 16D). Based on the result of rheological experiments, the authors identified the self-healing capability of this supramolecular hydrogels, and its macroscopic self-healing performance was also observed because of the dynamic reversibility of the β-CD/Fc inclusion complexes. As can be seen from Figure 16E, the supramolecular hydrogel piece was separated into two parts, and then they were reintegrated. After 24 h of keeping contact, the preceding fissure disappeared, and the two parts fused into one integrated gel piece. Interestingly, when the contact surfaces were treated with NaClO as oxidant, the healing phenomenon was not observed. When the GSH was subsequently spread as a reductant on the contact surfaces, the two hydrogel parts re-adhered together into a whole one (Figure 16F). Namely, the self-healing capability of the supramolecular hydrogel were tuned by using oxidizing and reducing agents. The present hydrogel is anticipated to be applied as smart drug-delivery carrier with redox-controlled drug-release property or medical soft materials with self-repairing ability.

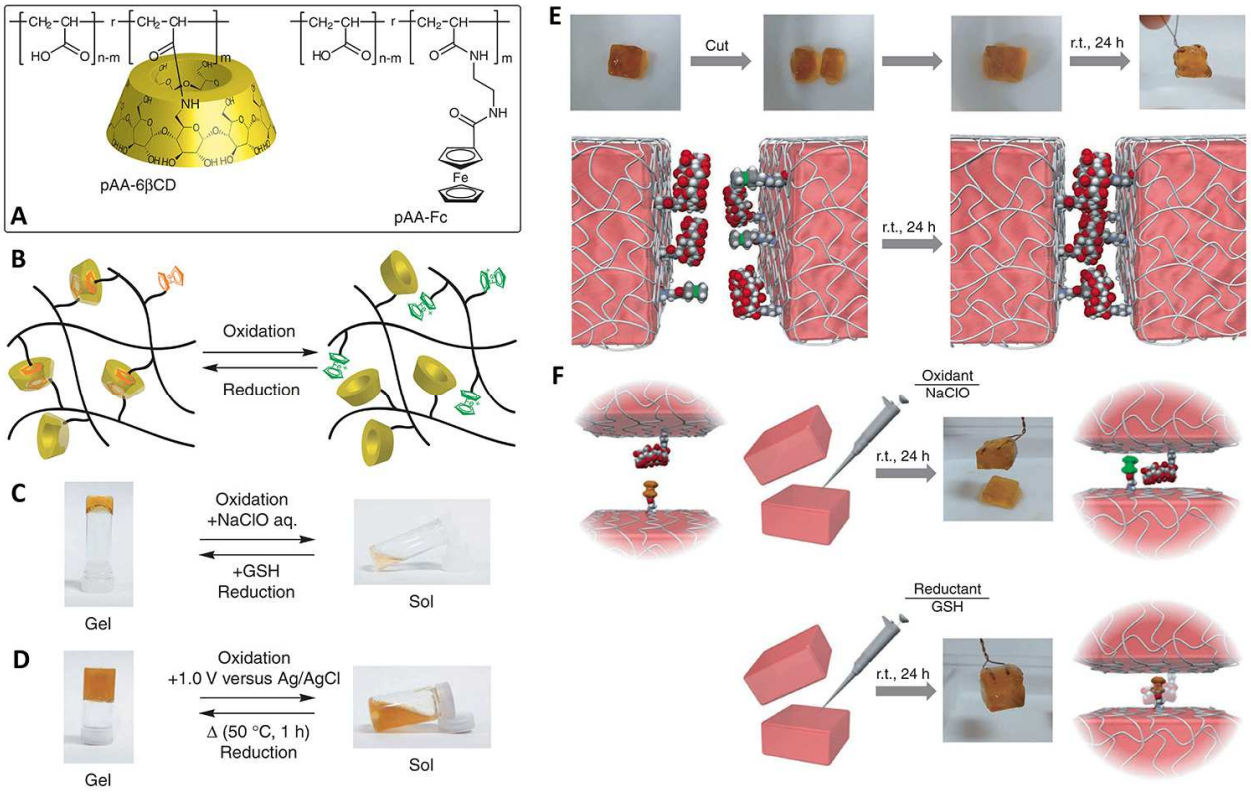

Figure 16. (A) Molecular structures of pAA-6βCD containing host β-CD rings in the side chain and pAA-Fc bearing side-chain Fc guest groups. (B) Schematic mechanism of sol–gel change. (C) Sol–gel transformation induced by chemical reagents. (D) Sol–gel transformation under the different electrochemical atmosphere. (E) Macroscopic self-healing experiments by cutting and re-attaching and the corresponding mechanism. (F) Redox-responsive healing experiments and the corresponding mechanism. Reproduced with permission from Ref. [73]. Copyright 2011 Springer Nature.

Making use of the β-CD/Fc host–guest inclusion system, Harada and co-workers [75] prepared a distinctive supramolecular hydrogel actuator whose action was driven by redox reactions. First, the supramolecular cross-linker was synthesized via directly blending the Fc guest molecule (Fc-AAm) and the β-CD host one (β-CD-AAm). The supramolecular hydrogel was then fabricated via the

copolymerization of acrylamide (AAm) and *N*,*N*'-methylenebis(acrylamide) (MBAAm) in the presence of the supramolecular cross-linker and the initiator of 2,2'-azobis[2-(2-imidazolin-2-yl)-propane] dihydrochloride (VA-044). Figure 17A presents the molecular composition of the formed βCD-Fc hydrogel. The supramolecular crosslinked interaction inside the hydrogel was proven by the results of immersing experiments in an aqueous solution of competitive compounds. As shown in Figure 17B and C, AdCANa was adopted as the competitive guest, and β-CD was selected as the competitive host. The immersing treatment in both solutions led to the swelling of the hydrogel because of the disintegration of inclusion complexes of β-CD/Fc. In addition, the size of the βCD-Fc hydrogel was adjusted using redox reagents (Figure 17D, E). The oxidation with ceric ammonium nitrate (CAN) improved the size of the hydrogel, whereas the subsequent reduction restored its original size. This expansion–contraction behavior of βCD-Fc hydrogel was further applied to perform the mechanical work. As shown in Figure 17E, oxidation prompts the expansion of the supramolecular hydrogel and thus the descending location of the weight was observed. On the other hand, reduction resulted in the contraction of the hydrogel, and thus restored location of the weight. Specifically, the calculated mechanical work was 2.0 μJ. The authors believed that the present hydrogel containing supramolecular β-CD/Fc cross-links would find a specific application as an artificial muscle.

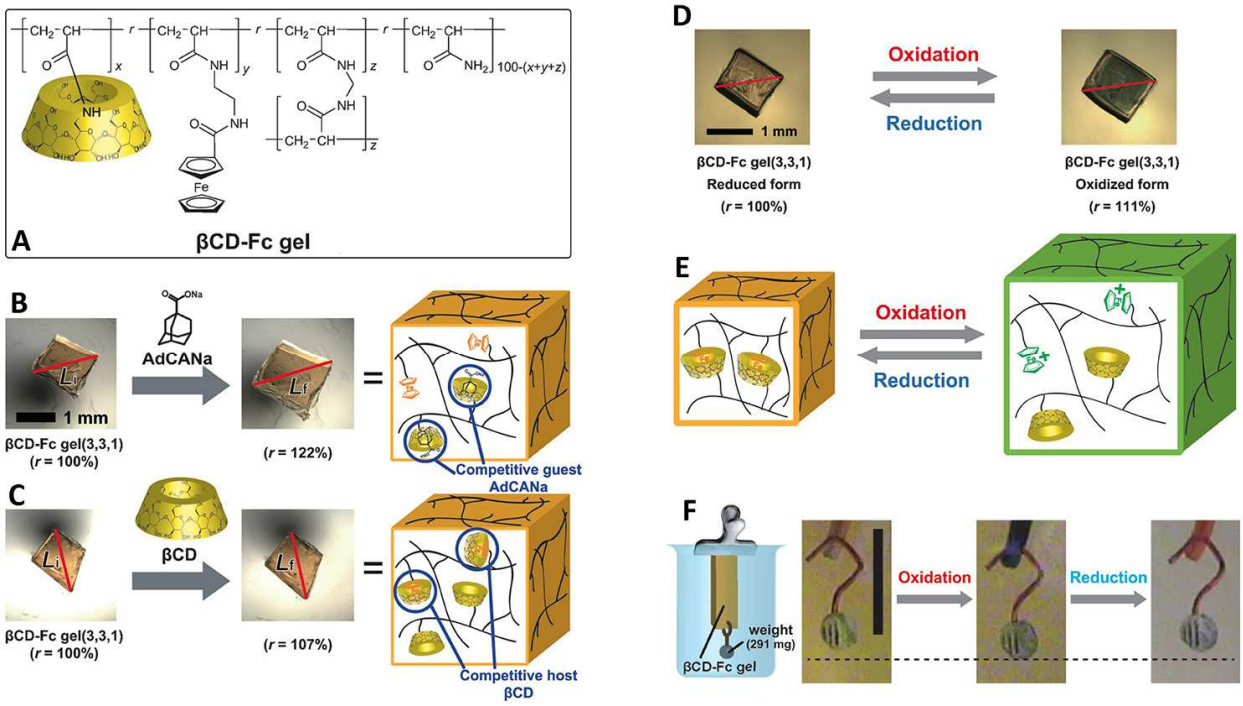

Figure 17. (A) Structure of the βCD-Fc hydrogel. Photos and schematic diagrams of the length variation of βCD-Fc hydrogel induced by (B) AdCANa and (C) β-CD. Photos (D) and schematic diagrams (E) of swelling or shrinking of the βCD-Fc hydrogel caused by oxidation/reduction stimuli. (F) Schematic diagram and photos of the action of βCD-Fc hydrogel. Reproduced with permission from Ref. [75]. Copyright 2013 Wiley-VCH Verlag GmbH & Co. KGaA, Weinheim.

A redox-responsive Fc-containing hydrogel assembly system was developed by Harada's group[140] to precisely identify an appropriate adhering object in visible scale. The system included the redox-responsive megascopic self-assembly of polymeric hydrogel side-chain functionalized via β-CD (βCD gel), Fc (Fc gel), and styrenesulfonic acid sodium salt (SSNa gel), respectively. The underlying recognition mechanisms are the β-CD/Fc host–guest inclusion action and cation-anion electrostatic incorporation between Fc^+ and SSNa. Figure 18 provides the molecular compositions of these hydrogels. The βCD and SSNa hydrogels were synthesized in water via copolymerization reactions of the corresponding monomers, in which ammonium

peroxodisulfate (APS) and *N*,*N*,*N*',*N*'-tetramethylethylenediamine (TEMED) were applied as catalyst. The homogeneous radical copolymerization was also carried out to prepare the Fc gel but using VA-044 as an initiator. When the βCD gel and Fc gel met together, and the intensive aggregation phenomenon was observed within a few minutes (Figure 18A). However, after oxidizing the Fc gel to the Fc^+ gel, this aggregation was not observed (Figure 18B). Moreover, after the competitive compounds (e.g. β-CD and sodium adamantine carbonate) were mixed into the outer solution, this aggregation was not formed either. The above experimental results manifest that the resulting adhering interaction between Fc and β-CD hydrogel pieces may be on account of the generation of inclusion compounds at the interfaces of these hydrogel pieces (Figure 18C). It was noted that no aggregation phenomenon took place in the mixture of Fc gel and SSNa gel (Figure 18D). The Fc^+ gel was adhered using the SSNa gel, however (Figure 18E). Similarly, the presence of a the host calix[6]arene hexasulfonic acid sodium salt (CS6) that possesses a comparatively high bonding constant with the Fc^+ units, prevented the visible assembly between the Fc^+ gel and SSNa gel. The above results confirm that the visual assembly between Fc^+ gel and SSNa gel may be explained by the electrostatic attraction at the interfaces of these hydrogel pieces (Figure 18F). In addition, a Fc/Fc^+ gel was further prepared by oxidizing half of the Fc gel in CAN aqueous solution for 10 min. Interestingly, a unique ABC-type visible assembly phenomenon was observed when the Fc/Fc^+ gel, βCD gel and SSNa gel pieces were mixed together, and this treatment led to the formation of the βCD gel–Fc/Fc+ gel–SSNa gel long pieces (Figure 18G). This characteristic visible assembly was taken into account by the host–guest interaction between β-CD and Fc and the electrostatic attraction between Fc^+ and SSNa (Figure 18H). In other words, by changing the redox state of the Fc units, the Fc gel discriminatively recognized βCD gel and SSNa

gel on a visible scale. As a result, the present smart macroscopic assembly systems were expected to find potential applications in the medical and functional device fields.

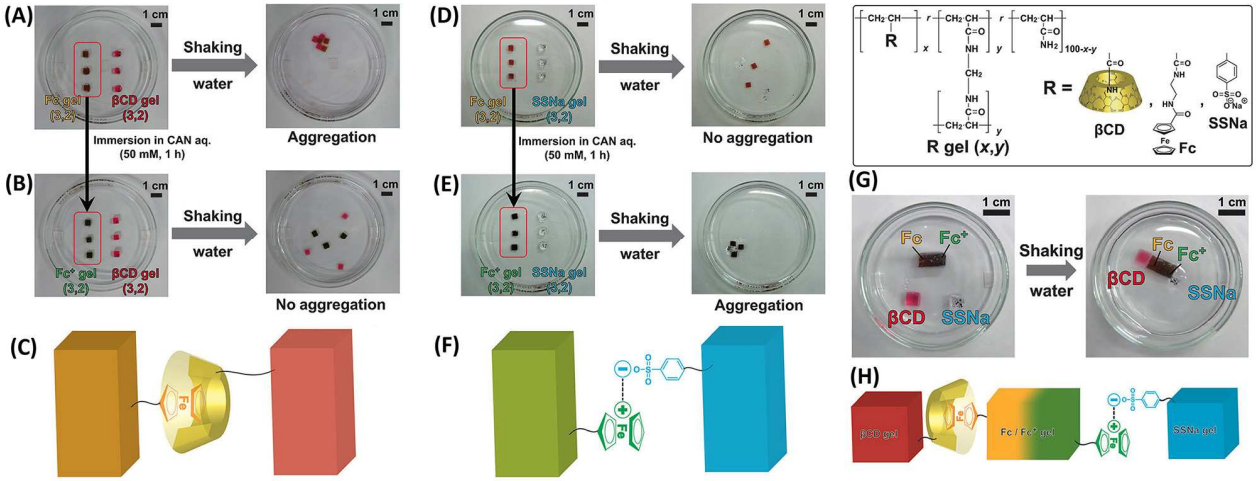

Figure 18. Structures of the βCD, Fc and SSNa hydrogels. (A-H) Pictures and schematic mechanisms of aggregation between these hydrogels. Reproduced with permission from Ref. [140]. Copyright 2014 Wiley-VCH Verlag GmbH & Co. KGaA, Weinheim.

Harada's group[78] further reported the preparation of a new supramolecular hydrogel containing two diverse classes of host–guest systems of β-CD with adamantane (Ad) and Fc, respectively, and the obtained hydrogel exhibited self-healing, swelling-shrinking, and shape-memory performances. Figure 19A provides the molecular composition of the formed host–guest βCD-Ad-Fc hydrogel. The host (βCD–AAm) and guest (Ad–AAm and Fc–AAm) monomers were first dissolved in the H_2O/DMSO mixture solvent. The βCD-Ad-Fc hydrogel was then produced via typical free-radical copolymerization of these inclusion complexes and AAm (or NIPAAM) in the presence of VA-044 initiator. Figure 19B shows the photograph of the formed supramolecular hydrogel. As expected, the βCD-Ad-Fc hydrogel exhibited the self-reparing property because of the presence of the

invertible dynamic non-covalent bondings (Figure 19C). The self-healing performance was even maintained in the presence of an oxidant, because the host–guest combination of β-CD and Ad was insensitive to the redox stimuli. Only highly competitive guest compounds such as AdCANa totally destroyed this self-healing property. In addition, the swelling-shrinking performance of the βCD-Ad-Fc hydrogel was adjusted during an oxidation-reduction cycle. Concretely, the hydrogel swelled upon oxidizing its Fc units to cationic Fc^+ species, whereas the following reduction of Fc^+ into Fc resulted in the shrinking of the hydrogel. Furthermore, the helical morphology of the βCD-Ad-Fc hydrogel belt fixed in the oxidizing CAN buffered solution was retained by the subsequent reduction treatment (Figure 19D). This shape-memory phenomenon did not take place without chemical redox treatment. Figure 19E indicates the possible shape-memory mechanism. It was proposed that the incorporation of two distinct supramolecular bondings afforded the hydrogels with redox-responsive shape-memory performance. The present supramolecular hydrogels were anticipated to find potential applications as intelligent soft materials owing to their highly bionic performances.

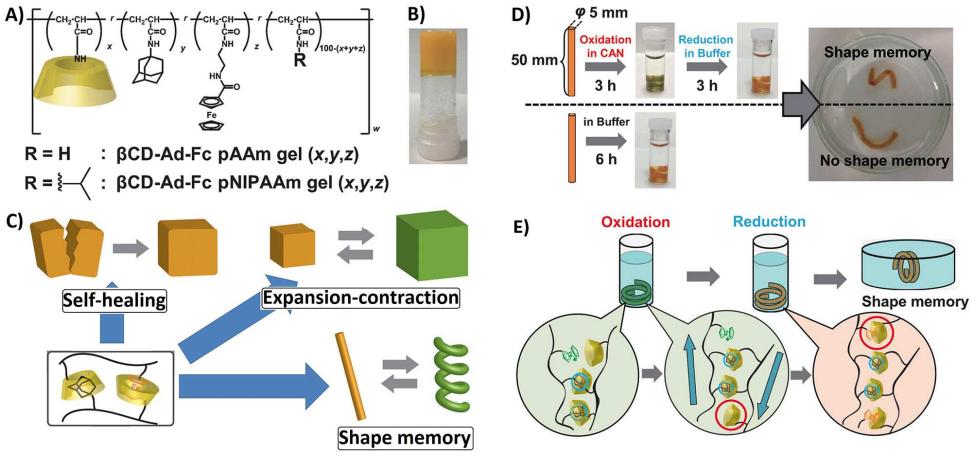

Figure 19. Molecular structure (A) and photo (B) of βCD-Ad-Fc hydrogels. (C) Schematic of three characteristic performances of βCD-Ad-Fc hydrogel. (D) Shape-change experimental procedure for the βCD-Ad-Fc hydrogel. (E) Proposed mechanism of the shape-memory. Reproduced with

permission from Ref. [78]. Copyright 2015 Wiley-VCH Verlag GmbH & Co. KGaA, Weinheim.

Jiao et al.[141] prepared the supramolecular hydrogels by using poly(β-cyclodextrin) (P-CD) and Fc-grafted poly(acrylic acid) (PAA-Fc, Figure 20A), and confirmed its high-efficiency dye removal capacity for waste water treatment. The P-CD was prepared by reacting β-CD with epichlorohydrin under alkaline conditions, and the PAA-Fc was obtained by the amidation graft modification of PAA with Fc-CONH-$(CH_2)_2$-NH_2. The produced PAA-Fc and P-CD were mixed at their different ratios in water, resulting in the formation of host-guest supramolecular hydrogels. The internal network structure and property of these hydrogels was tuned by changing the P-CD concentrations. The gel-sol transformation took place upon using redox stimulation and a competitive molecule (Figure 20B). Specifically, the treatment of NaClO or AdCANa dramatically lowered the viscosity of this hydrogel and finally resulted in the formation of sol solution. Subsequently, the addition of reducing GSH into the sol solution led to the regeneration of the solid hydrogel state. The hydrogels prepared in this work had different adsorption mechanisms for poisonous bisphenol A and methylene blue, and the adsorption process was easily regulated by changing environmental pH values. The host-guest combination was believed to be the possible adsorbing mechanism of bisphenol A by this hydrogel, while methylene blue was adsorbed owing to H-bonding and electrostatic attraction. However, the present supramolecular hydrogel exhibited similar adsorption ability for bisphenol A and methylene blue, and the determined maximum amounts were 23.61 mg/g for the former and 24.64 mg/g for the latter, respectively. This work afforded a new and feasible approach for designing and fabricating eco-friendly supramolecular hydrogel adsorbents.

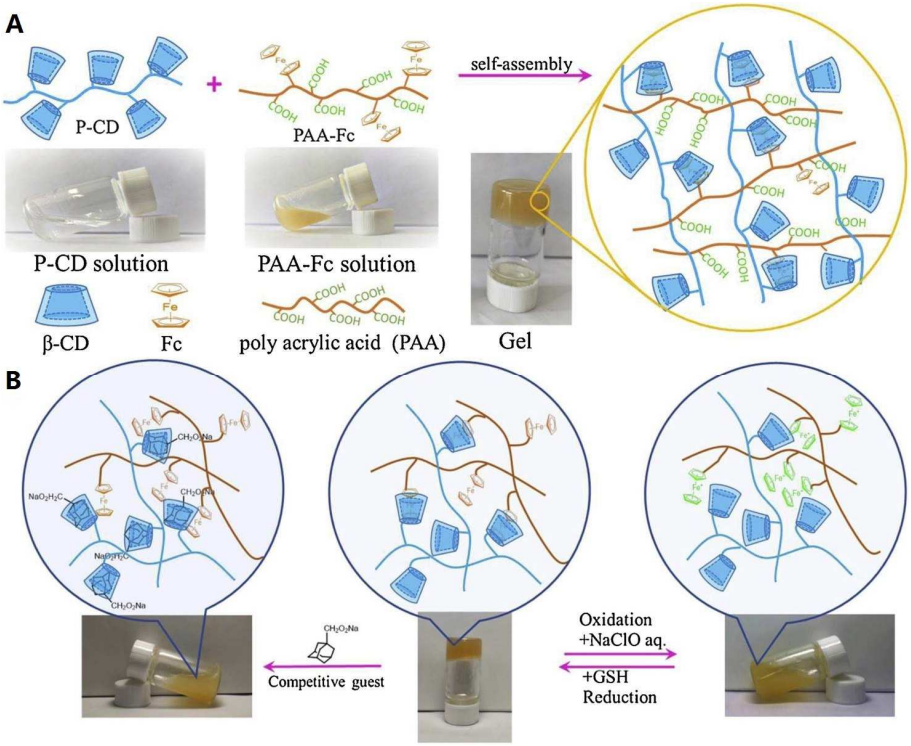

Figure 20. Schematic preparation route to supramolecular P-CD/PAA-Fc hydrogel (A) and its sol-gel transition (B). Reproduced with permission from Ref. [141]. Copyright 2019 Elsevier B.V.

Zhang et al.[142] reported a new redox-triggered shape-memory polymer (SMP) hydrogel that was synthesized through crosslinking β-CD-grafted chitosan (β-CD-CS) and Fc-terminated branched ethylene imine polymer (Fc-PEI). The SMP was used to prepare a hydrogel film, and there were two cross-linking types, namely the dynamic, invertible and redox-sensitive β-CD/Fc bonding and the covalent Schiff base linkages from glutaraldehyde as a cross-linker. This material was able to be driven to form the required shapes in the reduced state and regained its primary shape after being oxidized. Both the restoration ratio and the immobility ratio were determined to be more than 70%. Specifically, when Fc groups were kept in the reduced state, the SMP was rigid and did not easily change shape due to the presence of supramolecular host-guest and covalent crosslinks. After Fc groups were changed into Fc^+ species upon using the oxidant $(NH_4)Ce(NO_3)_6$, the disassembly of

the host-guest combinations took place. The resulting material became soft and easily transformed under an external force. By soaking the distorted sample into the reducing $NaHSO_3$ solution with the external pressure, the distortion of the sample would be maintained owing to the recovery of the host-guest combination. When the sample was subsequently immersed in the oxidizing $(NH_4)Ce(NO_3)_6$ solution again, the damage of the host-guest combinations led to the recovery of its initial shape. The redox-responsive host-guest supramolecular combination of β-CD/Fc acts as the "on-off", while the covalent bondings should contribute to maintaining the constant shape. In addition, after encapsulating GOD into the hydrogel network, the resulting product exhibited a shape-memory performance under the action of glucose, and both the restoration and immobility ratios also reached more than 70%.

Kuckling et al.[143] reported a dual cross-linked supramolecular hydrogel (DCSH) that was applied as sensor for the determination of small molecules (Figure 21). The DCSH was obtained via synchronously incorporating the host–guest β-CD/Fc complex cross-linkers and the photo-responsive crosslinking of 2-(dimethylmaleimido)-*N*-ethylamine (DMIEA). The RAFT copolymerization of DMAAM and 2-vinyl-4,4-dimethylazlactone led to P(DMAAm-*co*-VDMA). Subsequently, the obtained P(DMAAm-*co*-VDMA) was functionalized with DMIEA and β-CD (or Fc) to generate P(DMAAm-*co*-VDMA)-CD [or P(DMAAm-*co*-VDMA)-Fc]. The contents of cross-linkers were calculated by ^{1}H NMR to be 1.4% of β-CD and 3.7% of DMIEA in P(DMAAm-*co*-VDMA)-CD, and 4.3% of Fc and 2.3% of DMIEA in P(DMAAm-*co*-VDMA)-Fc, respectively. As expected, the targeted supramolecular DCSH was prepared by mixing the host polymer P(DMAAm-*co*-VDMA)-CD with the guest one P(DMAAm-*co*-VDMA)-Fc in water, which was explained by the host-guest combination between β-CD and Fc in side chains. After the addition of

the competitive guest compound of adamantane amine (Ada), the formed colloidal DCSH changed into a liquid sol due to the stronger interaction between Ada and β-CD. The DCSH system was also formed by spin-coating the mixture of host and guest polymers onto a pretreated gold surface, followed by the photo-cross-linking of DMIEA groups. The resulting thickness of DCSH film was determined to be 375 nm. The DCSH layer had the swelling ratio of 11.3 and the refractive index of 1.387. After being treated by Ada solution, the thickness of DCSH film dramatically increased to 528 nm, and the corresponding swelling ratio was improved to 16.0, while the refractive index was reduced to 1.362. These results proved that Ada served as an adjusting agent to destroy the host–guest β-CD/Fc combination in the thin DCSH film, but the covalent photo-crosslinking was strong enough to maintain its colloidal state. Finally, the DCSH was also employed as a surface plasmon resonance (SPR) combined with optical waveguide spectroscopy (SPR-OWS) sensor to monitor some small molecular compounds that have stronger binding ability to β-CD than the Fc unit. The new method demonstrated by the present DCSH system is hopeful to serve as an efficient SPR sensor for targeted detection of small biological molecules.

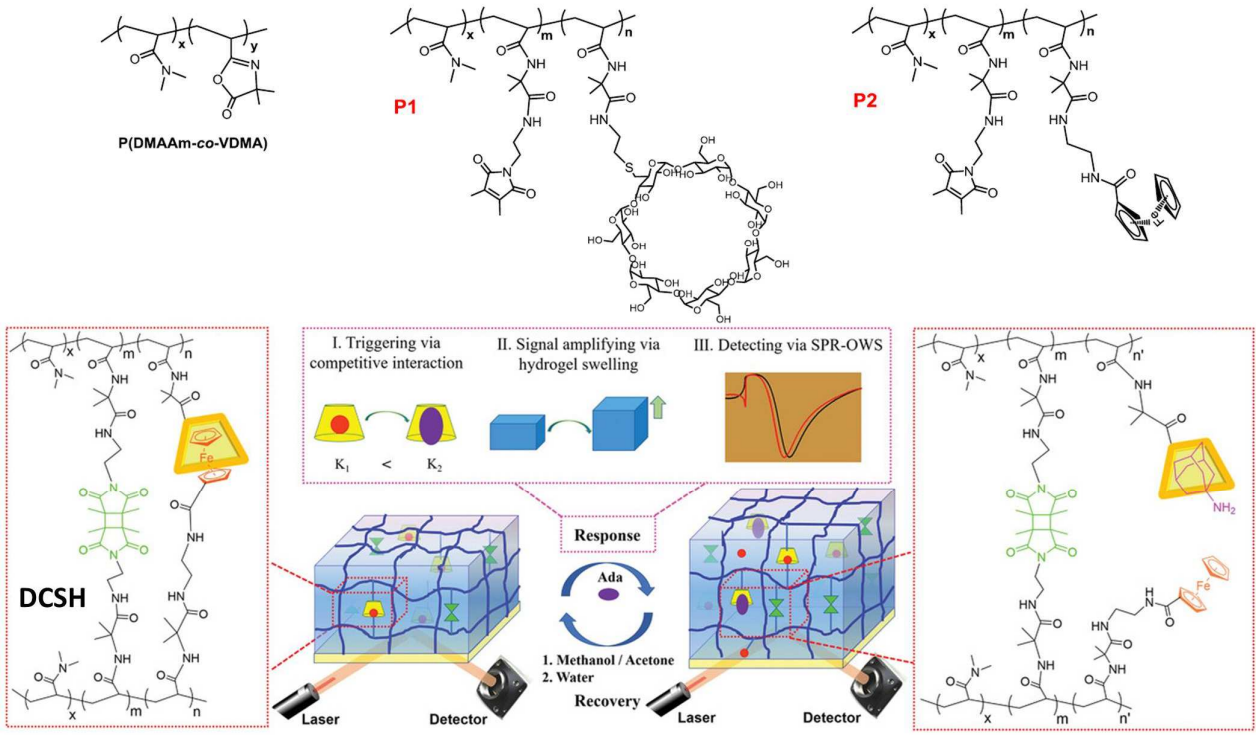

Figure 21. Structures of host and guest polymers used to fabricate DCSH hydrogel, schematic swelling behavior of DCSH and its response mechanism. Reproduced with permission from Ref. [143]. Copyright 2019 WILEY-VCH Verlag GmbH & Co. KGaA, Weinheim.

Duan et al.[144,145] reported a supramolecular cellulose hydrogel fabricated using β-CD-grafted cellulose and Fc-modified cellulose. Cellulose was first reacted with epichlorohydrin in NaOH aqueous solution to give epoxy cellulose, the epoxy groups of which served as cross-linking bridges upon combination with the OH groups of β-CD to generate the β-CD-cellulose host polymer with a grafting degree of 0.32% wt. The Fc-cellulose guest polymer with grafting rate of 0.5% wt was synthesized by the esterification reaction of ferrocenecarboxyl chloride (Fc-COCl) with cellulose. The supramolecular hydrogel was then fabricated by mixing the β-CD-cellulose and Fc-cellulose at the β-CD/Fc molar ratio of 1:1. The performance of the obtained hydrogel was significantly influenced by the host-guest β-CD/Fc combination. Both competing host and guest compounds

affected the mechanical property of this supramolecular cellulose hydrogel. Concretely, the compressive strength of the hydrogel sharply decreased from 41.0 to 9.8 kPa after the soaking treatment in the β-CD solution. Similarly, the treatment of adamantine carboxylic acid led to the decrease of compressive strength from 41.0 to 6.8 kPa. This decrease in compressive strength was explained by the decreased degree of crosslinking in the supramolecular cellulose hydrogel resulted from the inhibition of competitive guest or host molecules. In addition, the compressive strength of the supramolecular cellulose hydrogel was regulated by changing the redox state of Fc groups, which caused the complexing/separating of the β-CD/Fc system (Figure 22A). As expected, the cellulose hydrogel exhibited desirable self-healing property. As shown in Figure 22B, it took 24 h to heal two hydrogel pieces into an integral one. However, the self-healing phenomenon was not observed when the bonding surfaces were coated by the competitive guest (Figure 22C) or host solutions (Figure 22D). These results indicated that the self-healing performance of the cellulose hydrogel was attributed to the host-guest combination on the joint surfaces. Also, the authors reported a supramolecular hydrogel using the host-guest combination between the Fc-modified cellulose and the β-CD-grafted chitosan[146]. The resulting cellulose-chitosan composite hydrogel also showed good self-healing capacity and presented potential applications in medicine, textiles, sports, cosmetics, and hygiene product manufacture.

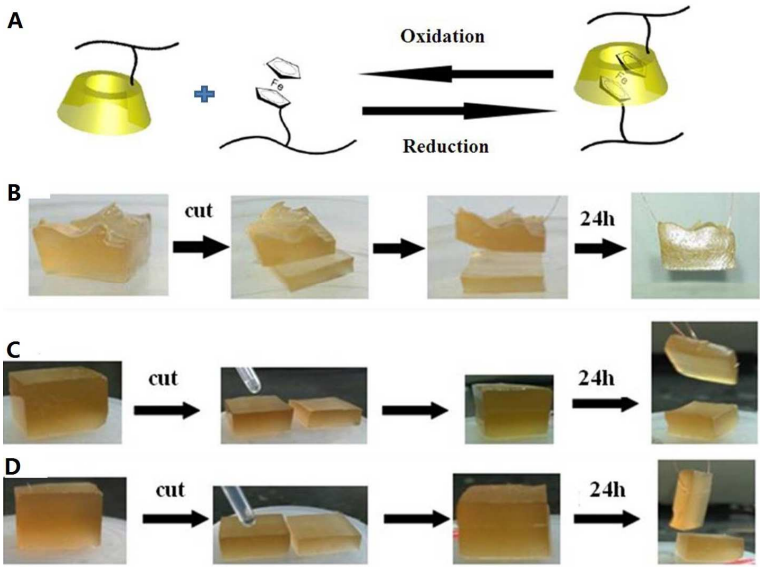

Figure 22. (A) Schematic structures of β-CD- and Fc-modified cellulose polymers and the corresponding supramolecular hydrogel. (B) Cutting-rejoining experimental procedure. Inhibitory effects of adamantane carboxylic acid (C) and β-CD (D) on the self-healing ablility of hydrogel. Reproduced with permission from Ref. [144]. Copyright 2014 BioResources.

Yuan et al.[77,147] fabricated the host random copolymer poly(*N*,*N*-dimethylacrylamide-*r*-glycidol methacrylate-β-CD) P(DMA-*r*-GMA-CD) and the guest random copolymer poly (*N*,*N*-dimethylacrylamide-*r*-2-hydroxyethylmethacrylate-Fc) P(DMA-*r*-HEMA-Fc), and the corresponding redox-sensitive supramolecular hydrogels with self-healing characteristic (Figure 23). The post-polymerization method was adopted to prepare both random copolymers containing pendent β-CD or Fc groups. The RAFT copolymerization of DMA and GMA led to P(DMA-*r*-GMA) that was then functionalized with β-CD and a Fc derivative, respectively, to generate the corresponding P(DMA-r-GMA-CD) and P(DMA-*r*-HEMA-Fc). Both the resulting polymers wer dissolved in H_2O to provide stable solutions (Figure 23A, 23B), but the mixing of these two solutions resulted in the formation of the supramolecular hydrogels owing to the β-CD/Fc host–

guest combination reactions (Figure 23C). As can be seen from Figure 23C and 23D, the obtained supramolecular hydrogels showed reversible sol–gel transformation by changing the potentials between +0.50 V and −0.10 V. In addition, the same phenomenon was also induced by the addition of suitable redox chemicals. Concretely, the treatment of the oxidant $FeCl_3$ led to the transformation from the solid gel to a liquid sol (Figure 23E), and the subsequent treatment of the reductant ascorbic acid resulted in the restoration of the solid hydrogel (Figure 23C). Furthermore, the results of cytotoxicity test on C26 cell line indicated that these hydrogels had good biocompatibility, and thus they were safe and suitable for biomedical applications.

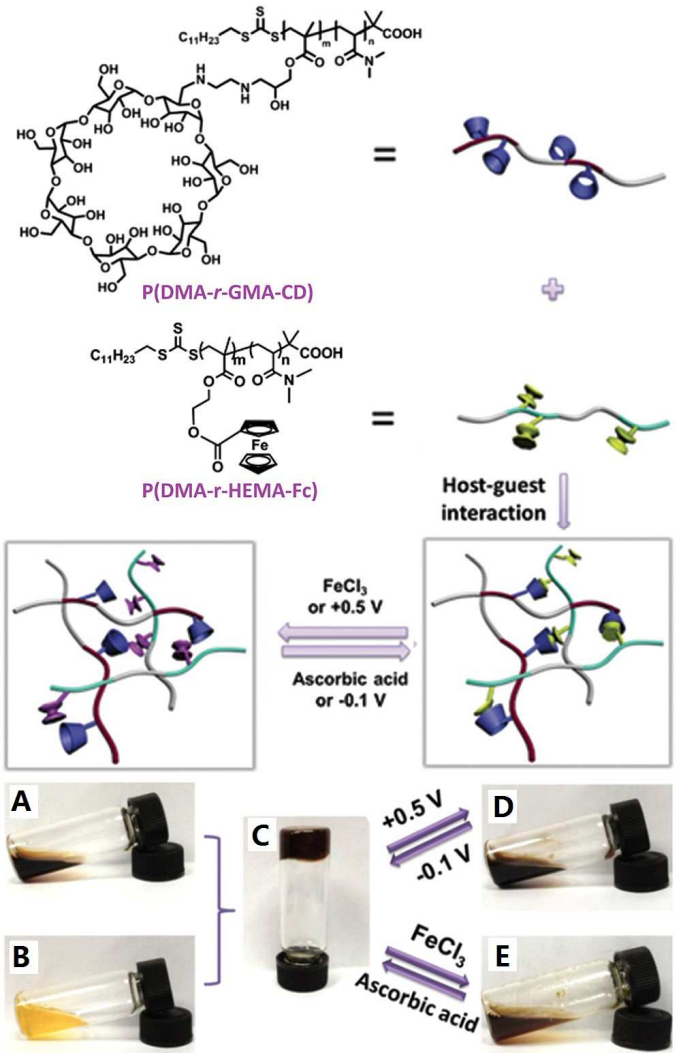

Figure 23. Schematic formation and redox-responsiveness of supramolecular hydrogel prepared using two polymer side-chain containing β-CD and Fc units, respectively. Pictures of P(DMA-*r*-HEMA-Fc) (A) and P(DMA-*r*-GMA-CD) (B) in H_2O at 20 wt%. (C) Picture of P(DMA-*r*-GMA-CD)/P(DMA-*r*-HEMA-Fc) supramolecular hydrogel. (C, D) Sol-gel transformation triggered by electrochemical treatment. (C, E) Sol-gel transformation triggered by redox agents. Reproduced with permission from Ref. [77]. Copyright 2015 Royal Society of Chemistry.

Xiong et al.[148] reported a strategy used to fabricate oxidation-triggered degradable nanogels for Fe^{3+}-chelating application. Figure 24A shows the molecular structure of the used oxidation-sensitive host-guest β-CD/Fc-containing supramolecular crosslinker, and the nanogel (oxNG–DFO) was prepared via the copolymerization of this crosslinker, metal chelating deferoxamine (DFO) and AAm monomers. The obtained nanogels exhibited excellent chelating activity to Fe^{3+} ions and oxidation-triggered degradable behavior. As shown in Figure 24B, after the addition of $FeCl_3$ into the nanogel solution, a clear yellow-brown color was immediately observed, indicating the successful chelation of Fe^{3+} with the nanogels. The DFO conjugated to the nanogels was further confirmed by centrifugal filtration experiment (Figure 23B), and the collected concentrate and filtrate were measured, respectively, by UV-vis. spectroscopy at 430 nm. The yellow-brown solution showeds absorption, while the filtrate had no absorption. These results illustrated the fact that DFO was successfully introduced into nanogels. Furthermore, a similar method was also applied to fabricate bulk hydrogels. As shown in Figure 24C, the increase of the oxidative stress

levels much improved the degradation rate of the hydrogel. Furthermore, the results of cytotoxicity test on J774A.1 mouse monocyte/macrophage cells demonstrated that the cytotoxicity of the chelator was reduced by conjugating DFO to the nanogels. Therefore, these oxidation-responsive nanogels and hydrogels are anticipated to find favorable applications in chemical oxidation sensing and drug delivery.

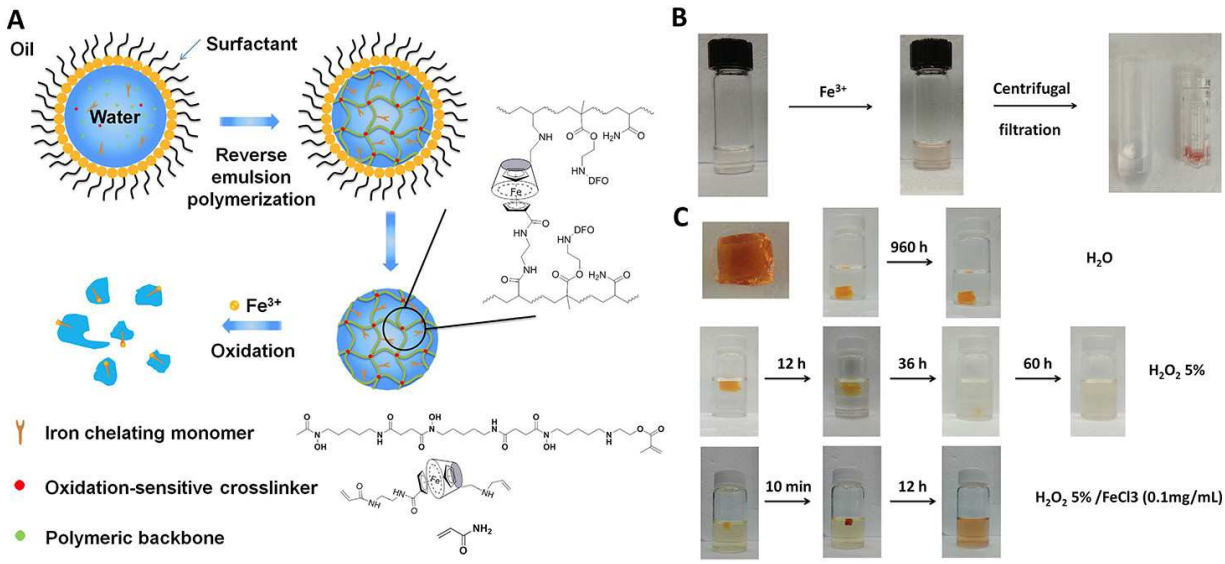

Figure 24. (A) Schematic fabrication of nanogels. (B) Photos of color change of nanogels after the addition of $FeCl_3$ (left) and centrifugal filtration result (right). (C) Oxidation-triggered degradable behavior of the bulk hydrogel. Reproduced with permission from Ref. [148]. Copyright 2016 Springer Nature.

Zhao et al.[149] reported the multi-responsive 2D and 3D supramolecular hydrogel legos in terms of the β-CD/Fc host-guest combination. Two host hydrogels (RH and NRH, Figure 25a) and one guest hydrogel (NRG, Figure 25A) were used in these systems. They were prepared by introduction of β-CD host or Fc guest units into the same polyacrylamide hydrogel network cross-linked by

N,*N*'-methylenebisacrylamide. Concretely, the RH hydrogel containing β-CD and carboxyl groups in the side chain was fabricated by radical copolymerization of β-CD-AAm, AAm, methylacrylicacid (MAA) and BIS with the aid of APS and TEMED in water. Another side-chain β-CD-containing host hydrogel NRH was prepared through a similar process in the absence of MAA. The guest hydrogel NRG, bearing pendant Fc units, was synthesized by copolymerization of Fc-modified acrylamide (Fc-AAm), AAm and BIS in DMSO, followed by dialysis treatment against deionized water. The NRH hydrogel was non-responsive, while the RH hydrogel was in response to both pH and ionic strength (IS) owing to the presence of carboxylic acid units. As expected, rapid and strong adhesion took place between these host and guest hydrogels because of the β-CD/Fc-based host-guest bonding effect. As shown in Figure 25B, RH and NRG hydrogels were manually jointed together to produce a two-layer lamina in which the β-CD/Fc host-guest combination acted as the cohesion force. Interestingly, while the pH value was adjusted from 7 to 2, the lamina bent toward the RH side due to the shrinking of the RH part. Nevertheless, when the IS was decreased from 100 to 5 mM, the lamina bent towards the NRG side owing to the expansion of the RH part. The original shape of the two-layer lamina was restored by adjusting the environmental pH or IS, and this hydrogel lamina showed excellent multi-cycle reversible bending behavior. Based on this unique reversible bending behavior, this laminate was successfully used to fabricate a smart device to detect the change of environmental pH and IS. By using the host-guest bonding force among these hydrogels and the pH- and IS-responsive properties of RH hydrogel, the authors further established a series of legos with complex geometric structures and investigated their responsive behaviors. As shown in Figure 25C, a "steering wheel" lego was constructed using a closed circular NRH (blue), three rod-shaped RH (red), and four small NRG portions (brown) as

linkage blocks, and the reversible variation amongst four different shapes was achieved by adjusting the swelling-deswelling behavior of the RH hydrogel circle at various environmental pH and IS. Figure 25D presents the jointing sequence of another two-dimensional (2D) hydrogel steeling wheel, by using a pH-sensitive RH circle, three NRH strips and four small NRG linkage blocks, and its reversible shape transformation to a 3D tower owing to the contracting of the RH hydrogel ring by changing the environmental pH from 7 to 2. The steering wheel of hydrogel lego was separated because of the dissociation of the host-guest complexes, as a result of the oxidation of the Fc groups in the NRG hydrogels by potassium persulfate. A new hydrogel ring lego was also reassembled using six freshly as-prepared NRG blocks and the disassembled NRH circle and RH arms, and a reversible shape change was regulated between this 2D ring and the corresponding 3D crown by controlling the environmental pH. The present host and guest hydrogels and supramolecular assembly strategies are anticipated to have great potential to be used to fabricate stimuli-responsive materials.

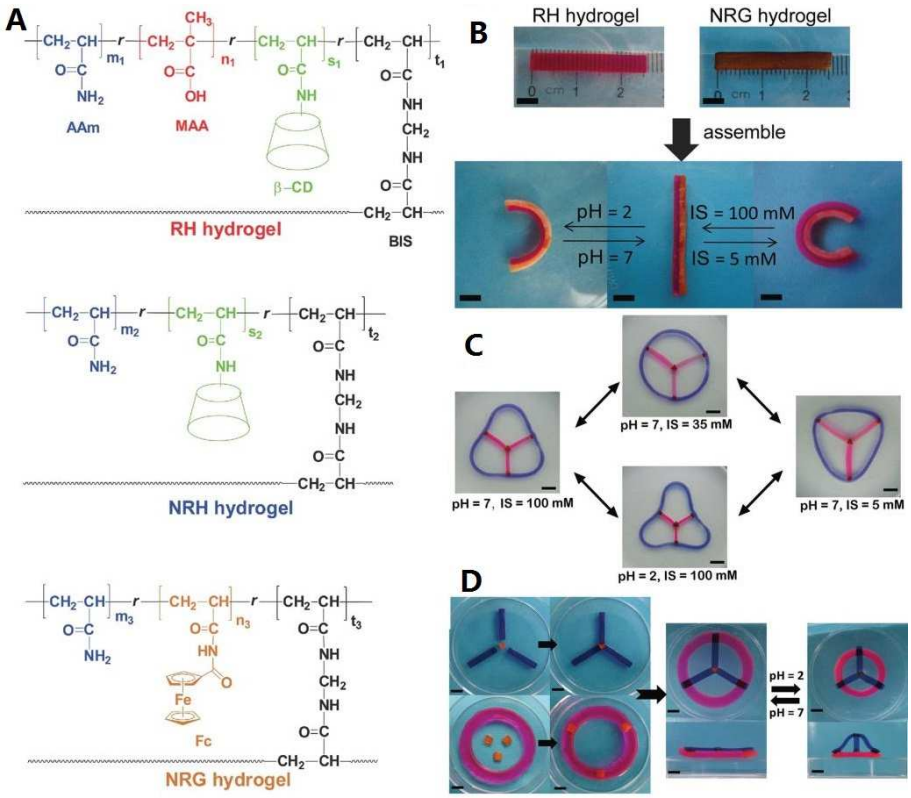

Figure 25. A) Molecular structures of three host and guest hydrogels. B) Responsive behavior of hydrogel lamina. C) Shape changes of hydrogel rings. d) Shape variation of the 2D- and 3D-hydrogel lego. Reproduced with permission from Ref. [149]. Copyright 2014 WILEY-VCH Verlag GmbH & Co. KGaA, Weinheim.

Wang and co-workers[156] described the redox- and temperature-sensitive behaviors of a new bi-gel belt fabricated using side-chain Fc-modified polyacrylamide hydrogel (PAM-Fc) as the guest hydrogel and poly(*N*-isopropylacrylamide) hydrogel grafted by pendant β-CD units (PNIPAAm-CD) as the host hydrogel. The PAM-Fc hydrogel was produced via the copolymerization of AAm, Fc-AAm and *N*,*N*'-methylenebis (acrylamide). The PNIPAAm-CD hydrogel was synthesized via copolymerization of NIPAAM, 6-acrylamido-β-CD (AAm-CD) and *N*, *N*'-methylenebisacrylamide with the aid of TEMED and APS. As shown in Figure 26A, the bi-gel belt was fabricated via the macroscopic host-guest β-CD/Fc-based hydrogel assembly of a PNIPAAm-CD gel strip and a

PAM-Fc gel strip. As expected, the resulting bi-gel belt exhibited a reversible bonding-separating transformation through changing the redox state of Fc moieties in PAM-Fc part. When the Fc groups were oxidized to Fc^+ cations by CAN, the bi-gel strip was separated to two free hydrogel strips. In contrast, after the treatment by GSH reductant, the two separated hydrogel parts were bonded together in order to rebuild the original bi-gel belt. The bi-gel belt exhibited a bending behavior with the enhancement of temperature (Figure 26B) because of the heat-induced dehydration of the PNIPAAm-CD part. Its bending speed and degree was regulated upon varying the outside temperature and the LCST of the PNIPAAm-CD part. Specifically, the high surrounding temperature induced a rapid bending speed accompanied by a largely curved angle, while LCST was tuned by changing the β-CD content in PNIPAAm-CD gel. Based on the reversible bending behavior, the bi-gel belt was further utilized to develop a temperature-sensitive on-off. As shown in Figure 26C, at low temperature (23 ^oC), the bi-gel belt showed straight shape, and the circuit was in the non-connected state; when the temperature was improved to 70 ^oC, the bending to the left was observed for the bi-gel belt, and the circuit was then in the connected state. In short, the present dual responsive integrated hydrogel should find various applications such as temperature-sensitive switches, sensor and remote controls.

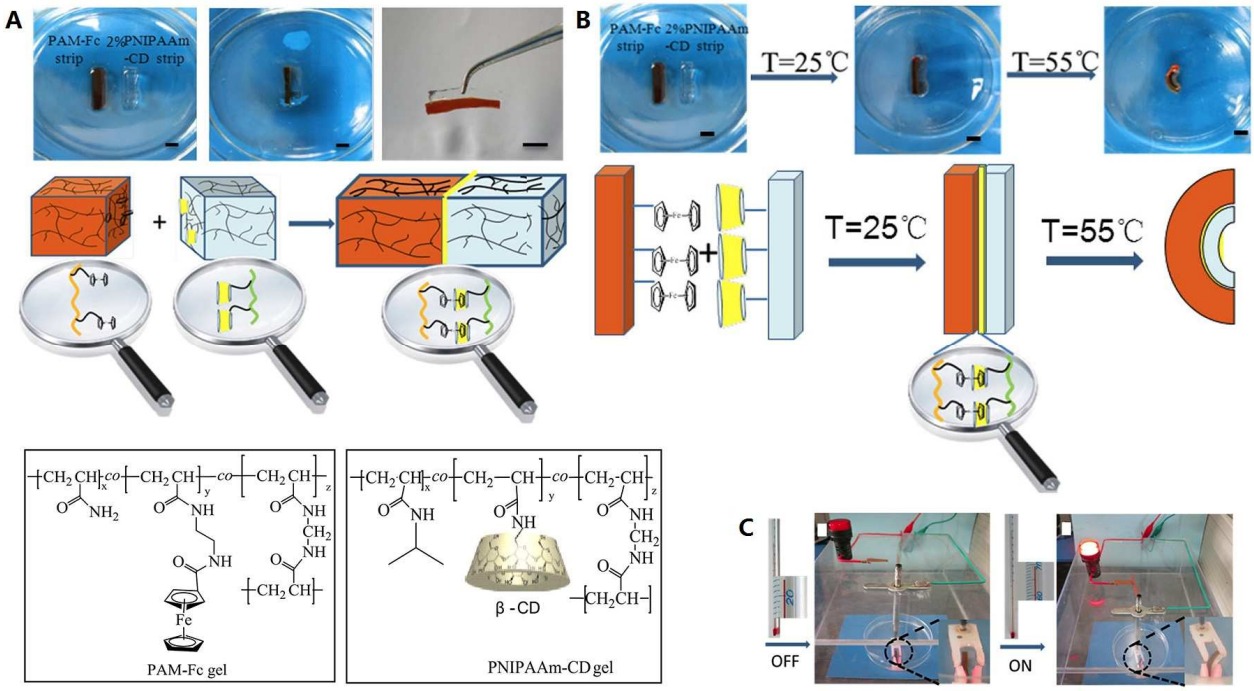

Figure 26. Macroscopic assembly between the host and guest hydrogels (a) and the bending behavior of the resulting bi-gel belt (b). Temperature-sensitive on-off fabricated using the bi-gel belt (c). Reproduced with permission from Ref. [156]. Copyright 2015 Springer Nature.

Recently, Tang et al.[157] synthesized deformable hydrogel composites based on a Janus bilayer MWCNTs/host-guest complex structure. As shown in Figure 27A and 27B, the host MWCNT-CD hydrogel was fabricated via direct copolymerization of the monomers AAm, BIS, CD-vinyl and MWCNTs-vinyl, and the guest MWCNT-Fc hydrogel was synthesized by a similar method, in which the Fc-vinyl monomer was used to replace CD-vinyl monomer. Swelling experiments demonstrated that the swelling ratio of MWCNT-CD hydrogel was twice as high as that of the MWCNT-Fc hydrogel. The two hydrogels were further combined to build the bilayer hydrogel actuator through the β-CD/Fc-based host-guest bonding force. The as-prepared bilayer hydrogel actuator MWCNT-CD-Fc was black (Figure 27C). After the hydrogel actuator was actuated in water, its deformation took place within 1 min. The actuator curved towards the MWCNT-Fc layer

because of the higher swelling ratio of MWCNT-CD hydrogel side. The resulting hydrogel actuator was characterized by the bending motion in aqueous solution. The present strategy provides a good example of how to prepare a high-performance hydrogel actuator that possesses potential applications in simulating behaviors of artificial muscles and humidity sensors.

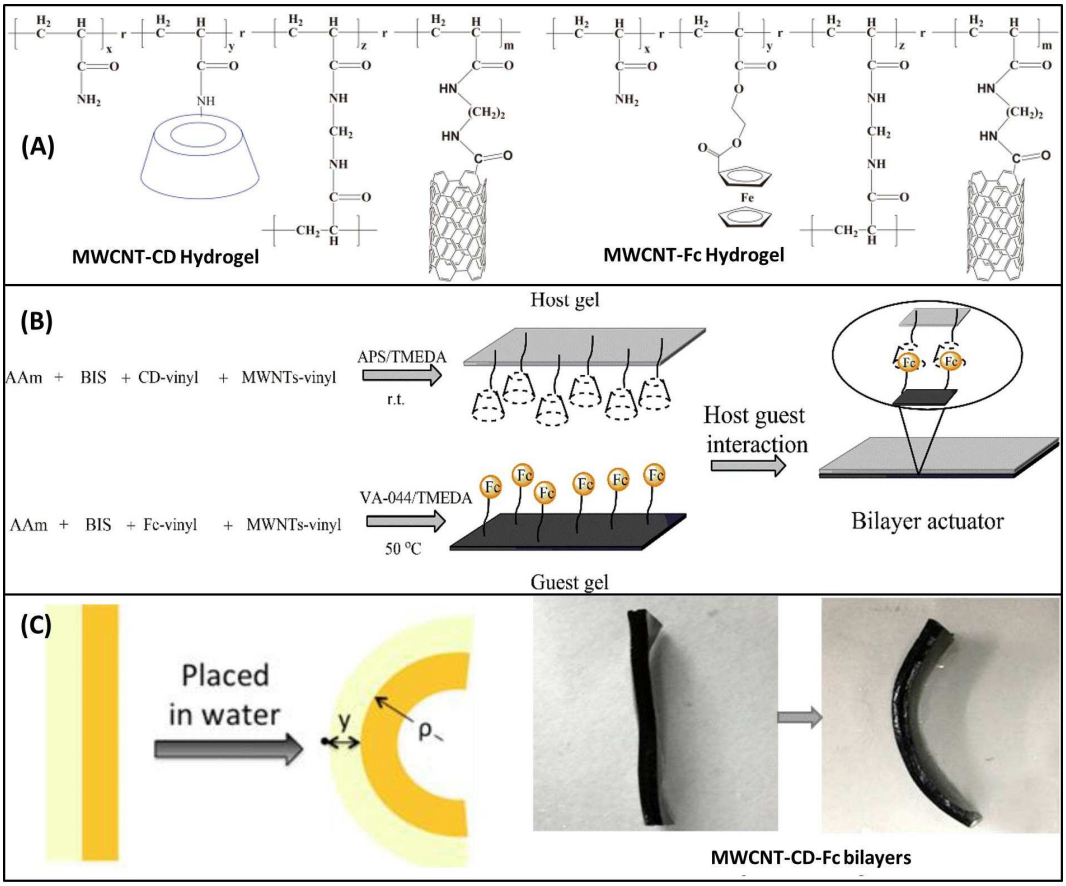

Figure 27. (A) Chemical compositions of MWCNT-CD and MWCNT-Fc hydrogels. (B) Diagrammatic fabrication of the bilayer hydrogel actuator. (C) Shape change of the MWCNT-CD-Fc bilayers. Reproduced with permission from Ref. [157]. Copyright 2019 Elsevier Ltd.

Jiang and co-workers[158] designed and prepared a new electrochemically responsive hydrogel. As shown in Figure 28, the supra-crosslink (Fc-SCL) was fabricated by mixing a β-CD-functionalized CdS quantum dot (CD@QD) and a Fc-modified monomer (2-acryloyloxyethyl

ferrocenecarboxylate, Fc-M) according to the β-CD/Fc-based host-guest combination. The copolymerization of the Fc-SCL and the *N*,*N*-dimethylacrylamide monomer led to the generation of the organic-inorganic hybrid hydrogel (Fc-Gel). The inclusion complex of β-CD/Fc was fully identified by thermogravimetric analysis (TGA), IR and CV measurements. The formation of Fc-Gel hydrogel was also proven by the results of dynamic rheology measurements, and this hydrogel still retained the fluorescent property of QDs. The β-CD/Fc host-guest bonding force was believed to act as an important role in the preparation of the hydrogel. Owing to the redox-responsive characteristic of this combination, it is anticipated that the mechanical and fluorescent performances of the supramolecular hybrid hydrogel might be regulated using electrochemical stimuli.

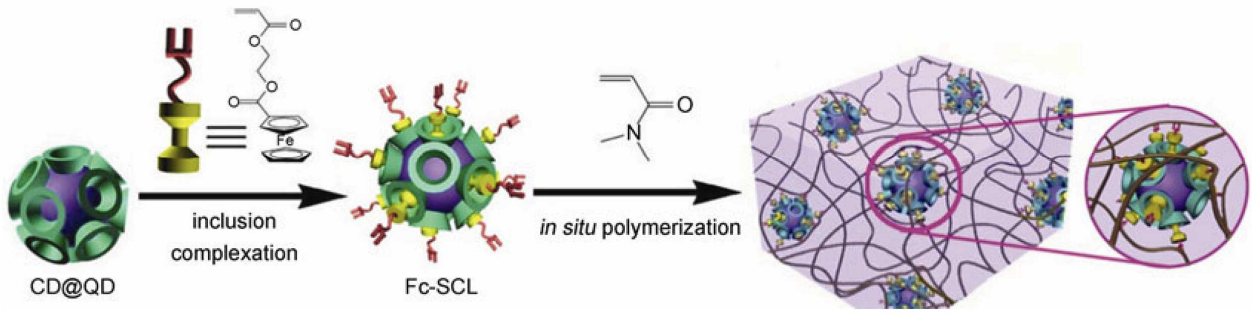

Figure 28. Diagrammatic preparation of Fc-SCL and Fc-Gel hydrogel. Reproduced with permission from Ref. [158]. Copyright 2012 Springer Nature.

Guo's group[159] reported the preparation of supramolecular hydrogels with dramatically stretchable, stab-resistant and adhesive properties according to a β-CD/Fc-based host-guest combination. The β-CD-containing linear polymer (polyβ-CD) was synthesized by the copolymerization of β-CD and epichlorohydrin under alkaline condition. The macromolecular

supramolecular cross-linker (MSCL, Figure 29A) was then prepared by mixing polyβ-CD and the polymerizable Fc monomer (A-TG-Fc, Figure 29A) modified by a hydrophilic and flexible spacer in water. As shown in Figure 29A, a transparent aqueous solution was obtained, confirming the generation of β-CD/Fc host-guest inclusion linkages. The supramolecular hydrogels were further fabricated by facile free-radical copolymerization of MSCL and acrylamide. The obtained hydrogels were well characterized by SEM, rheology and mechanical tests. These hydrogels exhibited excellent tensile property with the highest adhesive strength of 32 kPa (Figure 29B), and they could be stretched up to 30 times of their initial length without rupture. The hydrogel was also pierced using sharp tips of scissors (or pencil) without breaking, confirming its excellent puncture resistance property (Figure 29C). Also, these hydrogels showed a strong adhesion ability to the surfaces of hydrophilic glass and hydrophobic porcine skin (Figure 29D). The author believed that these distinguished properties should be attributed to the use of polyβ-CD and the incorporation of a flexible linker to the Fc monomer. The former led to a local high content of host-guest inclusion complex in the hydrogel network, while the latter provided its flexible sliding ability. Thus, under outside forces, the present supramolecular hydrogel not only dissipated external forces through the dissociation of the β-CD/Fc inclusion complex, but also maintained its network integrity through the rapid re-complexation between the host and guest groups after dissociation. This work provides a new design strategy for the preparation of supramolecular soft materials by using the β-CD/Fc-based host-guest combination.

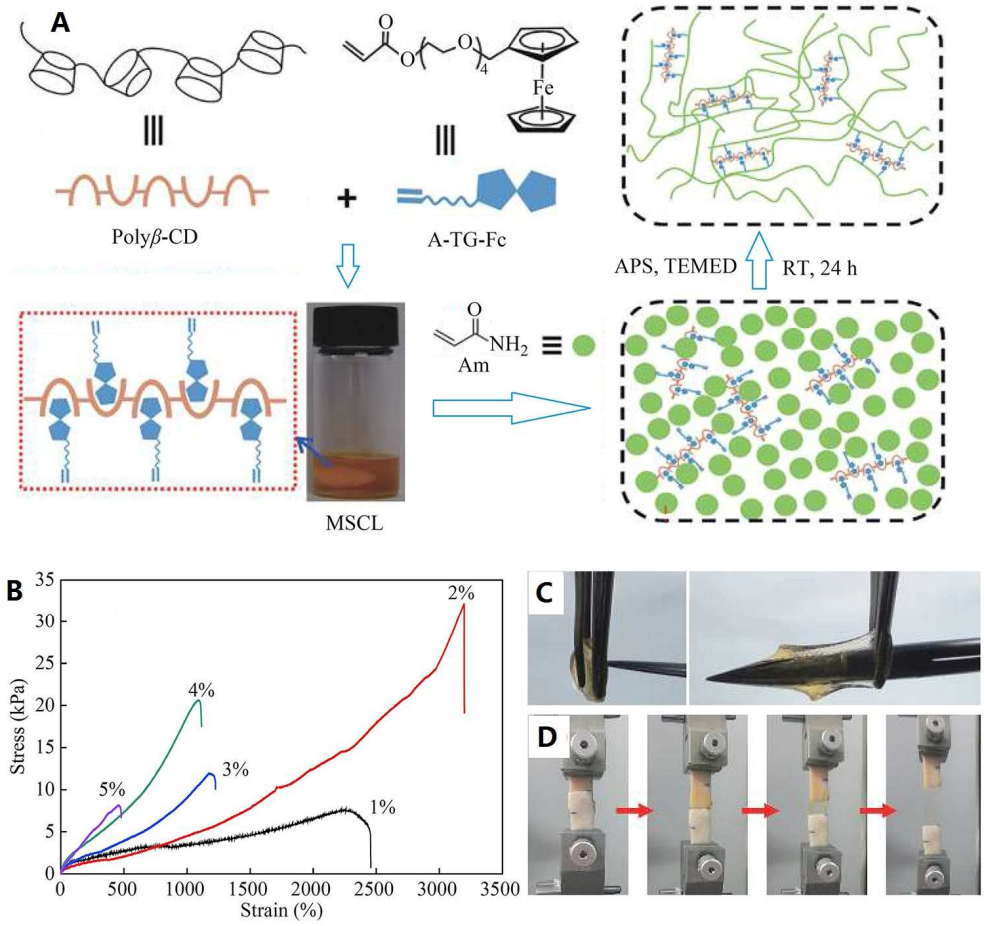

Figure 29. (A) Schematic fabrication of MSCL and the corresponding supramolecular hydrogel. (B) Tensile testing curves of the hydrogels with different concentrations of MSCL. (C) Pictures exhibiting the stab resistance of the hydrogel. (D) Pictures of the stretching process of the hydrogel adhered between two pieces of porcine skin. Reproduced with permission from Ref. [159]. Copyright 2018 China Academic Journal Electronic Publishing House.

Jiang et al.[160] reported the design and fabrication of multi-responsive supramolecular hydrogels by using β-CD-functionalized CdS quantum dots (CD@QD) and diblock copolymer poly(*N*,*N*'-dimethylacrylamide)-*b*-poly(*N*-isopropylacrylamide) with a Fc-modified terminal [Fc-p(DMA-*b*-NIPAM), Figure 30] as building blocks. The reversible addition fragmentation chain-transfer (RAFT) polymerization method was used to produce the targeted Fc-p(DMA-*b*-NIPAM). For this

goal, a novel Fc-functionalized RAFT agent (Fc-CTA) was synthesized and used for the polymerization of DMA, and the resulting homopolymer Fc-pDMA was then utilized as macromolecular initiator for the RAFT polymerization of NIPAM to provide the final diblock copolymer Fc-p(DMA-*b*-NIPAM). Owing to the β-CD/Fc host-guest combination, mixing Fc-p(DMA-*b*-NIPAM) and CD@QD in water led to the generation of a multi-arm architecture, namely Fc-HIC, with a QD core and a lot of block copolymer arms. As shown in Figure 30, when the environment temperature is improved to more than the LCST of pNIPAM, the aggregation of pNIPAM block results in the formation of microdomains that act as another cross-link factor, and thus, as expected the transformation of liquid Fc-HIC into solid hydrogel was observed. This sol-gel change was confirmed by the results of steady and dynamic rheology tests, and the gelation point was determined to be 40.5 ºC. The sol-gel transition of Fc-HIC hydrogel was tuned via changing the environmental temperature and the redox state of Fc groups. The addition of a competitive host or guest also led to the separation of the β-CD/Fc inclusion complexes and thus induced the gel-sol transition.

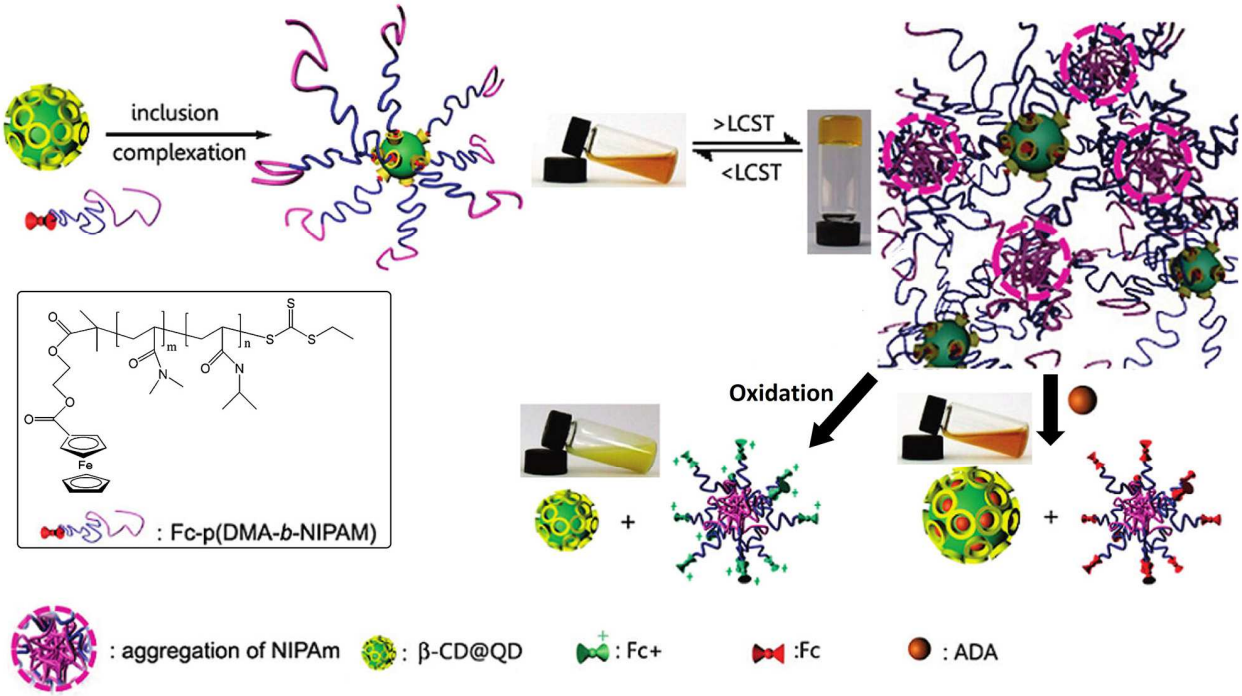

Figure 30. Diagrammatic formation and disassembly of Fc-HIC hydrogel. Reproduced with permission from Ref. [160]. Copyright 2011 American Chemical Society.

3.1.2. Poly-(β-CD)/Dual-(Fc) hydrogels

Li et al. [161] developed a novel bio-safe supramolecular hydrogel consisting of β-CD-modified alginate (Alg-β-CD) and Fc-terminated pluronic F127 (F127-Fc) and investigated its gel–sol transition characteristic under various outside stimuli including temperature, oxidants and glucose. The Alg-β-CD was produced by the amido link condensation reaction between mono-6-deoxy-6-ethylenediamine-β-CD (6-CD-EDA) and sodium alginate with the aid of EDC and *N*-hydroxysuccinimide (NHS), and the degree of substitution (DS) was calculated to be 12.4%. The F127-Fc was fabricated via the esterification reaction between Pluronic F127 and carboxyferrocene with the help of DCC and DMAP, and the final DS was determined to be 24.3%. The targeted hydrogel was fabricated through the mixture of Alg-β-CD with F127-Fc in the PBS aqueous solution with pH 7.4. The authors believed that the crosslinking forces in this hydrogel network

were the β-CD/Fc host-guest combination and the temperature-dependent hydrophobic interaction among poly(propylene oxide)(PPO) parts. At high temperature (e.g. 37 ºC), the PPO parts of F127-Fc were water-insoluble, which led to the generation of micelles (Figure 31). The formed F127-Fc micelles were then combined by β-CD/Fc inclusion to provide the sol-to-gel transformation of the supramolecular hydrogel. The PPO parts of F127-Fc became water-soluble at low temperature (e.g. 4 ºC), which caused the gel-to-sol transition. As expected, oxidizing Fc to Fc^+ by sodium hypochlorite (NaOCl) achieved the gel-to-sol transformation of the supramolecular hydrogel. The authors further fabricated the GOD-entrapped supramolecular hydrogel, and the introduction of glucose also triggerred the gel-to-sol transformation. This is because the oxidation of glucose by GOD produced hydrogen peroxide that further oxidized Fc to Fc^+, and thus led to the disassembly of β-CD/Fc bonding sites. The good biocompatibility of the present supramolecular hydrogel was proven based on the results of the agar diffusion test.

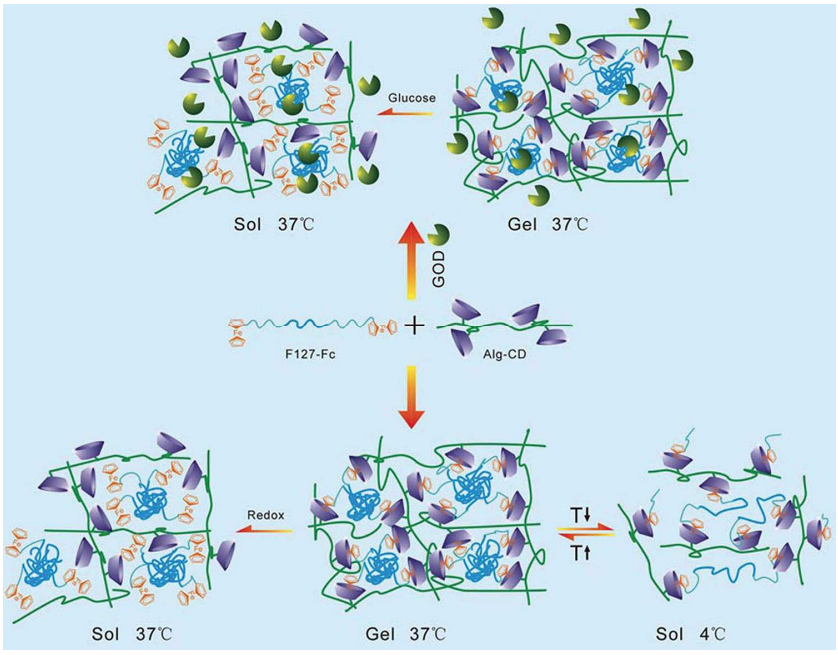

Figure 31. Sketch map of the sol–gel transformation of Alg-β-CD/F127-Fc hydrogel. Reproduced

with permission from Ref. [161]. Copyright 2012 Royal Society of Chemistry.

Zhou et al.[162] reported the stimuli-triggered gel-sol transformation of supramolecular hydrogels fabricated using two building blocks, namely linear β-CD-containing polymer and pluronic F127 with two ferrocene terminals (Figure 32). The host polymer P(EPI-β-CD) was prepared in alkali condition by the reaction of β-CD and epichlorohydrin, while the macromolecular cross-linker Fc-F127-Fc was synthesized by the esterification modification of pluronic F127 by ferrocenecarboxylic acid containing a middle block of PPO and two polyethylene oxide (PEO) blocks. The corresponding supramolecular hydrogel was fabricated using the mixed aqueous solution of the above host polymer and cross-linker. Several stimuli such as temperature, oxidizing agent and glucose triggerred the gel–sol phase transition of the obtained hydrogel. This characteristic was explained by the presence of two reversible dynamic cross-linkages in the hydrogel network, namely the heat-sensitive hydrophobic interaction among PPO parts and the β-CD/Fc host-guest bonding. Concretely, by changing the temperature between 4 ^{o}C and 37 ^{o}C, the convertible sol-gel transformation was observed. After the treatment with H_2O_2, the gel-sol transformation also occurred because of the destruction of the β-CD/Fc inclusion complexes. The GOD was further immobilized into the hydrogel matrix leading to a glucose-sensitive hydrogel. GOD oxidizes glucose to produce the oxidant H_2O_2, thus the gel-sol transition phenomenon was also observed in the presence of glucose. Considering the good biocompatibility of its two building blocks, this supramolecular hydrogel was anticipated to show great potential in medical applications.

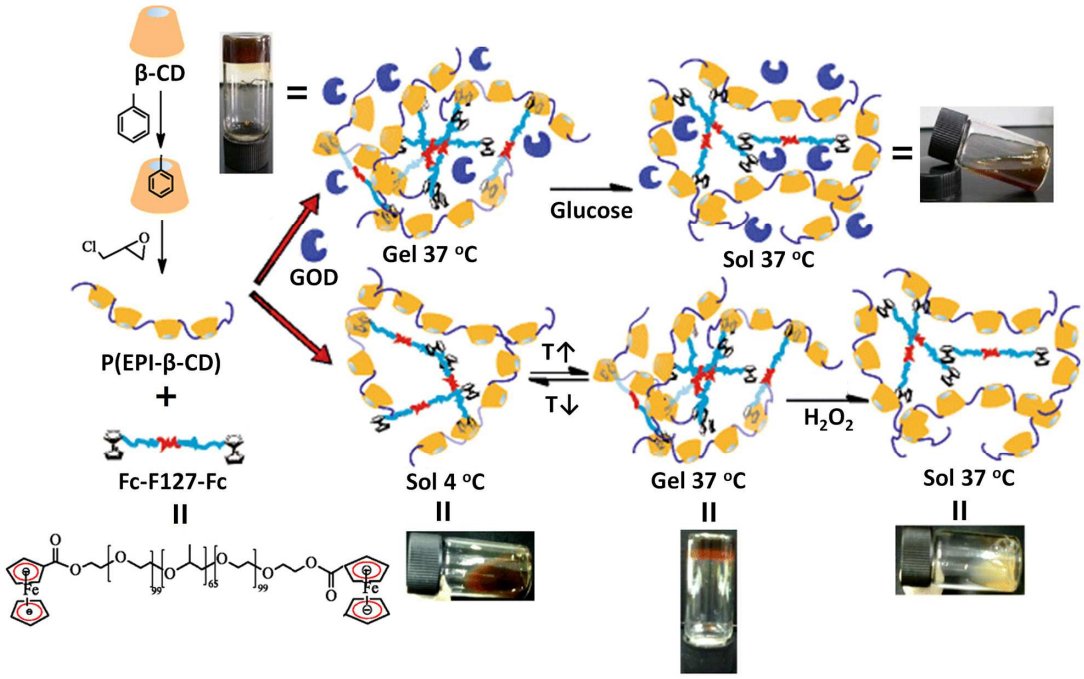

Figure 32. Sol–gel transformation of the P(EPI-β-CD)/Fc-F127-Fc supramolecular hydrogel. Reproduced with permission from Ref. [162]. Copyright 2014 Springer Nature.

3.1.3. Poly-(β-CD)/Mono-(Fc) hydrogels

Wang et al.[163] prepared a water-soluble supramolecular copolymer CDCS-FcPEG using β-CD-modified chitosan and Fc-terminated PEG as building blocks, and they investigated its gelation behavior induced through the generation of crystalline inclusion complex of α-CD and PEG (Figure 33). Based on the results of XRD, the authors believed that the formation of the supramolecular hydrogel CDCS-FcPEG/α-CD was due to the physical crosslinking between the pipe-like crystalline structures produced by the ring-wearing complexation of α-CD to PEG chain segments.

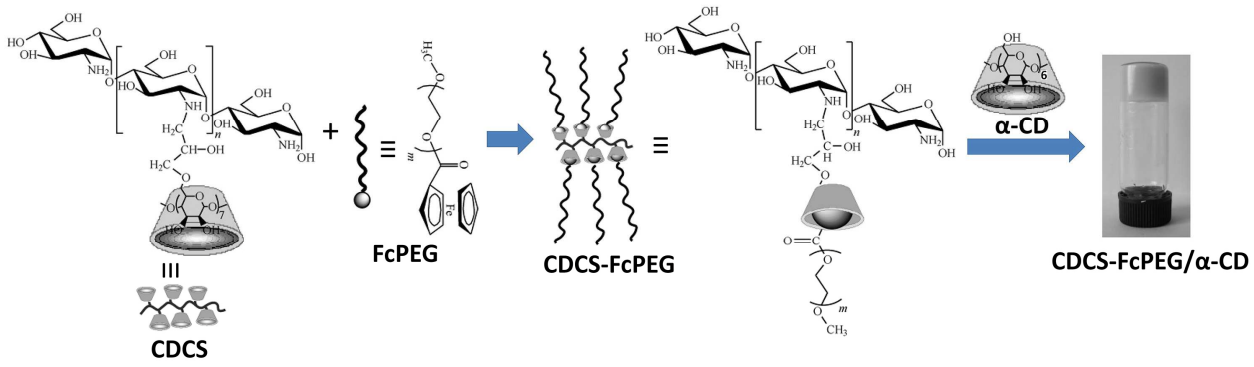

Figure 33. Formation of the CDCS-FcPEG/α-CD hydrogel. Reproduced with permission from Ref. [163]. Copyright 2012 China Academic Journal Electronic Publishing House.

3.1.4. Mono-(β-CD)/Dual-(Fc) hydrogels

Fang et al.[164] prepared a new multiple responsive supramolecular hydrogel (Figure 34) utilizing the β-CD/Fc-based host-guest bonding force between 6-deoxy-6-amino-β-cyclodextrin (β-CDNH$_2$) and *N*,*N*′-bis(ferrocenyl-methylene) diaminobutane (FBI) in aqueous phase. The gel-sol transformation was observed upon heating, and on the contrary, cooling resulted in the renewal of the β-CDNH$_2$/FBI hydrogel. Similarly, the addition of HCl gas led to the transformation from gel state to sol solution, and the sol-to-gel conversion was successfully accomplished by adding NH_3 gas. These results indicated that the protonation and deprotonation of the amino group in β-CDNH$_2$ tuned the generation and disassembly of the hydrogel. As expected, the addition of the oxidant [$Ce(NH_4)_2(NO_3)_6$] also led to the gel-to-sol transformation, which was attributed to the oxidation of Fc units to Fc^+ cations and the subsequent decomposition of the β-CD/Fc inclusion compounds. SEM images (Figure 34) revealed that the network structure of the hydrogel was characterized by belt-like fibers that further interwoven into 3D networks. According to the results of ^{1}H NMR, FT-IR, CV and XRD, the authors believed that the driving forces for the hydrogel generation originated from the β-CD/Fc host-guest bonding force between FBI and β-CDNH$_2$ and the intermolecular H-

bonding among the β-CDNH$_2$ molecules. Figure 34 provides the proposed formation process. FBI first interacts with β-CDNH$_2$ to generate the inclusion complexes of FBI/β-CDNH$_2$, then their aggregation led to the formation of dimers, trimers, and even "oligomers" through H-bonding interaction. Subsequently, these "oligomers" further reassemble into "polymers", belt-like fibers and even interweaving network of the hydrogel.

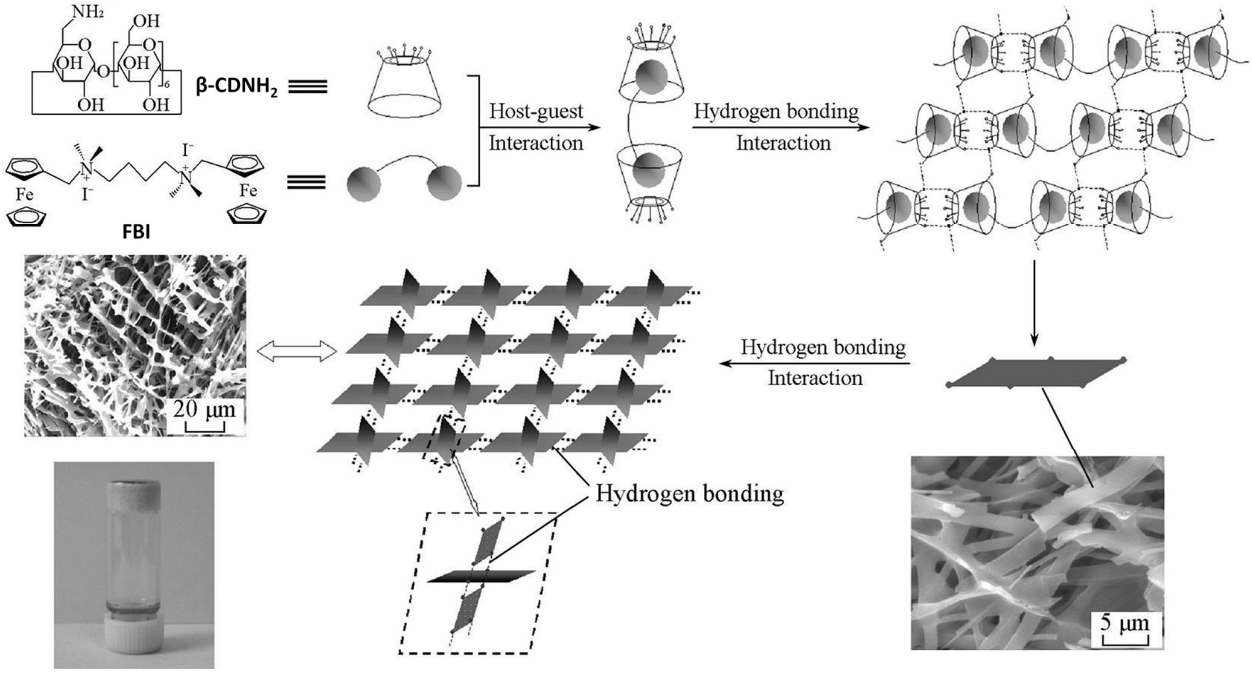

Figure 34. Formation of the β-CDNH$_2$/FBI hydrogel. Reproduced with permission from Ref. [164]. Copyright 2008 China Academic Journal Electronic Publishing House.

3.1.5. Mono-(β-CD)/Mono-(Fc) hydrogels

Wang et al.[165] described supramolecular hydrogels that were formed upon dual host–guest bonding between α-CD and Fc-functionalized PEG (FcPEG-2000) (Figure 35). PEG with low molecule weight (M_n = 2000, PEG-2000) was first modified using Fc as mono-end group. The resulting FcPEG-2000 further self-assembled in the presence of α-CD to generate supramolecular

hydrogel even at low concentration ($C_{FcPEG\text{-}2000}$ = 17 mg ml^{-1}), which was due to the double host–guest combination. Interestingly, the oxidation of Fc units to Fc^+ groups or the addition of β-CD did not cause the disassembly of the hydrogel. On the one hand, the resulting Fc^+ terminal would be conducive to lock more α-CD molecules, resulting in more channel-type crystalline regions as physical cross-linking sites. On the other hand, the synergy effect of the intermolecular inclusion of β-CD/Fc and the intermolecular inclusion of α-CD/PEG chains was helpful for the gelatinization action. In addition, the present supramolecular hydrogel possessed the desirable shear-thinning performance.

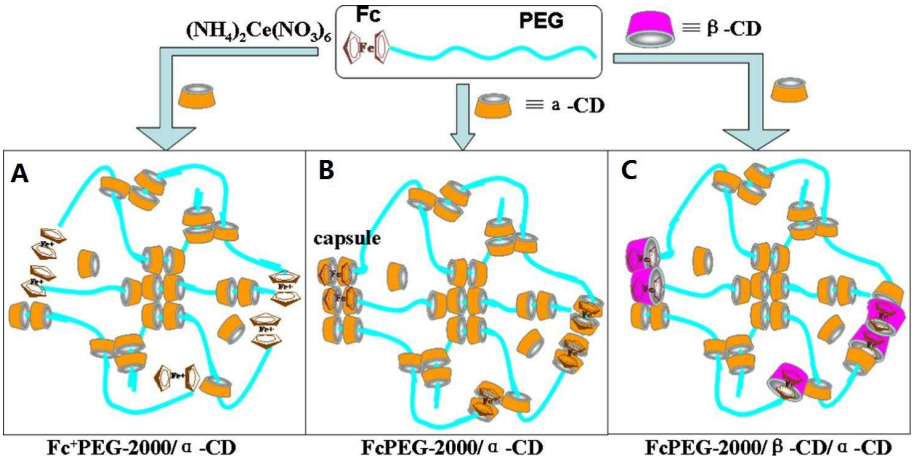

Figure 35. Schematic diagrams of supramolecular hydrogels formed by FcPEG-2000 and α-CD. Reproduced with permission from Ref. [165]. Copyright 2013 Elsevier Ltd.

Osakada et al.[166] synthesized two Fc-containing amphiphilic compounds [py-N-$(CH_2)_nOCH_2Fc$]Cl (Fc-py-a, n = 8; Fc-py-b, n = 10, py = C_5H_5N) that formed micelles and hydrogels (Figure 36). The resulting micelles and hydrogel showed invertible self-assembly-disassembly behavior under outside redox stimuli. Fc-py-a and Fc-py-b encapsulated the dye molecules (e.g. Nile red and pyrene) dispersed in water. Figure 36 shows the variation in the

aggregation process of Fc-py-a and Fc-py-b. Amphiphilic Fc-py-a first formed spherical micelles, which suffered from the sphere-to-rod transition at higher concentration due to the electrostatic repulsive force among the resulting spherical micellar surfaces. After adding NaOCl oxidant and α-CD, the micelles were broken, because the Fc^+ groups and the pseudorotaxane of α-CD were not helpful for the formation of stable micelles. The bigger Fc-py-b suffered from a similar experience, whereas its pseudorotaxane with α-CD led to the formation of a bulky hydrogel. After oxidizing the Fc groups to Fc^+ units, the hydrogel changed into a sol solution, too. Similarly, the solid hydrogel re-formed after addition of GSH as reductant. The sensitive and smart transformations of micelles and hydrogel were expected to be applicable in new stimuli-responsive systems.

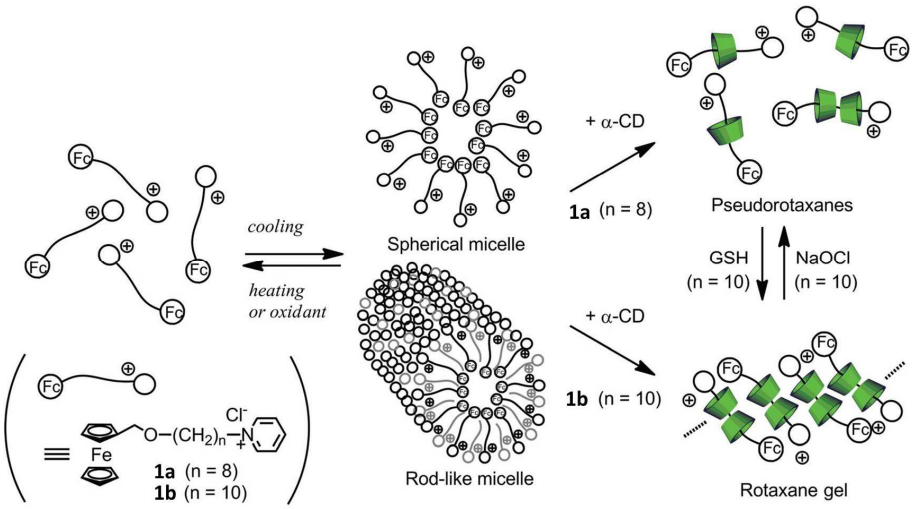

Figure 36. The aggregation and competing supramolecular assembly of Fc-py-a and Fc-py-b. Reproduced with permission from Ref. [166]. Copyright 2013 Royal Society of Chemistry.

3.2. PA/Fc hydrogels

PAs, a new class of macrocyclic host molecules, have been developed rapidly in supramolecular chemistry, material science, and medical applications because of their unique characteristics

including easy synthesis, available chemical modifiability, rigid electron-rich architecture and tunable cavity size[167-173]. PAs are able to identify appropriate cations and bind some neutral molecules. Especially, the formation of supramolecular inclusion complexes was achieved using PAs and Fc (1:1, mole/mole) units according to hydrophobic interaction, the corresponding binding constant being 1.27×10^5 M^{-1}[174-176]. At present, there are reports concerning PA/Fc-based host-guest supramolecular hydrogels. A few remarkable illustrations will be discussed in this section.

Recently, Ni and coworkers[75] reported a smart supramolecular hydrogel with multi-stimuli responsiveness whose expanding ratio were immensely improved by formation of pillar[6]arene (WP6)/Fc-based host-guest complexes. Concretely, a Fc-containing polymer hydrogel network G1c (Figure 37A) was fabricated via radical copolymerization reaction of Fc-modified acrylate, acrylamide and *N*,*N*'-methylenebisacrylamide. The resulting G1c hydrogel cross-linked by covalent bonds was then treated using a WP6 aqueous solution to give the supramolecular hydrogel G1c·WP6 (Figure 37A). Compared with the sample (G1c) treated with pure water, there is an around 11-fold weight enhancement for the formed G1c·WP6. This is explained by the generation of highly hydrophilic WP6/Fc inclusions in the network of hydrogel and the strong electrostatic repulsive force among the formed pendant inclusion complexes with negatively charged COO^- groups on the surfaces. The two hydrogels of G1c and G1c·WP6 were investigated and compared for their responsiveness to outside environmental factors such as pH, redox, competitive compounds and temperature. As shown in Figure 37B, the addition of HCl, namely the acidification treatment, resulted in the violent shrinking of G1c·WP6 in diameter, while this diameter was recovered after the alkalinization treatment using NaOH. This reversible change is explained by the protonation and deprotonation of WP6 ring that causes decomposition and formation of the

host–guest assembly between WP6 and Fc. Unlike G1c·WP6, the pH-responsive behavior of G1c (Figure 37C) should account for by degradation or oxidation of some Fc units in the presence of O_2 under acidic condition, and thus the following addition of NaOH scarcely arouses any diameter variation. Moreover, the oxidation of Fc to Fc^+ transformed the network of G1c·WP6 into a pseudo zwitterionic structure, thus leading to the contracting of G1c·WP6 (Figure 37D). On the contrary, the addition of oxidant gave rise to the swelling behavior of G1c (Figure 37E) because of the enhanced Fc^+ hydrophilicity. The encapsulation of DOX·HCl was further accomplished by steeping the dried G1c·WP6 in the DOX·HCl solution. As shown in Figure 37A, the controlled release of DOX·HCl was observed in an acidic environment, indicating that the supramolecular hydrogel might be potentially applicable as controlled drug delivery carrier. Furthermore, the authors anticipated that this smart hydrogel would find hopeful applications in the fields of extractants, artificial muscles and actuators.

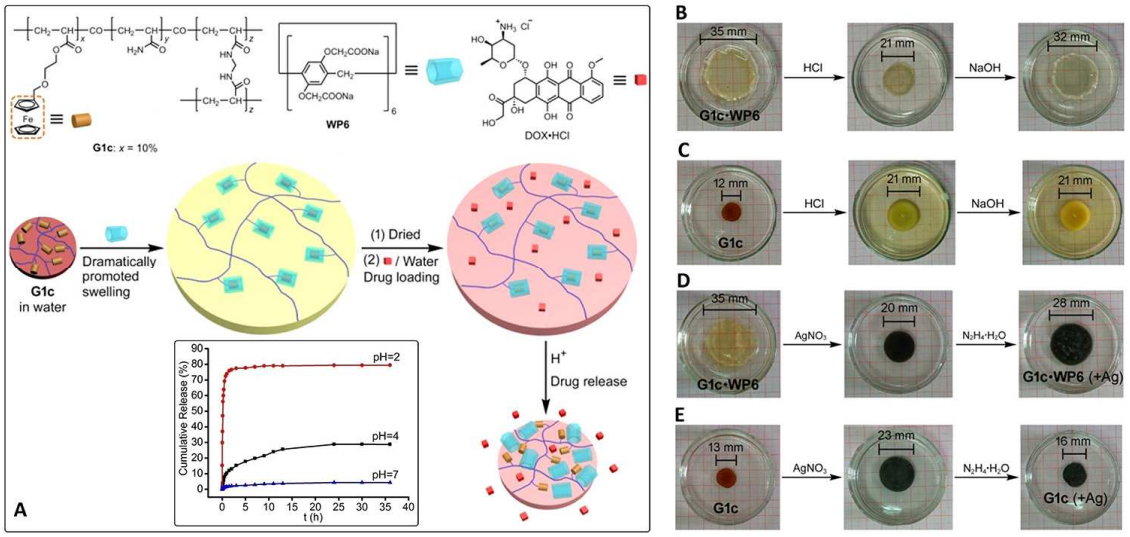

Figure 37. (A) Schematic formation of well-expanding G1c·WP6 hydrogel and the pH-controlled drug release. (B, C) pH-sensibility of G1c·WP6 and G1c hydrogels. (D, E) Redox-sensibility of G1c·WP6 and G1c hydrogels. Reproduced with permission from Ref. [75]. Copyright 2016

American Chemical Society.

Wang et al.[177] reported a new strategy to fabricate warm/cool-tone switchable thermochromic hydrogel Fc-gel·EGP6 as a multifunctional smart window through the orthogonal incorporation of the characteristic performance of pillar[6]arene/Fc-based host–guest inclusion. First, the Fc-containing gel (Fc-gel) was fabricated via copolymerization of acrylamide, Fc-functionalized acrylamide (FcAm) and MBAAm with the aid of AIBN. Then, the obtained dry Fc-gel was treated in an aqueous solution of the ethylene glycol chain-functionalized pillar[6]arene (EGP6) to give the supramolecular Fc-gel·EGP6 hydrogel (Figure 38). The internal morphology of the resulting hydrogel was confirmed to be highly homogeneous and porous because of the generation of the hydrophilic EGP6/Fc-based host-guest inclusion combination. Interestingly, EGP6 showed a unique thermo-responsiveness with transformation between transparency at 25 ^{o}C and opaqueness at 40 ^{o}C, while the Fc units exhibited a reversible orange-green conversion under different redox atmosphere. EGP6 and Fc units conducted their own function not only in a non-interference way but also in a mutual promotion way. Accordingly, the transmittance and color of the Fc-gel·EGP6 hydrogel were reversibly modulated by changing the environmental temperature and redox conditions (Figure 38). Based on these fascinating properties, the present Fc-gel·EGP6 hydrogel was expected to be usable as a new functional material for the preparation of warm/cool tone-adjustable smart windows.

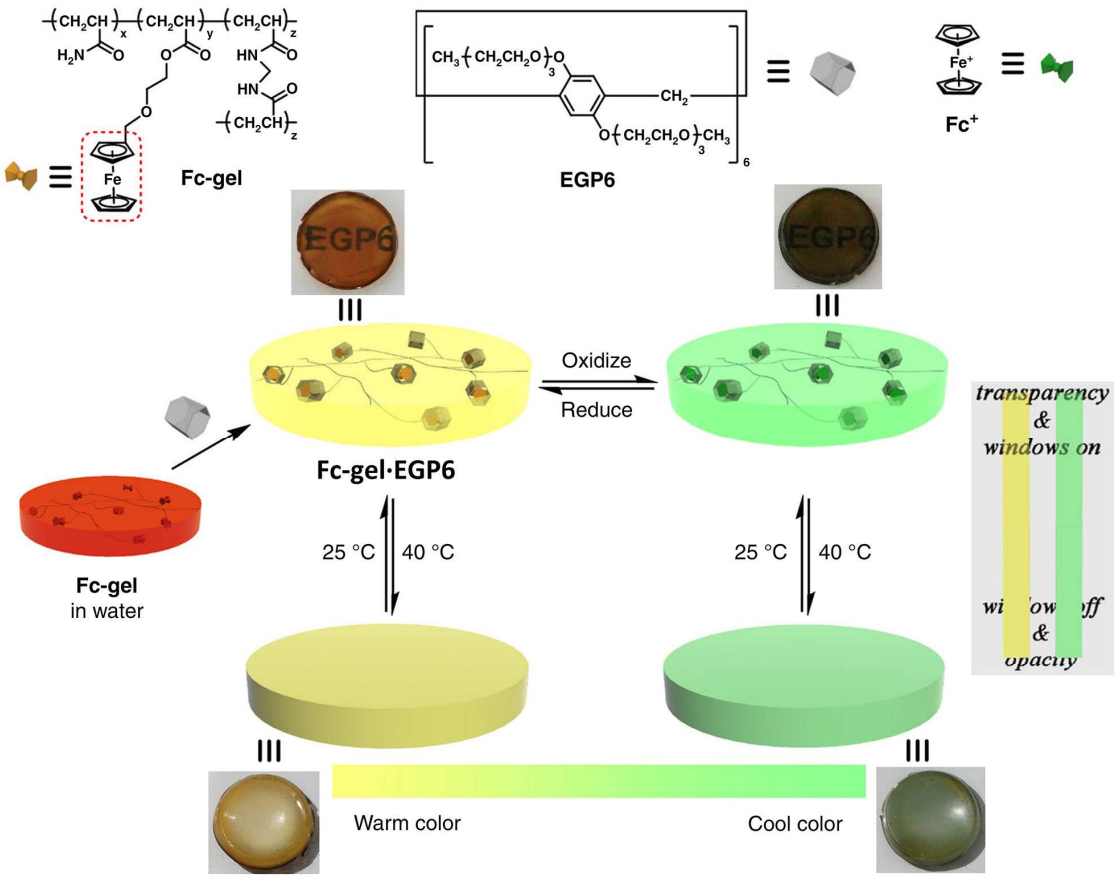

Figure 38. (A) Fabrication of supramolecular Fc-gel·EGP6 hydrogel as multifunctional smart windows. Reproduced with permission from Ref. [177]. Copyright 2018 Springer Nature.

3.3. Supramolecular hydrogels upon self-assembly of Fc-containing peptides

Fc-modified peptides are a class of fascinating molecules that might be used to prepare highly ordered materials because of their characteristic molecular configuration, high hydrophobicity and redox performance of the Fc groups[178-182]. Fc-modified peptide conjugates gelate with the help of environmental stimuli, and the Fc moiety is able to serve as a structural scaffold to stabilize peptide secondary structural motifs[183-192]. In addition, Fc-containing peptide hydrogels with potential biocompatibility are potentially usable as promising biosensors due to their facile

preparation process and sensitive redox functionality.

Zhang and coworkers[193] presented a new method to prepare supramolecular hydrogels with multi-stimuli responsive behaviors by using ferrocenoyl phenylalanine (Fc-F, Figure 39A) as a hydrogelator. The critical gelation concentration of Fc-F was determined to be 2–3 $mg \cdot mL^{-1}$ in water. As shown in Figures 39B-39D, AFM, SEM and TEM images indicated that the resulting hydrogels possessed ordered fibrils with a width in the range of 30–80 nm and a length of over 1 mm. The Fc-F hydrogel was very stable and kept without change for at least nine months when the environmental pH was maintained to about 7.0. According to the results of DFT computation and the various structural studies, the authors proposed that the supramolecular hydrogel showed a stepwise hierarchical assembly to form ordered fibrils (Figure 39E). The driving forces include π–π stacking, H-bonds and hydrophobic interactions. Reversible and rapid gel–sol transitions were observed when the environmental conditions, such as pH, temperature, redox potential and agitating treament, were changed (Figure 39F). Interestingly, the Fc-F hydrogel can be used as an electron-transfer matrix for the immobilization of enzyme (e.g. GOD, Figure 39G), in which the hydrogel not only offers an aqueous microenvironment to immobilize enzyme but also could be used as an electron-transfer adjuster for the electron transfer of enzyme using the easy electron transfer from the Fc units. The resulting hydrogel was also applied as a drug delivery carrier (Figure 39H). Owing to the enantiomeric feature of phenylalanine parts, the Fc-F hydrogel presents chirality, and thus is anticipated to find potential applications in supporting the asymmetric synthesis catalysts and chiral separation. In addition, the Fc-F hydrogel was found to show excellent resistance towards salt stress, and the formation of this hydrogel is not affected by the existence of highly concentrated NaCl, phosphate and transition-metal compounds. Moreover, the

authors further used the Fc-F hydrogel as electrochemical immune-sensor that have the ability to detect human IgG and tumor necrosis factor α, as well as a cancer biomarker prostate specific antigen[194-197]. In a word, Fc-F is anticipated to act as a Superduper template used to fabricate new, multi-responsive hydrogelators in the future. The Fc-F hydrogels thus present significant meanings to develop biosensors for clinical uses.

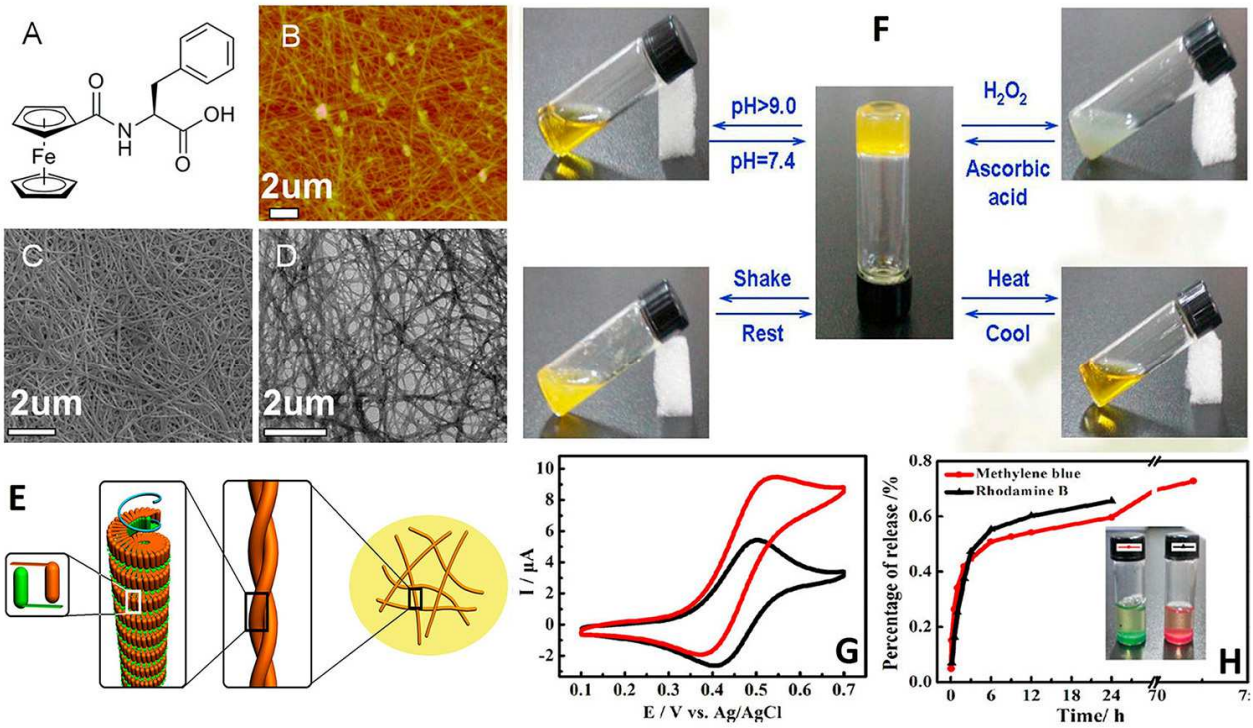

Figure 39. (A) Molecular constitution of the hydrogelator Fc-F. (B-D) AFM, SEM, and TEM pictures of Fc-F hydrogels. (E) Schematic diagram of the proposed formation mechanism of Fc-F hydrogel. (F) Convertible gel–sol transformation of Fc-F hydrogels. (G) CV profiles of the GOD/Fc-F hydrogels (red: PBS of pH 7.4, black: without glucose). (H) Drug release profiles of Fc-F hydrogels. Reproduced with permission from Ref. [193]. Copyright 2013 American Chemical Society.

Qi et al.[198] reported the use of Fc–diphenylalanine (Fc–FF) and Fc-modified tripeptides (Fc-FFH, Fc-FFD, Fc-FFF, and Fc-FFS) to form self-supporting hydrogels. Fc–FF showed a morphological transformation from moderately stable nanospheres to well-defined nanofibers via application of an external mechanical force (i.e. shaking), and this change further resulted in the generation of the self-supporting hydrogel, as shown in Figure 40A. In addition, TEM and SEM results confirmed the sol-to-gel transition, in which the micromorphology of Fc-FF assemblies changed from nanoscale spheres to nanofibers. The self-assembly process involving Fc-FF was effectively regulated by converting the redox state of the Fc units. The authors also found that Fc-modified tripeptides arranged into a particular configuration and aggregated into thin shells for the stabilization of the nanoemulsion droplets (Figure 40B) [199]. The resulting nanoemulsions remained stable at 25 °C for more than four months. Interestingly, the enthalpy-triggered phase transformation from nanoemulsions to hydrogels was observed by lowering the temperature when using Fc-FFH as an emulsifying agent, but the other three Fc-modified tripeptides nanoemulsions remained stable. According to the results of thermostability studies, the Fc-FFH nanoemulsion transformed into solid hydrogel when the environmental temperature was below 25 °C. TEM analysis indicated that the Fc-FFH hydrogel was composed of 3D interlaced nanofibers, and the Fc-FFH nanoemulsion kept its emulsification state above 25 °C. Along with the increase of temperature, the nanoemulsion showed the improved diameter and shell thickness. The Fc-tripeptide nanoemulsion was oxidized to form smaller micellar assemblies under electrochemical treatment. The functional bio-organometallic nanoemulsion and hydrogel with tailored structure were believed to have great potential in medicine, food and cosmetic industries.

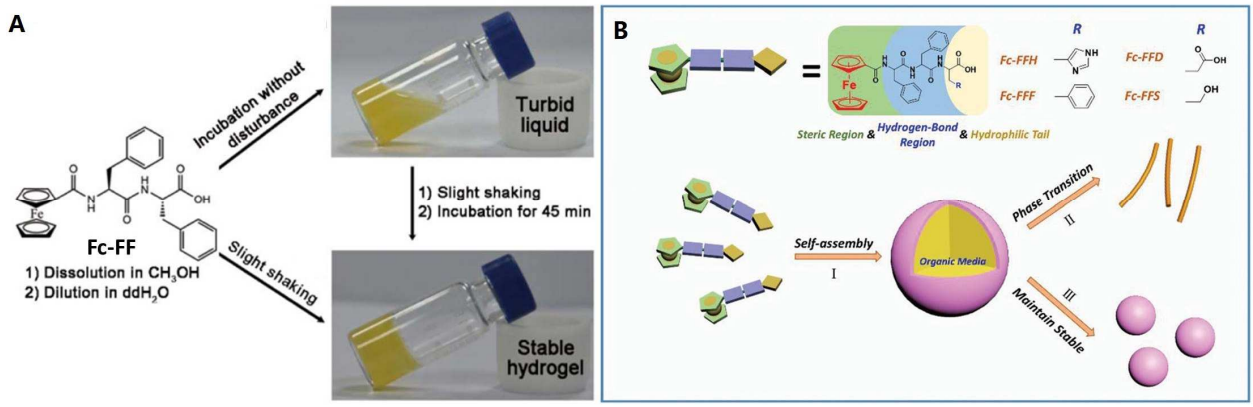

Figure 40. A) Molecular structure of Fc–FF and the formation process of hydrogel. Reproduced with permission from Ref. [198]. Copyright 2013 IOP Publishing Ltd. B) Molecular structure of the four Fc-tripeptides Fc-FFH, Fc-FFD, Fc-FFF, and Fc-FFS, proposed formation of nanoemulsion and its phase transformation. Reproduced with permission from Ref. [199]. Copyright 2017 Royal Society of Chemistry.

3.4. Other supramolecular Fc-containing hydrogels

Wang and coworkers[200] reported a self-healing and multi-sensitive supramolecular hydrogel fabricated from Fc-functionalized chitosan (FcCS). FcCS was prepared using the grafting reaction of chitosan with ferrocenecarboxylic acid assisted by EDC and NHS. The structure of FcCS was well confirmed through ^{1}H NMR, FT-IR and X-ray diffraction (XRD) measurements, and the grafting degree of Fc group was calculated to be 8.2%. Using an aqueous solution of acetic acid as the solvent, the FcCS solution was fabricated at a concentration of 10 mg mL^{-1}, and then cooled, leading to the formation of the corresponding hydrogel. The aggregated microdomain of the hydrophobic Fc groups in the side chain was believed to serve as convertible cross-linking sites for the formation of the hydrogel. The FcCS hydrogel showed self-repairing behavior. As indicated in Figure 41A, the hydrogel disc was separated into two parts that were then jointed together. After 4

h, a restored disk was obtained and was able to be stretched to twice the diameter of the initial one. Furthermore, results of rheology analyses also confirmed that the hydrogel had excellent and rapid self-healing property. Interestingly, as shown in Figures 41B-41D, possessed multi-stimuli-responsiveness toward pH, redox, and several metal cations including Cd^{2+}, Cr^{3+}, Pb^{2+}, and Cu^{2+}. In addition, doxorubicin hydrochloride (DOX·HCl) was easily encapsulated into the FcCs hydrogel network, and its controllable release was observed at different pH values (Figures 41E). This FcCs hydrogel is anticipated to find potential applications as biomedical and other functional materials.

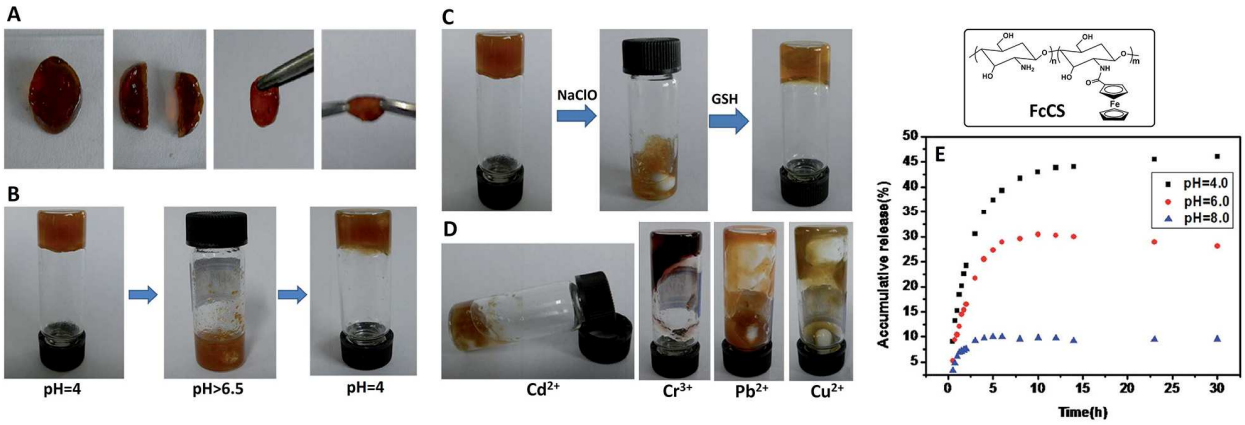

Figure 41. FcCS supramolecular hydrogel. (A) Self-healing process of FcCS hydrogel. pH- (B), Redox- (C) and metal ion-responsiveness (D) of FcCS hydrogel. (E) Release curves of DOX·HCl from the FcCS hydrogel. Reproduced with permission from Ref. [200]. Copyright 2014 Royal Society of Chemistry.

Das et al.[201] reported the preparation of new redox-responsive 3D-printable supramolecular hydrogels due to the presence of the dynamic borate ester bond between ferroceneboronic acid (FcBA) and guanosine. As shown in Figure 42, the green G-quadruplex hydrogel containing Fc^{+} units was fabricated through the heat treatment of FcBA and guanosine in KOH aqueous solution

at 80 ^{o}C. After being preserved at environment temperature for 4-5 days, the unstable green hydrogel was then voluntarily altered to the brown, Fc-bearing hydrogel. It was confirmed that K^{+} ion was the most appropriate species to insert the interior of G-quadruplex in order to maintain its architecture and generate the corresponding supramolecular hydrogel. Both the green and brown hydrogels were analyzed via UV-vis. and ^{11}B NMR spectroscopies, TEM, circular dichroism, powder XRD, CV and rheological tests. The brown Fc-containing hydrogel possessed excellent syringeability and thixotropy, which would be beneficial to the 3D printing. The Fc and Fc^{+}-containing hydrogels were set, respectively, into two syringes, and various shapes were printed adopting a 22G needle as shown in Figure 42a-d. Compared to the Fc^{+}-containing hydrogel, the brown Fc-bearing hydrogel produced geometrical shapes with more sharp and distinguishable edges. Thus, the Fc-containing hydrogel was found more appropriate for 3D printing and had better shape-keeping strength. As shown in Figure 42e-h, the brown Fc-containing hydrogel was put into a 3D printer, and a 3D square block and a 3D circular diagram were printed based on predefined "Computer Added Design'' (CAD) architectures. This 3D printable Fc-based hydrogel is expected to find various applications such as tissue regeneration, drug loading and wastewater treatment.

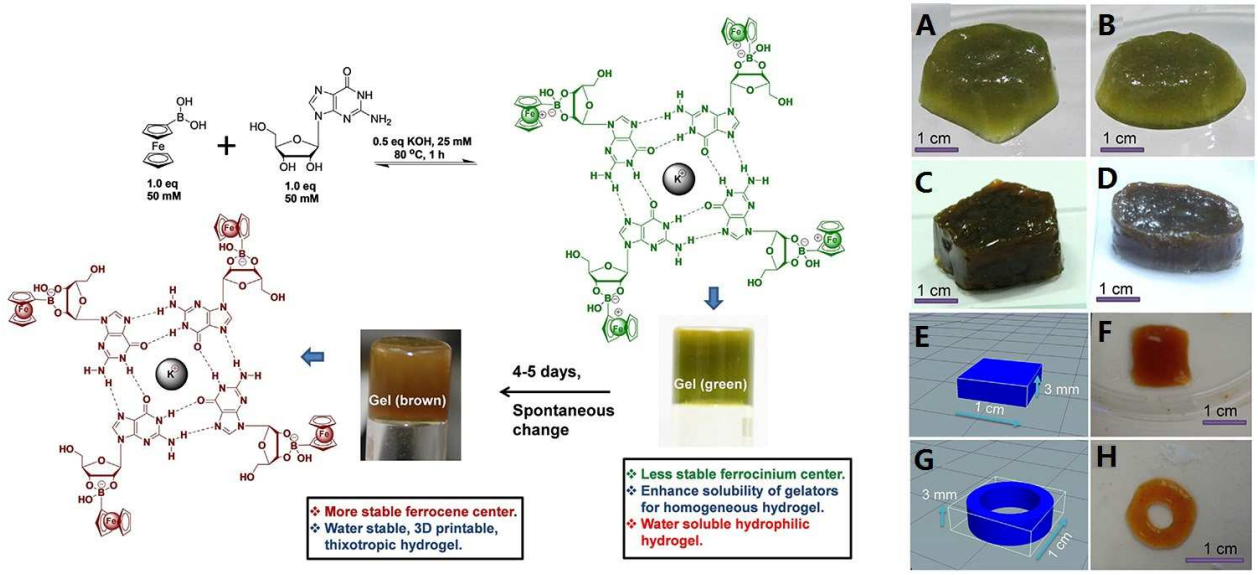

Figure 42. Schematic fabrication of Fc-containing G-quadruplex hydrogel and its 3D-printability. (A-D) Printed shapes of hydrogels by syringe-extrusion. CAD designed 3D block (E) and circular (G) patterns. 3D-printed block (F) and circular (H) objects by using the present hydrogel. Reproduced with permission from Ref. [201]. Copyright 2018 Wiley-VCH Verlag GmbH & Co. KGaA, Weinheim.

Kondo et al[202] prepared a new cationic gemini surfactant Fc-11-4-11-Fc that showed gel-sol transition in response to electrochemical oxidation-reduction (Figure 43). The water-soluble Fc-11-4-11-Fc was prepared by the quaternization reaction between 11-ferrocenylundecyl bromide and *N,N,N',N'*-tetramethyl-1,4-diamino alkane. The Fc-11-4-11-Fc micelle solution still keept a relatively high viscosity in the presence of LiBr, and therefore it showed gelation capacity. When the Fc-11-4-11-Fc hydrogel was treated by a constant voltage (+0.6 V), its viscosity gradually decreased (Figure 43A), and the solid hydrogel slowly changed into a liquid sol, and the color change from yellow to green was observed at the same time (Figure 43B). This color alteration is explained by oxidation of Fc groups to Fc^+ cations (Figure 43C).

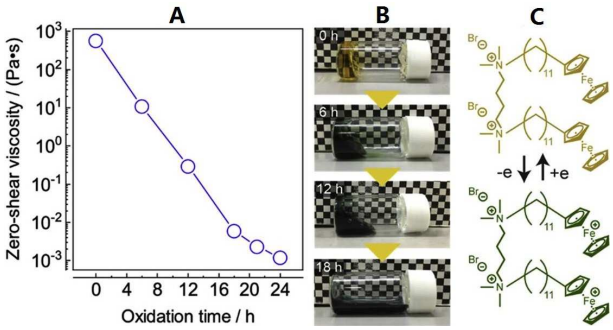

Figure 43. (A) Zero-shear viscosity curve and (B) pictures of the Fc-11-4-11-Fc solutions. (C) Reversible redox reaction of Fc-11-4-11-Fc. Reproduced with permission from Ref. [202]. Copyright 2019 Elsevier B.V.

4. Fc-containing microgels

Microgels are composed of chemically cross-linked 3D polymer networks that are similar to the structure of traditional hydrogels, whereas they are colloidal particles with a size range from tens of nanometers to several microns[203-206]. They have the ability to dramatically swell or shrink under various outside stimuli including temperature, pH, ionic strength, electrochemistry, electric field, solvents and enzymes, which affords a chance to controllably regulate their physicochemical performances[207-211]. Also, microgels feature the characteristics of chemical functionality, macromolecular structure, adaptative ability, penetrability, and deformability in a unique manner to combine the "best" of the colloid, polymer and surfactant fields[212-216]. This may open a new door for a variety of promising applications such as sensors, catalysis, nanotechnology, medicine and separation technology. Fc and its derivatives show chemically and electrochemically convertible redox performance and form host–guest combinations with macrocyclic host molecules. So, the introduction of Fc into microgels enables the formation of redox-responsive and

supramolecular microgels. The resulting Fc-containing microgels generally show electrochemically and chemically convertible redox behavior.

Vancso et al[217] first reported a new and versatile approach to prepare PFS-based redox-responsive organometallic microgel particles using the microfluidics technique (Figure 44). Organometallic microgels were synthesized from the PFS-based macromolecular cross-linkers containing acrylate units (PFS M1, Figure 44B) or vinylimidazole units (PFS M2, Figure 44F) in the side chain. To prepare the PFS M1 microgels, a glass chip with a T-junction was used to produce oil-in-water droplets in a H_2O/toluene mixed solvent system (Figure 44A). Subsequently, the crosslinked microgels were generated after treatment by UV irradiation. SEM indicated that cross-linked PFS M1 microgels were provided as microspheres with uniform size and smooth outside surface, and their diameters depended on the adopted water-to-oil flow rate ratios (Figure 44C,D). A flow-focusing PDMS device was selected to generate water-soluble and cross-linkable PFS M2 microgels (Figure 44E). The subsequent UV irradiation treatment resulted in the generation of cross-linked PFS M2 microgels that had rough apparent surface and a homogeneous size of about 20 mm (Figure 44G,H). Significantly, the cross-linked PFS M1 microgels served as reducing agent and template to *in-situ* prepare AgNPs when immersed in a saturated solution of $AgPF_6$. The resulting AgNPs were found to cover the external surface of the microgel microspheres (Figure 44I,J). In addition, a fluorescent dye (Rhodamine 6G) was further encapsulated into the micro-network of the cross-linked PFS M1 microgels, and its controllable release was achieved by the oxidation of Fc groups with $FeCl_3$.

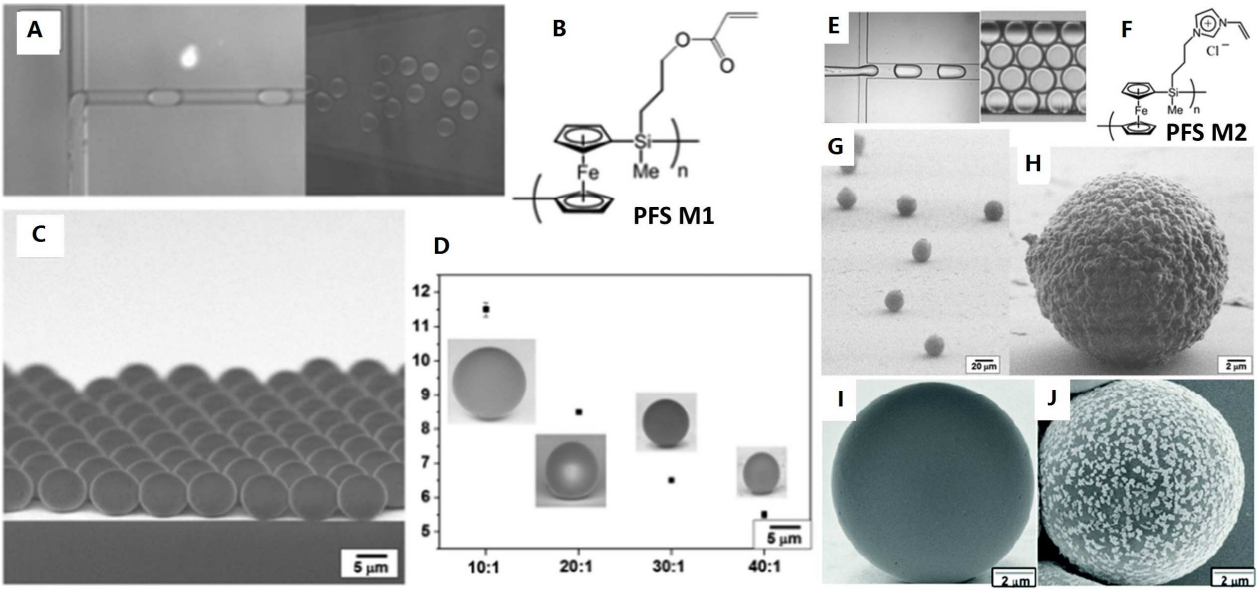

Figure 44. (A,E) Pictures showing the head-on formation of droplets. Structures of PFS M1 (B) and PFS M2 (F). SEM photo (C) and diameter change (D) of PFS M1 microgels. (G, H) SEM photos of PFS M2 microgels. (I) SEM photos of an individual PFS M1 microgel particle (I) and the AgNPs-coated one (J). Reproduced with permission from Ref. [217]. Copyright 2014 Royal Society of Chemistry.

Mugo et al.[218] used Fc-containing microgels to construct H_2O_2-responsive optical devices (etalons). As shown in Figure 45A, NIPAM, acrylic acid, and MBAAm were first copolymerized using the free-radical precipitation polymerization technique to prepare MG-AAc microgels with a cross-linking network. Then, the resulting MG-AAc microgels were modified with ferrocenylmethanol by esterification. TEM pictures indicated that both MG-AAc and MG-Fc microgels exhibited spherical shape, and the diameter for the former was 400 ± 10 nm (Figure 45B), while for the latter, the diameter was 340 ± 8 nm (Figure 45C). After MG-Fc microgels were oxidized by H_2O_2, the resulting MG-Fc^+ microgels presented a smaller diameter of 120 nm or so (Figure 45D). Based on the response characteristic of MG-Fc microgels to H_2O_2, the MG-Fc

microgels were further employed to prepare Fc-containing etalons through anchoring the microgels between two thin Au layers, and the response of the etalons towards H_2O_2 was estimated. It was found that the optical performance of the formed etalons relied on the H_2O_2 concentration in the range of 0.6-35 mM. Interestingly, H_2O_2 generated from an enzymatic reaction of glucose oxidized by GOD was quantitatively detected using the MG-Fc etalons. The H_2O_2-responsive etalons have the potential to monitor species of broad relevance and quantify products of biological reactions.

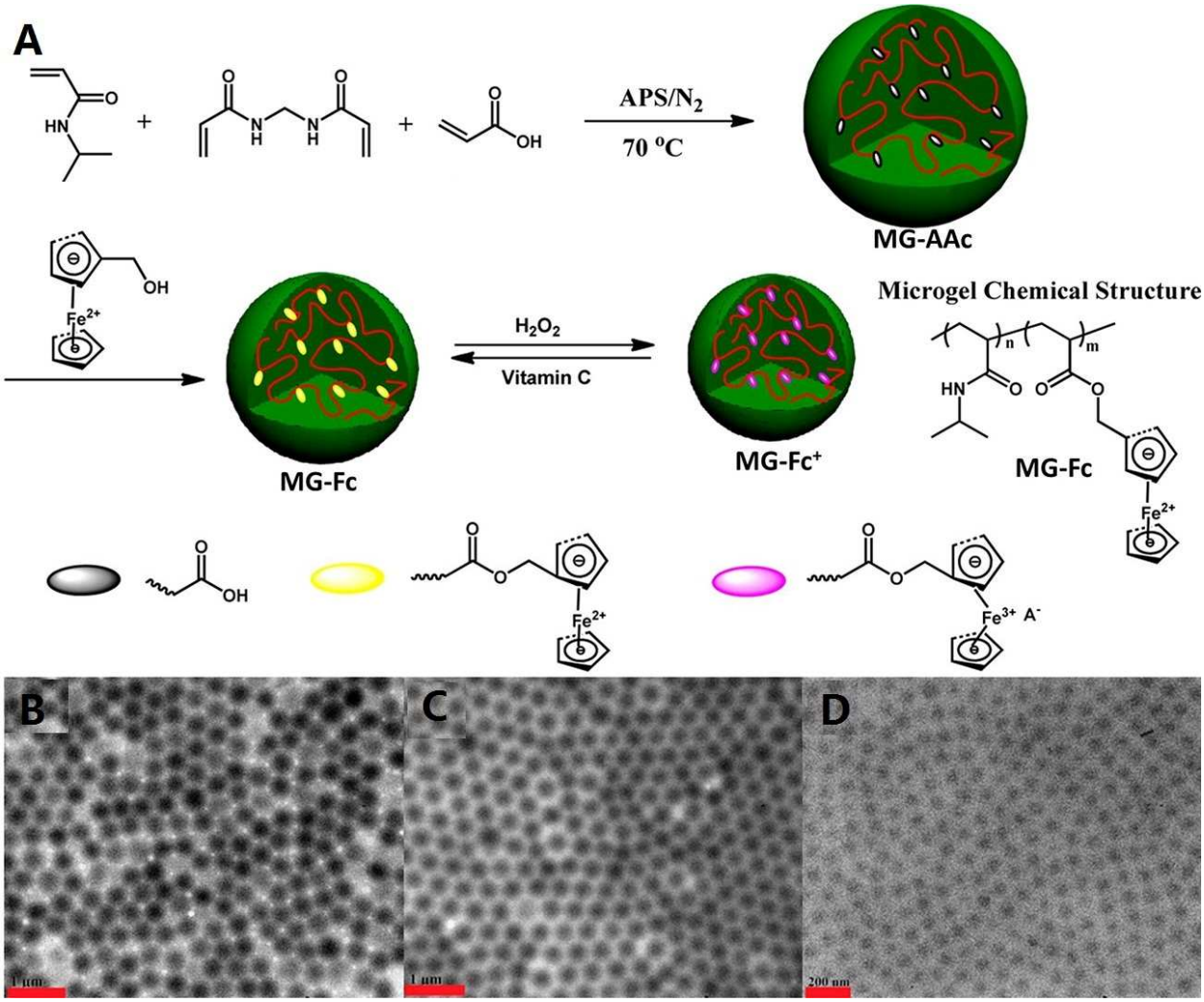

Figure 45. (A) Diagrammatic preparation and redox-responsiveness of MG-Fc microgels. TEM pictures of MG-AAc (B), MG-Fc (C), and MG-Fc$^+$ (D) microgels. Reproduced with permission

from Ref. [218]. Copyright 2016 American Chemical Society.

Karbarz et al.[219] prepared a new Fc-containing microgel that showed reversible size change using electrochemically induced volume phase transition. The precursor p(NIPAM-DASS-AC) microgels were first fabricated by radical copolymerization of NIPAM, sodium acrylate and DASS as shown in Figure 46A. Subsequently, the p(NIPAM-BISS-AC) microgels were functionalized using aminoferrocene based on the amide reaction, resulting in the formation of p(NIPAM-DASS-AC-Fc) microgels (Figure 46B). The p(NIPAM-DASS-AC-Fc) microgels were characterized by both SEM and TEM (Figure 46C and D), and the spherical shape were demonstrated for these microgels. Also, a gold electrochemical-quartz-crystal-microbalance electrode (Au EQCM) was functionalized by the p(NIPA-BISS-AC-Fc) microgels following coordination of the efficiently chemisorptive disulfide bridges, and the electrochemical responsiveness of the modified Au EQCM was detected. The p(NIPA-BISS-AC-Fc) layers exhibited shrinking or expanding shape relying on the amount of the oxidized Fc units. It was possible to adjust the oxidation degree of Fc groups using an electrochemical method, and the shrinking–expanding change was reversible and repeatable.

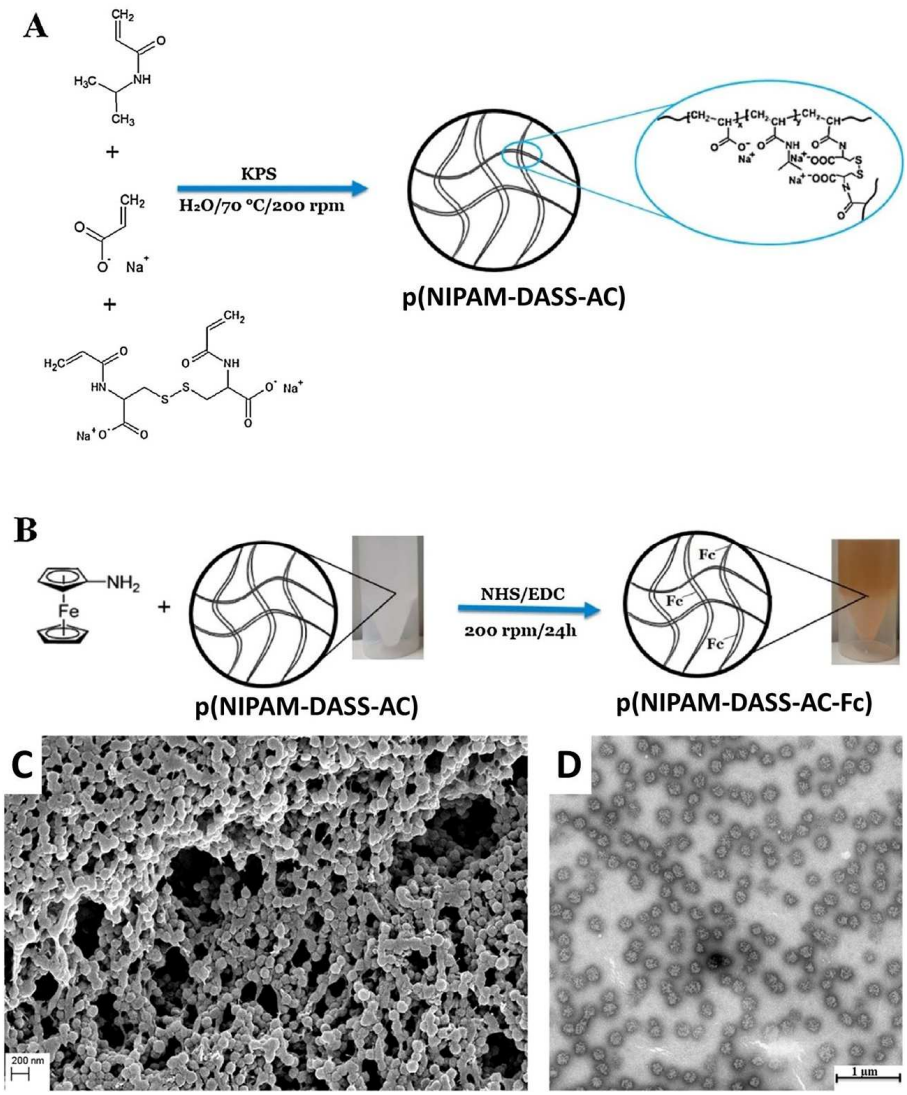

Figure 46. Graphical preparation of p(NIPAM-DASS-AC) (A) and p(NIPAM-DASS-AC-Fc) (B) microgels. SEM (C) and TEM (D) pictures of p(NIPAM-DASS-AC-Fc) microgels. Reproduced with permission from Ref. [219]. Copyright 2018 Elsevier Ltd.

Recently, Plamper et al[220] reported new cargo shuttling based on the electrochemical switching of p(NIPAM-*co*-VFc) microgels with the Fc-enriched (collapsed/hard) cores and a NIPAM-rich shells that were synthesized via a facile one-shot precipitation copolymerization (Figure 47A). The p(NIPAM-*co*-VFc) microgels showed the typical core–shell structure, while the core was found to disappear partially after electrochemical oxidation because of the repulsion between the Fc^+ groups.

In the electrochemical oxidation process, only 50% of Fc groups were oxidized into Fc^+ ions, and the core radius was found to be reduced from 102 ± 11 nm to 56 ± 4 nm (Figure 47C). After oxidation, the radius of the total core–shell particles was found to increase from 311 nm ± 16 nm to 384 nm ± 47 nm (Figure 47B and 47C). These results indicated that the shell made an addressable response to electrochemical oxidation, but the core responded slowly to the oxidation. Interestingly, when the oxidation was chemically conducted using $FeCl_3$, a faster oxidation of Fc was observed in the cores of microgels. The complete oxidation resulted in the chemically oxidized microgels that had a contrary architecture against the original microgels. The chemically oxidized microgels showed the core–shell architecture with the much improved core radius (129 ± 17 nm) and a less expanding shell with a total radius of 386 ± 34 nm (Figure 47D). Based on the reversible electrochemical hydrophilicity-hydrophobicity transformation property, the microgels were further used to load a bactericidal drug of triclosan that could be controllably released to effectively kill bacteria. Moreover, results of cell tests indicated that the p(NIPAM-*co*-VFc) microgels showed good biocompatibility. The property of the Fc-containing microgels to load/release small molecules based on the switching polarity is promising for future biomedical applications, especially in the fields of smart drug delivery systems and biosensors.

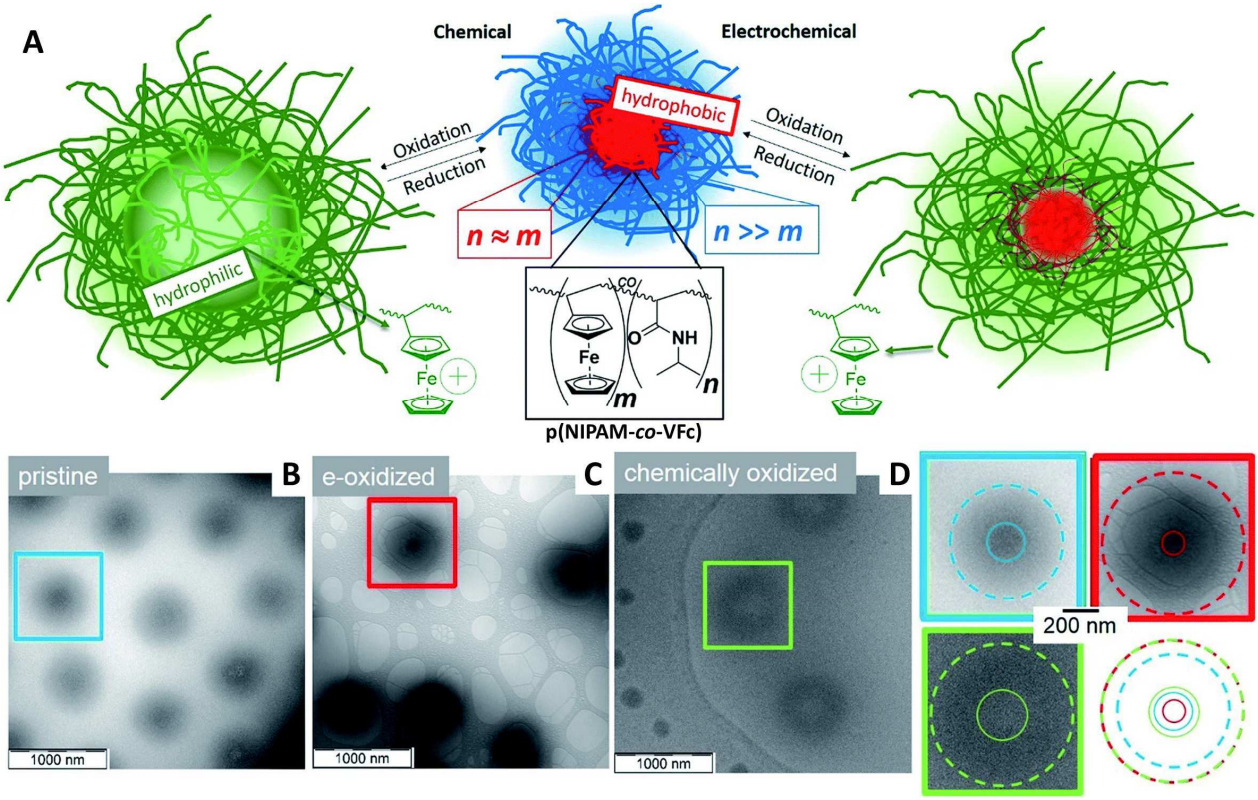

Figure 47. Schematic redox-responsiveness of p(NIPAM-*co*-VFc) microgels. Cryo-TEM pictures of p(NIPAM-*co*-VFc) microgels reduced by pristine (B) and oxidized by electrochemical (C) and chemical (D) methods. Reproduced with permission from Ref. [220]. Copyright 2019 Royal Society of Chemistry.

Yuan et al[221] reported electrochemical stimuli-responsive pickering emulsions fabricated from Fc-based microgels for the recycling of enzyme in biocatalysis. The Fc-based microgels were prepared from β-CD modified 8-arm poly(ethylene glycol) (PEG-CD) and the Fc functionalized analogue (PEG-Fc) via the β-CD/Fc-based host-guest bonding (Figure 48A). TEM analysis indicates that the microgels were spherical and their diameters were about 200 nm (Figure 48B). After the microgels were treated with a +0.80 V potential, their diameters were sharply reduced from 340 to 10 nm based on dynamic light scattering analysis, demonstrating the disassembly of

the particles. The TEM images also provided powerful proof for this phenomenon (Figure 48C). After treatment applying a potential of +0.20 V, the microgels were rebuilt. As shown in Figure 48B and 48D, no significant change was observed in the particle morphology after a redox cycle. The microgels (10 wt %) was further dispersed in a mixed solvent consisting in hexane and H_2O (v:v = 1:1) to give a pickering emulsion. The prepared pickering emulsion provided favorable micro-environment for an enzyme-biocatalyzed reaction. It was found that the specific activity of lipases was much enhanced in the pickering emulsion. The potential-controlled disassembly and assembly of this pickering emulsion enabled the efficient separation of reaction products and the recycling of the used enzymes. The present Fc-based microgels and the corresponding pickering emulsion provide new chance for high-efficiency and clean biocatalytic reactions.

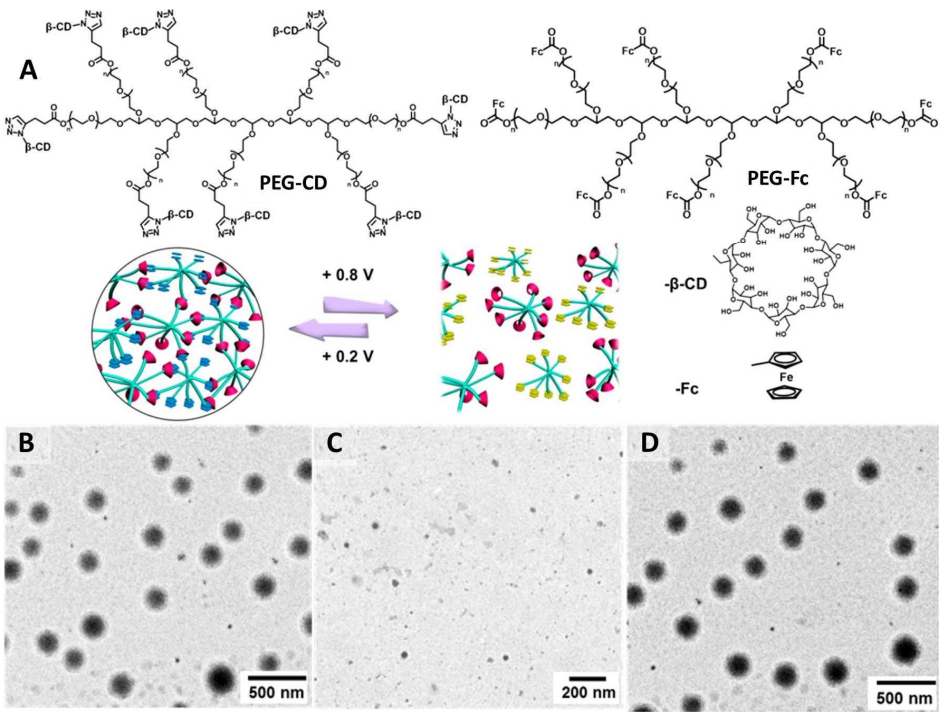

Figure 48. (A) Chemical structures of PEG-CD and PEG-Fc, and assembly and disassembly of the corresponding microgel under the potential stimuli. TEM pictures of the original microgels (B) before treatment, (C) oxidized by +0.80 V of potential, and (D) reduced by +0.20 V of potential.

Reproduced with permission from Ref. [221]. Copyright 2016 American Chemical Society.

In a recent study, Pich's group [222] prepared Fc-containing microgels with supramolecular redox-cleavable crosslinks (Figure 49). A supramolecular Fc-containing redox-cleavable crosslinker was first obtained via host-guest interaction between methacrylate-functionalized β-CD and vinylferrocene. Whereafter, the precipitation copolymerization of the supramolecular crosslinker with *N*-vinylcaprolactam gave a range of supramolecular Fc-containing microgels. By changing the contents of this crosslinker, the resulting Fc-containing microgels showed hydrodynamic radii of 100-200 nm. Also, the Fc-containing microgels exhibited reversibly temperature-responsive swelling/deswelling behavior. Besides, the microgels would be degraded under chemical ($FeCl_3$ or H_2O_2) or electrochemical stimulus. And, the more the supramolecular crosslinker had, the faster the degradation occurred. The redox-triggered degradation behavior of the Fc-containing microgels gives a chance to load/release drug molecules. It was found that DOX could be encapsulated into the Fc-containing microgels and may be released under H_2O_2 stimulus. This work gives out a good idea to develop novel redox-responsive drug delivery carriers.

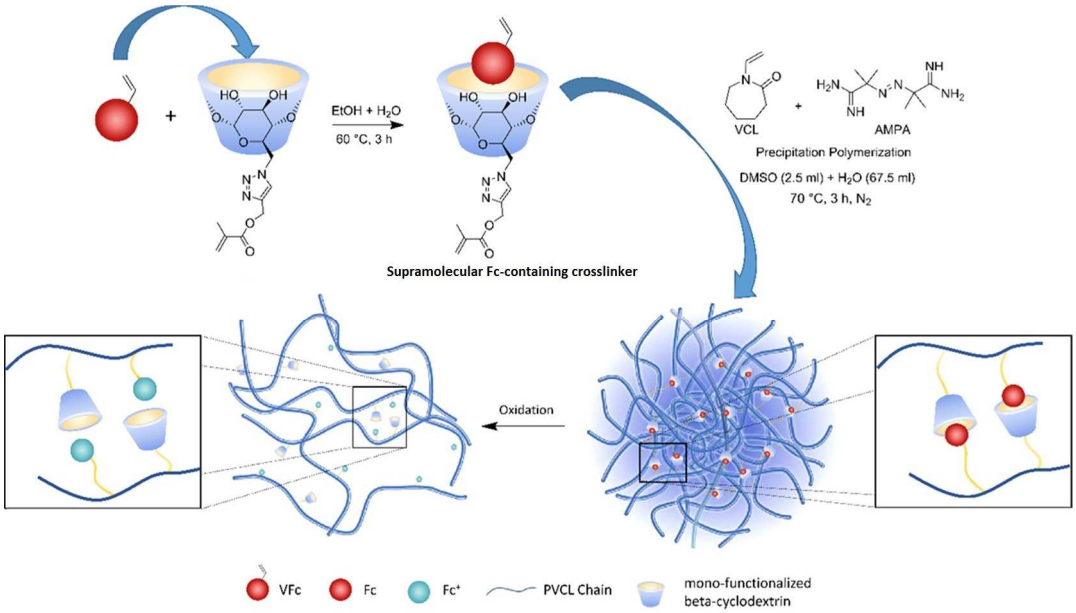

Figure 49. Preparation of Fc-containing redox-responsive microgels. Reproduced with permission from Ref. [222]. Copyright 2020 American Chemical Society.

5. Conclusion and outlook

Fc-containing hydrogels are becoming more and more popular as a new class of advanced materials, especially as biomedical, shape-memory and self-healing materials. In this review, we have discussed the preparation of the various classes of Fc-containing hydrogels fabricated by covalent cross-linking and supramolecular assemblies. The continuous and intensive exploitation of new strategies for the fabrication of Fc-containing hydrogels has resulted in many new organometallic hydrogels with promising performances. The remarkable features of Fc-containing hydrogels are on account of the invertible change of Fc and Fc^+ moieties adjusted using chemical or electrochemical treatment and the characteristic host–guest dynamic combination of Fc units with macrocyclic host molecules. The Fc moiety involves characteristics such as polarity, charge and bonding ability that are invertibly controlled by changing outside redox conditions. The

introduction of Fc into the hydrogel network structures consecutively produces electrochemically or chemically addressable remote-switchable materials with adjustable specific performances. The interconversion Fc/Fc^+ is rapid, highly efficiency and perfectly reversible. Therefore, a variety of innovative structures are produced in smart Fc-containing hydrogels in a controlled manner. In the supramolecular Fc-containing hydrogels, the application of a certain magnitude of voltage or chemicals by triggering the redox reaction of the Fc moiety also changes Fc-based host–guest interactions in the system. Therefore, the supramolecular Fc-containing hydrogels generally show self-healing and shape-memory properties as well as convertible sol-gel transformation process.

Fc-containing hydrogels are creating many opportunities available in the field of various advanced materials. Research on Fc-containing hydrogels is still in its initial period, however, and intensive focus should further be paid to the design, development and practical applications. The following points should be considered. First, the variety of Fc-containing polymers used to prepare Fc-containing hydrogels is relatively limited. The most commonly used polymer frameworks mainly involve the PFS, PS and PEI types. More Fc-containing polymers should be exploited for the construction of Fc-containing hydrogels. For example, many kinds of Fc-containing polymers could be easily prepared by controlled and living polymerizations such as ROMP, ATRP and RAFT[223-227]. Furthermore, some biomacromolecules, for example, proteins, peptides, collagens and polysaccharides, will be excellent carriers to fabricate Fc-containing hydrogels, thus endowing Fc-containing hydrogels with good biocompatibility and biodegradability.

Secondly, the supramolecular Fc-containing hydrogels are now mainly prepared based on the host–guest interactions, but the adopted families are still few. The most commonly used host molecule is still the β-CD, and the host–guest interactions based on host PAs [228-231] are rarely reported.

PAs should also be promising for the preparation of Fc-containing supramolecular hydrogels because of their favorable characteristics such as easy synthesis, versatile chemical modifiability, rigid electron-rich architectures and tunable cavity sizes. Other macrocyclic host molecules, such as calixarenes[232-238] and cucurbiturils[239-244], still keep unexplored in Fc-containing supramolecular hydrogels. Host–guest interactions have a significant impact on the architectures, properties and functionalities of macrocycle-based hydrogels. Macrocyclic compounds should be regarded as adjustable building blocks for the fabrication of diverse supramolecular hydrogels that often have exceptional self-healing characteristics owing to their high selectivity for guest molecules and reversible non-covalent features[245,246].

Thirdly, metal coordination is stronger than the majority of non-covalent interactions, but weaker than typical covalent interactions. Hydrogels fabricated via metal coordination may combine the unique performances of physically and chemically cross-linking hydrogels. Based on metal coordination, the resulting hydrogels might have many remarkable performances such as biocompatibility, recoverability, self-healing, and redox activity[247-253]. The incorporation of metal coordination interactions into Fc-containing hydrogels may result in the potential synergism between different metal centers bringing about unpredictable physical and chemical properties and stimuli-responsiveness. The future of supramolecular Fc-containing hydrogels, especially in the bio-medical field, will seek to take advantage of their characteristic chemical and mechanical performances in new applications towards enhancing health outcomes.

Last but not least, more attention should be paid to the bio-safety of Fc-containing hydrogels and their evaluation. Focus should be paid on the biocompatibility, biodegradability, and nontoxicity of the unique Fc-containing hydrogels for their increase of applications in biomedicine and

biomaterial fields[254]. It will be necessary to understand their behaviors *in vitro* and *in vivo*. Unfortunately, the majority of the reported Fc-containing hydrogels are still at the proof-of-concept level, however, and *in vitro* and *in vivo* assays are hardly reported. In view of the complex microenvironment in the biological systems, *in vitro* and *in vivo* evaluations are urgently needed. In conclusion, to fully develop the multiple applications of Fc-containing hydrogels, their species should be broadened. It will be necessary to carry out more investigations and improvements to solve the above issues. Scientists from the various fields such as chemistry, polymers, materials and biomedicine should make closer cooperation to provide newer insights into the design and exploitation of Fc-containing hydrogels for their potential applications.

Acknowledgement

This work was financially supported by the National Natural Science Foundation of China (No. 21978180), the Science & Technology Department of Sichuan Province (No. 2018HH0038), the Fundamental Research Fund for the Central Universities of China, ceshigo (www.ceshigo.com), the Université de Bordeaux and the Centre National de la Recherche Scientifique (CNRS). We also appreciate the valuable help of Dr. Wang Hui (Analytical & Testing Center of Sichuan University) and Dr. Jinwei Zhang (College of Biomass Science and Engineering, Sichuan University).

References

1. Y. Qiu, K. Park, Environment-sensitive hydrogels for drug delivery, Adv. Drug Deliv. Rev. 53 (2001) 321-339.
2. J.Y. Li, D.J. Mooney, Designing hydrogels for controlled drug delivery, Nat. Rev. Mater. 1

(2016) 16071.

3. I. Tokarev, S. Minko, Stimuli-Responsive Porous Hydrogels at Interfaces for Molecular Filtration, Separation, Controlled Release, and Gating in Capsules and Membranes, Adv. Mater. 22 (2010) 3446-3462.
4. N. Annabi, A. Tamayol, J.A. Uquillas, M. Akbari, L.E. Bertassoni, C. Cha, G. Camci-Unal, M.R. Dokmeci, N.A. Peppas, A. Khademhosseini, 25th Anniversary Article: Rational Design and Applications of Hydrogels in Regenerative Medicine, Adv. Mater. 26 (2014) 85-124.
5. J. Li, L.T. Mo, C.H. Lu, T. Fu, H.H. Yang, W.H. Tan, Functional nucleic acid-based hydrogels for bioanalytical and biomedical applications, Chem. Soc. Rev. 45 (2016) 1410-1431.
6. D.D. Diaz, D. Kuhbeck, R.J. Koopmans, Stimuli-responsive gels as reaction vessels and reusable catalysts, Chem. Soc. Rev. 40 (2011) 427-448.
7. D.L. Taylor, M.I.H. Panhuis, Self-Healing Hydrogels, Adv. Mater. 28 (2016) 9060-9093.
8. E.A. Appel, J. del Barrio, X.J. Loh, O.A. Scherman, Supramolecular polymeric hydrogels, Chem. Soc. Rev. 41 (2012) 6195-6214.
9. X.W. Du, J. Zhou, J.F. Shi, B. Xu, Supramolecular Hydrogelators and Hydrogels: From Soft Matter to Molecular Biomaterials, Chem. Rev. 115 (2015) 13165-13307.
10. Y.S. Zhang, A. Khademhosseini, Advances in engineering hydrogels, Science 356 (2017) eaaf3627.
11. K.J. De France, T. Hoare, E.D. Cranston, Review of Hydrogels and Aerogels Containing Nanocellulose, Chem. Mat. 29 (2017) 4609-4631.
12. S.K. Ahn, R.M. Kasi, S.C. Kim, N. Sharma, Y.X. Zhou, Stimuli-responsive polymer gels, Soft Matter 4 (2008) 1151-1157.

13. J.J. Shang, X.X. Le, J.W. Zhang, T. Chen, P. Theato, Trends in polymeric shape memory hydrogels and hydrogel actuators, Polym. Chem. 10 (2019) 1036-1055.
14. D. Roy, J.N. Cambre, B.S. Sumerlin, Future perspectives and recent advances in stimuli-responsive materials, Prog. Polym. Sci. 35 (2010) 278-301.
15. C.D.H. Alarcon, S. Pennadam, C. Alexander, Stimuli responsive polymers for biomedical applications, Chem. Soc. Rev. 34 (2005) 276-285.
16. A.K. Bajpai, S.K. Shukla, S. Bhanu, S. Kankane, Responsive polymers in controlled drug delivery, Prog. Polym. Sci. 33 (2008) 1088-1118.
17. A. Doring, W. Birnbaum, D. Kuckling, Responsive hydrogels - structurally and dimensionally optimized smart frameworks for applications in catalysis, micro-system technology and material science, Chem. Soc. Rev. 42 (2013) 7391-7420.
18. A.S. Hoffman, Stimuli-responsive polymers: Biomedical applications and challenges for clinical translation, Adv. Drug Deliv. Rev. 65 (2013) 10-16.
19. J.S. Kahn, Y.W. Hu, I. Willner, Stimuli-Responsive DNA-Based Hydrogels: From Basic Principles to Applications, Acc. Chem. Res. 50 (2017) 680-690.
20. B. Xue, V. Kozlovskaya, E. Kharlampieva, Shaped stimuli-responsive hydrogel particles: syntheses, properties and biological responses, J. Mat. Chem. B 5 (2017) 9-35.
21. S.J. Jeon, A.W. Hauser, R.C. Hayward, Shape-Morphing Materials from Stimuli-Responsive Hydrogel Hybrids, Acc. Chem. Res. 50 (2017) 161-169.
22. W. Lu, X.X. Le, J.W. Zhang, Y.J. Huang, T. Chen, Supramolecular shape memory hydrogels: a new bridge between stimuli-responsive polymers and supramolecular chemistry, Chem. Soc. Rev. 46 (2017) 1284-1294.

23. M. Huo, J. Yuan, L. Tao, Y. Wei, Redox-responsive polymers for drug delivery: from molecular design to applications, Polym. Chem. 5 (2014) 1519-1528.

24. N. Casado, G. Hernandez, H. Sardon, D. Mecerreyes, Current trends in redox polymers for energy and medicine, Prog. Polym. Sci. 52 (2016) 107-135.

25. W.Y. Wong, C.L. Ho, Organometallic Photovoltaics: A New and Versatile Approach for Harvesting Solar Energy Using Conjugated Polymetallaynes, Acc. Chem. Res. 43 (2010) 1246-1256.

26. Q.C. Dong, Z.G. Meng, C.L. Ho, H.G. Guo, W.Y. Yang, I. Manners, L.L. Xu, W.Y. Wong, A molecular approach to magnetic metallic nanostructures from metallopolymer precursors, Chem. Soc. Rev. 47 (2018) 4934-4953.

27. P. Nguyen, P. Gomez-Elipe, I. Manners, Organometallic polymers with transition metals in the main chain, Chem. Rev. 99 (1999) 1515-1548.

28. K.A. Williams, A.J. Boydston, C.W. Bielawski, Main-chain organometallic polymers: synthetic strategies, applications, and perspectives, Chem. Soc. Rev. 36 (2007) 729-744.

29. L. Zhao, X. Liu, L. Zhang, G.R. Qiu, D. Astruc, H.B. Gu, Metallomacromolecules containing cobalt sandwich complexes: Synthesis and functional materials properties, Coord. Chem. Rev. 337 (2017) 34-79.

30. H.B. Gu, R. Ciganda, P. Castel, S. Moya, R. Hernandez, J. Ruiz, D. Astruc, Tetrablock Metallopolymer Electrochromes, Angew. Chem. Int. Ed. 57 (2018) 2204-2208.

31. T.Y. Zhu, S.C. Xu, A. Rahman, E. Dogdibegovic, P. Yang, P. Pageni, M.P. Kabir, X.D. Zhou, C.B. Tang, Cationic Metallo-Polyelectrolytes for Robust Alkaline Anion-Exchange Membranes, Angew. Chem. Int. Ed. 57 (2018) 2388-2392.

32. T.Y. Zhu, Y. Sha, J. Yan, P. Pageni, M.A. Rahman, Y. Yan, C.B. Tang, Metallo-polyelectrolytes as a class of ionic macromolecules for functional materials, Nat. Commun. 9 (2018) 4329.

33. D. Astruc, C. Ornelas, J. Ruiz, Metallocenyl dendrimers and their applications in molecular electronics, sensing, and catalysis, Acc. Chem. Res. 41 (2008) 841-856.

34. I. Cuadrado, M. Moran, C.M. Casado, B. Alonso, J. Losada, Organometallic dendrimers with transition metals, Coord. Chem. Rev. 193-5 (1999) 395-445.

35. P. Wang, J.F. Sun, Z.C. Lou, F.G. Fan, K. Hu, Y. Sun, N. Gu, Assembly-Induced Thermogenesis of Gold Nanoparticles in the Presence of Alternating Magnetic Field for Controllable Drug Release of Hydrogel, Adv. Mater. 28 (2016), 10801-10808.

36. K. Hu, J.F. Sun, Z.B. Guo, P. Wang, Q. Chen, M. Ma, N. Gu, A Novel Magnetic Hydrogel with Aligned Magnetic Colloidal Assemblies Showing Controllable Enhancement of Magnetothermal Effect in the Presence of Alternating Magnetic Field, Adv. Mater. 27 (2015) 2507-2514.

37. L.Y. Tang, X.L. Chen, L. Wang, J.Q. Qu, Metallo-supramolecular hydrogels based on amphiphilic polymers bearing a hydrophobic Schiff base ligand with rapid self-healing and multi-stimuli responsive properties, Polym. Chem. 8 (2017), 4680-4687.

38. M. Haring, D.D. Diaz, Supramolecular metallogels with bulk self-healing properties prepared by in situ metal complexation, Chem. Commun. 52 (2016) 13068-13081.

39. A.Y.Y. Tam, V.W.W. Yam, Recent advances in metallogels, Chem. Soc. Rev. 42 (2013) 1540-1567.

40. X.Z. Yan, F. Wang, B. Zheng, F.H. Huang, Stimuli-responsive supramolecular polymeric materials, Chem. Soc. Rev. 41 (2012) 6042-6065.

41. J.Y. Zhang, C.Y. Su, Metal-organic gels: From discrete metallogelators to coordination polymers, Coord. Chem. Rev. 257 (2013) 1373-1408.

42. Y.H. Zheng, G.Y. Li, Y. Zhang, Organometallic Hydrogels, ChemNanoMat 2 (2016) 364-375.

43. D. Astruc, Why is Ferrocene so Exceptional, Eur. J. Inorg. Chem. (2017) 6-29.

44. R.L.N. Hailes, A.M. Oliver, J. Gwyther, G.R. Whittell, I. Manners, Polyferrocenylsilanes: synthesis, properties, and applications, Chem. Soc. Rev. 45 (2016) 5358-5407.

45. P. Li, H. Kang, C. Zhang, W. Li, Y. Huang, R. Liu, Reversible Redox Activity of Ferrocene Functionalized Hydroxypropyl Cellulose and Its Application to Detect H2O2, Carbohydr. Polym. 140 (2016) 35–42.

46. G. Gasser, I. Ott, N. Metzler-Nolte, Organometallic Anticancer Compounds, J. Med. Chem. 54 (2011) 3–25.

47. Z.P. Xiao, Z.H. Cai, H. Liang, J. Lu, Amphiphilic block copolymers with aldehyde and ferrocene-functionalized hydrophobic block and their redox-responsive micelles, J. Mater. Chem. 20 (2010) 8375–8381.

48. Q. Yan, J.Y. Yuan, Z.N. Cai, Y. Xin, Y. Kang, Y.W. Yin, Voltage-responsive vesicles based on orthogonal assembly of two homopolymers, J. Am. Chem. Soc. 132 (2010) 9268–9270.

49. H.B. Gu, S.D. Mu, G.R. Qiu, X. Liu, L. Zhang, Y.F. Yuan, D. Astruc, Redox-stimuli-responsive drug delivery systems with supramolecular ferrocenyl-containing polymers for controlled release, Coord. Chem. Rev. 364 (2018) 51-85.

50. W.E. Geiger, Organometallic electrochemistry: origins development, and future, Organometallics 26 (2007) 5738–5765.

51. G. Saravanakumar, J. Kim, W.J. Kim, Reactive-Oxygen-Species-Responsive Drug Delivery

Systems: Promises and Challenges, Adv. Sci. 4 (2017) 1600124.

52. N.G. Liu, D.R. Dunphy, P. Atanassov, S.D. Bunge, Z. Chen, G.P. Lopez, T.J. Boyle, C.J. Brinker, Photoregulation of mass transport through a photoresponsive azobenzene-modified nanoporous membrane, Nano Lett. 4 (2004) 551-554.

53. G.R. Qiu, X. Liu, B.R. Wang, H.B. Gu, W.X. Wang, Ferrocene-Containing Amphiphilic Polynorbornenes as Biocompatible Drug Carriers, Polym. Chem. 10 (2019) 2527-2539.

54. L. Zhang, G.R. Qiu, F.F. Liu, X. Liu, S.D. Mu, Y.R. Long, Q.X. Zhao, Y. Liu, H.B. Gu, Controlled ROMP synthesis of side-chain ferrocene and adamantane-containing diblock copolymer for the construction of redox-responsive micellar carriers, React. Funct. Polym. 132 (2018) 60-73.

55. X. Liu, Q.J. Ling, L. Zhao, G.R. Qiu, Y.H. Wang, L.X. Song, Y. Zhang, J. Ruiz, D. Astruc, H.B. Gu, New ROMP Synthesis of Ferrocenyl Dendronized Polymers, Macromol. Rapid Commun. 38 (2017) 1700448.

56. X. Liu, G.R. Qiu, L. Zhang, F.F. Liu, S.D. Mu, Y.R. Long, Q.X. Zhao, Y. Liu, H.B. Gu, Controlled ROMP Synthesis of Ferrocene-Containing Amphiphilic Dendronized Diblock Copolymers as Redox-Controlled Polymer Carriers, Macromol. Chem. Phys. 219 (2018) 1800273.

57. X. Liu, F.F. Liu, Y.L. Wang, H.B. Gu, Ferrocene-containing amphiphilic dendronized random copolymer as efficient stabilizer for reusable gold nanoparticles in catalysis, React. Funct. Polym. 143 (2019) 104325.

58. L. Peng, A.C. Feng, M. Huo, J.Y. Yuan, Ferrocene-based supramolecular structures and their applications in electrochemical responsive systems, Chem. Commun. 50 (2014) 13005-13014.

59. Z. P. Wang, H. Möhwald, C.Y. Gao, Preparation and Redox-Controlled Reversible Response of Ferrocene-Modified Poly (allylamine hydrochloride) Microcapsules, Langmuir 27 (2010) 1286−1291.

60. J.C. Eloi, D.A. Rider, G. Cambridge, G.R. Whittell, M.A. Winnik, I. Manners, Stimulus-responsive self-assembly: reversible, redoxcontrolled micellization of polyferrocenylsilane diblock copolymers, J. Am. Chem. Soc. 133 (2011) 8903−8913.

61. D.A. Rider, M.A. Winnik, I. Manners, Redox-controlled micellization of organometallic block copolymers, Chem. Commun. 43 (2007) 4483−4485.

62. D.R. van Staveren, N. Metzler-Nolte, Bioorganometallic chemistry of ferrocene, Chem. Rev. 104 (2004) 5931−5985.

63. R.L. Sun, L. Wang, H.J. Yu, Zain-ul-Abdin, Y.S. Chen, J. Huang, R.B. Tong, Molecular Recognition and Sensing Based on Ferrocene Derivatives and Ferrocene-Based Polymers. Organometallics 33 (2014) 4560-4573.

64. H.Z. Bu, S.R. Mikkelsen, A.M. English, Characterization of a ferrocene-containing Polyacrylamide-Based Redox Gel for Biosensor Use, Anal. Chem. 67 (1995) 4071-4076.

65. E.J. Calvo, C. Danllowlcz, L. Dlaz, A new Polycationic Hydrogel for 3-Dimensional Enzyme Wired Modified Electrodes, J. Electroanal. Chem. 369 (1994), 279-282.

66. H.Z. Bu, A.M. English, S.R. Mikkelsen, Modification of ferrocene-containing redox gel sensor performance by copolymerization of charged monomers, Anal. Chem. 68 (1996) 3951-3957.

67. F. Battaglini, E.J. Calvo, C. Danilowicz, A. Wolosiuk, Effect of ionic strength on the behavior of amperometric enzyme electrodes mediated by redox hydrogels, Anal. Chem. 71 (1999), 1062-1067.

68. B. Zoetebier, M.A. Hempenius, G.J. Vancso, Redox-responsive organometallic hydrogels for in situ metal nanoparticle synthesis, Chem. Commun. 51 (2015) 636-639.

69. B.V.K.J. Schmidt, M. Hetzer, H. Ritter, C. Barner-Kowollik, Complex macromolecular architecture design via cyclodextrin host/guest complexes, Prog. Polym. Sci. 39 (2014) 235-249.

70. S. Tan, K. Ladewig, Q. Fu, A. Blencowe, G.G. Qiao, Cyclodextrin-Based Supramolecular Assemblies and Hydrogels: Recent Advances and Future Perspectives, Macromol. Rapid Commun. 35 (20143) 1166-1184.

71. A. Harada, Y. Takashima, M. Nakahata, Supramolecular Polymeric Materials via Cyclodextrin-Guest Interactions, Acc. Chem. Res. 47 (2014) 2128-2140.

72. J.M. Casas-Solvas, E. Ortiz-Salmeron, I. Fernandez, L. Garcia-Fuentes, F. Santoyo-Gonzalez, A. Vargas-Berenguel, Ferrocene-beta-Cyclodextrin Conjugates: Synthesis, Supramolecular Behavior, and Use as Electrochemical Sensors, Chem.-Eur. J. 15 (2009) 8146-8162.

73. W.W. Feng, M. Jin, K. Yang, Y.X. Pei, Z.C. Pei, Supramolecular delivery systems based on pillararenes, Chem. Commun. 54 (2018) 13626-13640.

74. M. Nakahata, Y. Takashima, H. Yamaguchi, A. Harada, Redox-responsive self-healing materials formed from host–guest polymers, Nat. Commun. 2 (2011) 511.

75. M.F. Ni, N. Zhang, W. Xia, X. Wu, C.H. Yao, X. Liu, X.Y. Hu, C. Lin, L.Y. Wang, Dramatically Promoted Swelling of a Hydrogel by Pillar[6]arene–Ferrocene Complexation with Multistimuli Responsiveness, J. Am. Chem. Soc. 138 (2016) 6643-6649.

76. M. Nakahata, Y. Takashima, A. Hashidzume, A. Harada, Redox-Generated Mechanical Motion of a Supramolecular Polymeric Actuator Based on Host–Guest Interactions, Angew. Chem. Int.

Ed. 52 (2013) 5731-5735.

77. D.P. Hickey, R.C. Reid, R.D. Milton, S.D. Minteer, A self-powered amperometric lactate biosensor based on lactate oxidase immobilized in dimethylferrocene-modified LPEI, Biosens. Bioelectron. 77 (2016) 26-31.

78. L. Peng, H.J. Zhang, A.C. Feng, M. Huo, Z.L. Wang, J. Hu, W.P. Gao, J.Y. Yuan, Electrochemical redox responsive supramolecular self-healing hydrogels based on host–guest interaction, Polym. Chem. 6 (2015) 3652-3659.

79. K. Miyamae, M. Nakahata, Y. Takashima, A. Harada, Self-Healing, Expansion–Contraction, and Shape-Memory Properties of a Preorganized Supramolecular Hydrogel through Host–Guest Interactions, Angew. Chem. Int. Ed. 54 (2015) 8984-8987.

80. M.A. Hempenius, C. Cirmi, F. Lo Savio, J. Song, G.J. Vancso, Poly(ferrocenylsilane) Gels and Hydrogels with Redox-Controlled Actuation. Macromol. Rapid Commun. 31 (2010) 772-783.

81. X.F. Sui, X.L. Feng, M.A. Hempenius, G.J. Vancso, Redox active gels: synthesis, structures and applications. J. Mat. Chem. B 1 (2013) 1658-1672.

82. H. Li, P. Yang, P. Pageni, C.B. Tang, Recent Advances in Metal-Containing Polymer Hydrogels. Macromol. Rapid Commun. 38 (2017) 1700109.

83. J.L. Wu, L. Wang, H.J. Yu, Zain-Ul-Abdin, R.U. Khan, M. Haroon, Ferrocene-based redox-responsive polymer gels: Synthesis, structures and applications, J. Organomet. Chem. 828 (2017) 38-51.

84. R. Kuosmanen, K. Rissanen, E. Sievanen, Steroidal supramolecular metallogels, Chem. Soc. Rev. 49 (2020) 1977-1998.

85. R.X. Liang, L. Wang, H.J. Yu, A. Khan, B. Ul Amin, R.U. Khan, Molecular design, synthesis

and biomedical applications of stimuli-responsive shape memory hydrogels, Eur. Polym. J. 114 (2019) 380-396.

86. L. Wang, H. Yu, Synthesis, Properties and Applications of Ferrocene-Based Derivatives, Polymers and Hydrogels, SpringerBriefs in Molecular Science, Zhejiang University Press and Springer Nature Singapore 2018, Chapter 4, pp. 91-99.

87. S.M. George, S. Tandon, B Kandasubramanian, Advancements in Hydrogel-Functionalized Immunosensing Platforms, ACS Omega 5 (2020) 2060-2068.

88. S. Tamaru, I. Hamachi, Recent progress of phosphate derivatives recognition utilizing artificial small molecular receptors in aqueous media, Struct. Bond. 129 (2008) 95-125.

89. A.S. Abd-El-Aziz, C. Agatemor, W.Y. Wong, Macromolecules Incorporating Transition Metals: Tackling Global Challenges. Polymer Chemistry Series N°27. Royal Chemical Society Publishers, London, 2018, Chapters 2 and 5, pp. 12-39 and 130-191.

90. H.J. Schneider, M. Shahinpoor, Chemoresponsive Materials: Stimulation by Chemical and Biological Signals, Smart materials series, Royal Society of Chemistry Publishers 2015, Chapter 3, pp. 44-66.

91. M.W. Toepke, W.L. Murphy, Dynamic Hydrogels in Comprehensive Biomaterials, Metallic Ceramic and Polymeric Biomaterials, Vol 1. Elsevier Publisher, Amsterdam, 2011, P. Ducheyne Ed., Chapter 1.132, pp. 577.

92. M. Patenaude, N.M.B. Smeets, T. Hoare, Designing Injectable, Covalently Cross- Linked Hydrogels for Biomedical Applications, Macromol. Rapid Commun. 35 (2014) 598-617.

93. M, Hartlieb, K, Kempe, U.S. Schubert, Covalently cross-linked poly(2-oxazoline) materials for biomedical applications - from hydrogels to self-assembled and templated structures, J. Mat.

Chem. B 3 (2015) 526-538.

94. C.S. Patrickios, T.K. Georgiou, Covalent amphiphilic polymer networks, Curr. Opin. Colloid Interface Sci. 8 (2003) 76-85.

95. D.A. Foucher, B.Z. Tang, I. Manners, Ring-opening polymerization of strained, ring-tilted ferrocenophanes: a route to high-molecular-weight poly(ferrocenylsilanes), J. Am. Chem. Soc. 114 (1992) 6246-6248.

96. R.A. Musgrave, A.D. Russell, I. Manners, Strained Ferrocenophanes. Organometallics 32 (2013) 5654-5667.

97. D.E. Herbert, U.F.J. Mayer, I. Manners Strained metallocenophanes and related organometallic rings containing pi-hydrocarbon ligands and transition-metal centers, Angew. Chem. Int. Ed. 46 (2007) 5060-5081.

98. R.A. Musgrave, A.D. Russell, D.W. Hayward, G.R. Whittell, P.G. Lawrence, P.J. Gates, J.C. Green, I. Manners, Main-chain metallopolymers at the static-dynamic boundary based on nickelocene, Nat. Chem. 9 (2017) 743-750.

99. X.F. Sui, M.A. Hempenius, G.J. Vancso, Redox-Active Cross-Linkable Poly(ionic liquid)s, J. Am. Chem. Soc. 134 (2012) 4023-4025.

100. K.H. Zhang, X.L. Feng, C.N. Ye, M.A. Hempenius, G.J. Vancso, Hydrogels with a Memory: Dual-Responsive, Organometallic Poly(ionic liquid)s with Hysteretic Volume-Phase Transition, J. Am. Chem. Soc. 139 (2017) 10029-10035.

101. A. Rapakousiou, C. Deraedt, H.B. Gu, L. Salmon, C. Belin, J. Ruiz, D. Astruc, Mixed-Valent Click Intertwined Polymer Units Containing Biferrocenium Chloride Side Chains Form Nanosnakes that Encapsulate Gold Nanoparticles, J. Am. Chem. Soc. 136 (2014) 13995-13998.

102. N. Li, P.X. Zhao, M.E. Igartua, A. Rapakousiou, L. Salmon, S. Moya, J. Ruiz, D. Astruc, Stabilization of AuNPs by Monofunctional Triazole Linked to Ferrocene, Ferricenium, or Coumarin and Applications to Synthesis, Sensing, and Catalysis, Inorg. Chem. 53 (2014) 11802-11808.

103. L. Zhao, Q. Ling, X. Liu, C. Hang, Q. Zhao, F. Liu, H. Gu, Multifunctional triazolylferrocenyl Janus dendron: Nanoparticle stabilizer, smart drug carrier and supramolecular nanoreactor, Appl. Organomet. Chem. 32 (2017) e4000.

104. H.B. Gu, R. Ciganda, P. Castel, A. Vax, D. Gregurec, J. Irigoyen, S. Moya, L. Salmon, P.X. Zhao, J. Ruiz, R. Hernández, D. Astruc, Redox-Robust Pentamethylferrocene Polymers and Supramolecular Polymers, and Controlled Self-Assembly of Pentamethylferricenium Polymer-Embedded Ag, AgI, and Au Nanoparticles, Chem. Eur. J. 21 (2015) 18177-18186.

105. Y. Liu, S.D. Mu, X. Liu, Q.J. Ling, C.D. Hang, J. Ruiz, D. Astruc, H.B. Gu, Ferrocenyl Janus mixed-dendron stars and their stabilization of Au and Ag nanoparticles, Tetrahedron 74 (2018) 4777-4789.

106. X. Liu, F.F. Liu, D. Astruc, W. Lin, H.B. Gu, Highly-branched amphiphilic organometallic dendronized diblock copolymer: ROMP synthesis, self-assembly and long-term Au and Ag nanoparticle stabilizer for high-efficiency catalysis, Polymer 173 (2019) 1-10.

107. X.F. Sui, X.L. Feng, A. Di Luca, C.A. van Blitterswijk, L. Moroni, M.A. Hempenius, G.J. Vancso, Poly(N-isopropylacrylamide)–poly(ferrocenylsilane) dual-responsive hydrogels: synthesis, characterization and antimicrobial applications, Polym. Chem. 4 (2013) 337-342.

108. X.L. Feng, H.R. Wu, X.F. Sui, M.A. Hempenius, G.J. Vancso, Thin film hydrogels from redox responsive poly(ferrocenylsilanes): Preparation, properties, and applications in

electrocatalysis, Eur. Polym. J. 72 (2015) 535-542.

109. X.L. Feng, K.H. Zhang, P. Chen, X.F. Sui, M.A. Hempenius, B. Liedberg, G.J. Vancso, Highly Swellable, Dual-Responsive Hydrogels Based on PNIPAM and Redox Active Poly(ferrocenylsilane) Poly(ionic liquid)s: Synthesis, Structure, and Properties, Macromol. Rapid Commun. 37 (2016) 1939-1944.

110. R. Pietschnig, Polymers with pendant ferrocenes, Chem. Soc. Rev. 45 (2016) 5216-5231.

111. A. Akhoury, L. Bromberg, T.A. Hatton, Redox-Responsive Gels with Tunable Hydrophobicity for Controlled Solubilization and Release of Organics, ACS Appl. Mater. Interfaces 3 (2011) 1167-1174.

112. F.F. Liu, X. Liu, D. Astruc, H.B. Gu, Dendronized triazolyl-containing ferrocenyl polymers as stabilizers of gold nanoparticles for recyclable two-phase reduction of 4-nitrophenol, J. Colloid Interface Sci. 533 (2019), 161-170.

113. K. Kaniewska, J. Romański, M. Karbarz, Oxidation of ferrocenemethanol grafted to a hydrogel network through cysteine for triggering volume phase transition, RSC Adv. 3 (2013) 23816-23823.

114. S.D. Mu, W.T. Liu, L. Zhao, Y.R, Long, H.B. Gu, Antimicrobial AgNPs Composites of Gelatin Hydrogels Crosslinked by Ferrocene-Containing Tetrablock Terpolymer, Polymer 169 (2019) 80-94.

115. Y.R. Long, B. Song, C.T. Shi, W.T. Liu, H.B. Gu, AuNPs composites of gelatin hydrogels crosslinked by ferrocenecontaining polymer as recyclable supported catalysts, J. Appl. Polym. Sci. (2019). DOI: 10.1002/APP.48653.

116. Z.Y. Cheng, S.H. Liu, P.W. Beines, N. Ding, P Jakubowicz, W. Knoll, Rapid and Highly

Efficient Preparation of Water-Soluble Luminescent Quantum Dots via Encapsulation by Thermo- and Redox-Responsive Hydrogels, Chem. Mat. 20 (2008) 7215-7219.

117. X.J. Lin, K. Nishio, T. Konno, K. Ishihara, The effect of the encapsulation of bacteria in redox phospholipid polymer hydrogels on electron transfer efficiency in living cell-based devices, Biomaterials 33 (2012) 8221-8227.

118. K. Saha, S.S. Agasti, C. Kim, X.N. Li, V.M. Rotello, Gold Nanoparticles in Chemical and Biological Sensing, Chem. Rev. 112 (2012) 2739-2779.

119. B. Adhikari, S. Majumdar, Polymers in sensor applications, Prog. Polym. Sci. 29 (2004) 699-766.

120. Chen AC, Chatterjee S, Nanomaterials based electrochemical sensors for biomedical applications, Chem. Soc. Rev. 42 (2013) 5425-5438.

121. N.J. Ronkainen, H.B. Halsall, W.R. Heineman, Electrochemical biosensors, Chem. Soc. Rev. 39 (2010), 1747-1763.

122. P.J. Jiang, Z.J. Guo, Fluorescent detection of zinc in biological systems: recent development on the design of chemosensors and biosensors, Coord. Chem. Rev. 248 (2004), 205-229.

123. A. Rabti, N. Raouafi, A. Merkoci, Bio(Sensing) devices based on ferrocene-functionalized graphene and carbon nanotubes, Carbon 108 (2016), 481-514.

124. M. Saleem, H.J. Yu, L. Wang, Zain-ul-Abdin, H. Khalid, M. Akram, N.M. Abbasi, J. Huang, Review on synthesis of ferrocene-based redox polymers and derivatives and their application in glucose sensing, Anal. Chim. Acta 876 (2015) 9-25.

125. D. Astruc, Electron-transfer processes in dendrimers and their implication in biology,

catalysis, sensing and nanotechnology, Nat. Chem. 4 (2012) 255-267.

126. S. Takahashi, J. Anzai, Recent Progress in Ferrocene-Modified Thin Films and Nanoparticles for Biosensors, Materials 6 (2013) 5742-5762.

127. S.A. Merchant, D.T. Glatzhofer, D.W. Schmidtke, Effects of electrolyte and pH on the behavior of cross-linked films of ferrocene-modified poly(ethylenimine), Langmuir 23 (2007) 11295-11302.

128. M.T. Meredith, D.P. Hickey, J.P. Redemann, D.W. Schmidtke, D.T. Glatzhofer, Effects of ferrocene methylation on ferrocene-modified linear poly(ethylenimine) bioanodes, Electrochim. Acta 92 (2013) 226-235.

129. D.P. Hickey, F. Giroud, D.W. Schmidtke, D.T. Glatzhofer, S.D. Minteer, Enzyme Cascade for Catalyzing Sucrose Oxidation in a Biofuel Cell, ACS Catal. 3 (2013) 2729-2737.

130. J. Chen, R. Munje, N.P. Godman, S. Prasad, D.T. Glatzhofer, D.W. Schmidtke, Improved Performance of Glucose Bioanodes Using Composites of (7,6) Single-Walled Carbon Nanotubes and a Ferrocene-LPEI Redox Polymer, Langmuir 33 (2017) 7591-7599.

131. W.X. Li, Z.F. Ma, Conductive catalytic redox hydrogel composed of aniline and vinyl-ferrocene for ultrasensitive detection of prostate specific antigen, Sens. Actuator B-Chem. 248 (2017) 545-550.

132. Z.Y. Li, T. Konno, M. Takai, K. Ishihara, Fabrication of polymeric electron-transfer mediator/enzyme hydrogel multilayer on an Au electrode in a layer-by-layer process, Biosens. Bioelectron. 34 (2012) 191-196.

133. S.M. Mantooth, B.G. Munoz-Robles, M.J. Webber, Dynamic Hydrogels from Host-Guest Supramolecular Interactions, Macromol. Biosci. 19 (2019) 1800281.

134. L. Voorhaar, R. Hoogenboom, Supramolecular polymer networks: hydrogels and bulk materials, Chem. Soc. Rev. 45 (2016) 4013-4031.

135. H. Li, Y. Yang, F.F. Xu, T.X. Liang, H.R. Wen, W. Tian, Pillararene-based supramolecular polymers, Chem. Commun. 55 (2019) 271-285.

136. H. Svobodova, V. Noponen, E. Kolehmainen, E. Sievanen, Recent advances in steroidal supramolecular gels, RSC Adv. 2 (2012) 4985-5007.

137. M.R. Rao, S.S. Sun, Supramolecular Assemblies of Amide-Derived Organogels Featuring Rigid pi-Conjugated Phenylethynyl Frameworks, Langmuir 29 (2013) 15146-15158.

138. L. Zhang, X.F. Wang, T.Y. Wang, M.H. Liu, Tuning Soft Nanostructures in Self-assembled Supramolecular Gels: From Morphology Control to Morphology-Dependent Functions, Small 11 (2015) 1025-1038.

139. M. Burnworth, L.M. Tang, J.R. Kumpfer, A.J. Duncan, F.L. Beyer, G.L. Fiore, S.J. Rowan, C. Weder, Optically healable supramolecular polymers, Nature 472 (2011) 334-U230.

140. B. Zheng, F. Wang, S.Y. Dong, F.H. Huang, Supramolecular polymers constructed by crown ether-based molecular recognition, Chem. Soc. Rev. 41 (2012) 1621-1636.

141. L.R. Hart, J.L. Harries, B.W. Greenland, H.M. Colquhoun, W. Hayes, Healable supramolecular polymers, Polym. Chem. 4 (2013) 4860-4870.

142. N, Lanigan, X.S. Wang, Supramolecular chemistry of metal complexes in solution, Chem. Commun. 49 (2013) 8133-8144.

143. T. Matsue, D.H. Evans, T. Osa, N. Kobayashi, Electron-transfer reactions associated with host-guest complexation. Oxidation of ferrocenecarboxylic acid in the presence of b-cyclodextrin, J. Am. Chem. Soc. 107 (1985) 3411-3417.

144. C. Yuan, J.N. Guo, M. Tan, M.Y. Guo, L.H. Qiu, F. Yan, Multistimuli Responsive and Electroactive Supramolecular Gels Based on Ionic Liquid Gemini Guest, ACS Macro Lett. 3 (2014) 271-275.

145. I. Tomatsu, A. Hashidzume, A. Harada, Redox-responsive hydrogel system using the molecular recognition of beta-cyclodextrin, Macromol. Rapid Commun. 27 (2006) 238-241.

146. M. Nakahata, Y. Takashima, A. Harada, Redox-Responsive Macroscopic Gel Assembly Based on Discrete Dual Interactions, Angew. Chem. Int. Ed. 53 (2014) 3617-3621.

147. N. Hou, R. Wang, F. Wang, J.H. Bai, T.F. Jiao, Z.H. Bai, L.X. Zhang, J.X. Zhou, Q.M. Peng, Self-assembled hydrogels constructed via host-guest polymers with highly efficient dye removal capability for wastewater treatment, Colloid Surf. A-Physicochem. Eng. Asp. 579 (2019) 123670.

148. Z.Q. Dong, Y. Cao, Q.J. Yuan, Y.F. Wang, J.H. Li, B.J. Li, S. Zhang, Redox- and Glucose-Induced Shape-Memory Polymers, Macromol. Rapid Commun. 34 (2013) 867-872.

149. J. Li, C. D. Ji, X. Q. Yu, M.Z. Yin, D. Kuckling, Dually Cross-Linked Supramolecular Hydrogel as Surface Plasmon Resonance Sensor for Small Molecule Detection, Macromol. Rapid Commun. (2019), 1900189.

150. J.F. Duan, J.X. Jiang, C.R. Han, J. Yang, L.J. Liu, J.Z. Li, The Study of Intermolecular Inclusion in Cellulose Physical Gels, BioResources 9 (2014) 4006-4013.

151. J.F. Duan, X.J. Zhang, J.X. Jiang, C.R. Han, J. Yang, L.J. Liu, H.Y. Lan, D.Z. Huang, The Synthesis of a Novel Cellulose Physical Gel, J. Nanomater. (2014) 312696.

152. J.F. Duan, C.R. Han, L.J. Liu, J.X. Jiang, J.Z. Li, Y.Q. Li, C. Guan, Binding Cellulose and Chitosan via Intermolecular Inclusion Interaction: Synthesis and Characterisation of Gel, J.

Spectrosc. (2015) 179258.

153. H.J. Zhang, L. Peng, Y. Xin, Q. Yan, J.Y. Yuan, Stimuli-Responsive Polymer Networks with beta-Cyclodextrin and Ferrocene Reversible Linkage Based on Linker Chemistry, Macromol. Symp. 329 (2013) 66-69.

154. Z. Liu, Y. Wang, M. Purro, M.P. Xiong, Oxidation-Induced Degradable Nanogels for Iron Chelation, Sci. Rep. 6 (2016) 20923.

155. C.X. Ma, T.F. Li, Q. Zhao, X.X. Yang, J.J. Wu, Y.W. Luo, T. Xie, Supramolecular Lego Assembly Towards Three-Dimensional Multi-Responsive Hydrogels, Adv. Mater. 26 (2014) 5665-5669.

156. R.B. Tong, L. Wang, H.J. Yu, Zain-ul-Abdin, H. Khalid, M. Akram, Y.S. Chen, Redox and Temperature Dual Responsive Gel Based on Host–Guest Assembly, J. Inorg. Organomet. Polym. Mater. 25 (2015) 1053-1059.

157. Y.F. Zhang, F.P. Du, L. Chen, W.C. Law, C.Y. Tang, Synthesis of deformable hydrogel composites based on Janus bilayer multi-walled carbon nanotubes/host-guest complex structure, Compos. Pt. B-Eng. 164 (2019) 121-128.

158. P. Du, G.S. Chen, M. Jiang, Electrochemically sensitive supra-crosslink and its corresponding hydrogel, Sci. China-Chem. 55 (2012) 836-843.

159. L.Y. Wang, P.Z. Cheng, M.Y. Guo, Stretchable and Functional Supramolecular Hydrogels Based on the Template Effect of Poly(β-cyclodextrin), Acta Polym. Sin. (2018) 1097-1106.

160. P. Du, J.H. Liu, G.S. Chen, M. Jiang, Dual Responsive Supramolecular Hydrogel with Electrochemical Activity, Langmuir 27 (2011) 9602-9608.

161. L. Tan, Y. Liu, W. Ha, L.S. Ding, S.L. Peng, S. Zhang, B.J. Li, Stimuli-induced gel–sol

transition of multi-sensitive supramolecular β-cyclodextrin grafted alginate/ferrocene modified pluronic hydrogel, Soft Matter 8 (2012) 5746-5749.

162. Y.X. Zhou, X.D. Fan, W.B. Zhang, D. Xue, J. Kong, Stimuli-induced gel-sol transition of supramolecular hydrogels based on β-cyclodextrin polymer/ferrocene-containing triblock copolymer inclusion complexes, J. Polym. Res. 21 (2014) 359.

163. L. Wang, C.G. Guo, C.Q. Wang, Preparation and Gelation of Supramolecular copolymer Based on the Host-Guest Interaction between Cyclodextrin and Ferrocene. Journal of Functional Polymer 25 (2012) 335-341.

164. J.L. Yan, J. Liu, X. Chen, Y. Fang, Preparation and Properties of a Novel Multiple Responsive Supramolecular Hydrogel Based on Host-Guest Interaction, Chem. J. Chin. Univ.-Chin. 29 (2008) 124-129.

165. C.G. Guo, L. Wang, Y.K. Li, C.Q. Wang, Suprarmolecular hydrogels driven by the dual host–guest interactions between α-cyclodextrin and ferrocene-modified poly(ethylene glycol) with low-molecular-weight, React. Funct. Polym. 73 (2013) 805-812.

166. Y. Suzaki, H. Endo, T. Kojima, K. Osakada, Amphiphilic ferrocenylated alkylpyridinium: the formation of micelles and hydrogels and their disaggregation induced by an external stimulus, Dalton Trans. 42 (2013) 16222-16230.

167. S.Y. Dong, B. Zheng, F. Wang, F.H. Huang, Supramolecular Polymers Constructed from Macrocycle-Based Host-Guest Molecular Recognition Motifs, Acc. Chem. Res. 47 (2014) 1982-1994.

168. W. Xia, X.Y. Hu, Y. Chen, C. Lin, L.Y. Wang, A novel redox-responsive pillar[6]arene-based inclusion complex with a ferrocenium guest, Chem. Commun. 49 (2013) 5085-5087.

169. T. Ogoshi, S. Kanai, S. Fujinami, T.A. Yamagishi, Y. Nakamoto, para-bridged symmetrical pillar[5]arenes: Their Lewis acid catalyzed synthesis and host-guest property, J. Am. Chem. Soc. 130 (2008) 5022-5023.

170. G.C. Yu, X.R. Zhou, Z.B. Zhang, C.Y. Han, Z.W. Mao, C.Y. Gao, F.H. Huang, Pillar[6]arene/Paraquat Molecular Recognition in Water: High Binding Strength, pH-Responsiveness, and Application in Controllable Self-Assembly, Controlled Release, and Treatment of Paraquat Poisoning, J. Am. Chem. Soc. 134 (2012) 19489-19497.

171. J, Murray, K, Kim, T, Ogoshi, W, Yao, B.C. Gibb, The aqueous supramolecular chemistry of cucurbit[n]urils, pillar[n]arenes and deep-cavity cavitands, Chem. Soc. Rev. 46 (2017) 2479-2496.

172. K, Yang, Y.X. Pei, J. Wen, Z.C. Pei, Recent advances in pillar[n]arenes: Synthesis and applications based on host-guest interactions, Chem. Commun. 52 (2016) 9316-9326.

173. T. Ogoshi, T.A. Yamagishi, Y. Nakamoto, Pillar-Shaped Macrocyclic Hosts Pillar[n]arenes: New Key Players for Supramolecular Chemistry, Chem. Rev. 116 (2016) 7937-8002.

174. Q.P. Duan, Y. Cao, Y. Li, X.Y. Hu, T.X. Xiao, C. Lin, Y. Pan, L.Y. Wang, pH-Responsive Supramolecular Vesicles Based on Water-Soluble Pillar[6]arene and Ferrocene Derivative for Drug Delivery, J. Am. Chem. Soc. 135 (2013) 10542-10549.

175. X. Wu, L. Gao, X.Y. Hu, L.Y. Wang, Supramolecular Drug Delivery Systems Based on Water-Soluble Pillar[n]arenes, Chem. Rec. 16 (2016) 1216-1227.

176. G.C. Yu, M. Xue, Z.B. Zhang, J.Y. Li, C.Y. Han, F.H. Huang, A Water-Soluble Pillar[6]arene: Synthesis, Host-Guest Chemistry, and Its Application in Dispersion of Multiwalled Carbon Nanotubes in Water, J. Am. Chem. Soc. 134 (2012) 13248-13251.

177. S. Wang, Z.Q. Xu, T.T. Wang, T.X. Xiao, X.Y. Hu, Y.Z. Shen, L.Y. Wang, Warm/cool-tone switchable thermochromic material for smart windows by orthogonally integrating properties of pillar[6]arene and ferrocene, Nat. Commun. 9 (2018) 1737.

178. Y.F. Wang, W. Qi, R.L. Huang, X.J. Yang, M.F. Wang, R.X. Su, Z.M. He, Rational Design of Chiral Nanostructures from Self-Assembly of a Ferrocene-Modified Dipeptide, J. Am. Chem. Soc., 137 (2015) 7869-7880.

179. Z.F. Sun, Z.Y. Li, Y.H. He, R.J. Shen, L. Deng, M.H. Yang, Y.Z. Liang, Y. Zhang, Ferrocenoyl Phenylalanine: A New Strategy Toward Supramolecular Hydrogels with Multistimuli Responsive Properties, J. Am. Chem. Soc. 135 (2013) 13379-13386.

180. B. Adhikari, H.B. Kraatz, Redox-triggered changes in the self-assembly of a ferrocene-peptide conjugate, Chem. Commun. 50 (2014) 5551-5553.

181. N, Falcone, H.B. Kraatz, Supramolecular Assembly of Peptide and Metallopeptide Gelators and Their Stimuli-Responsive Properties in Biomedical Applications, Chem.-Eur. J. 24 (2018) 14316-14328.

182. B. Albada, N. Metzler-Nolte, Organometallic-Peptide Bioconjugates: Synthetic Strategies and Medicinal Applications, Chem. Rev. 116 (2016) 11797-11839.

183. R. Afrasiabi, H.B. Kraatz, Rational Design and Application of a Redox-Active, Photoresponsive, Discrete Metallogelator, Chem.-Eur. J. 21 (2015) 7695-7700.

184. T. He, N. Wang, Y.X. Liao, X. Wang, X.Q. Yu, A ferrocene-based multiple-stimuli responsive organometallogel, Soft Matter 10 (2014) 3755-3761.

185. K.T. Kim, G.W.M. Vandermeulen, D.A. Rider, C. Kim, M.A. Winnik, I. Manners, Gelation of helical polypeptide-random coil diblock copolymers by a nanoribbon mechanism, Angew.

Chem. Int. Ed. 44 (2005) 7964-7968.

186. T. Moriuchi, T. Hirao, Design of Ferrocene-Dipeptide Bioorganometallic Conjugates To Induce Chirality-Organized Structures, Acc. Chem. Res. 43 (2010) 1040-1051.

187. S. Chowdhury, G. Schatte, H.B. Kraatz, Rational design of bioorganometallic foldamers: A potential model for parallel beta-helical peptides, Angew. Chem. Int. Ed. 45 (2006) 6882-6884.

188. S. Chowdhury, G. Schatte, H.B. Kraatz, How useful is ferrocene as a scaffold for the design of beta-sheet foldamers, Angew. Chem. Int. Ed. 47 (2008) 7056-7059.

189. R. Afrasiabi, H.B. Kraatz, Small-Peptide-Based Organogel Kit: Towards the Development of Multicomponent Self-Sorting Organogels, Chem.-Eur. J. 19 (2013) 15862-15871.

190. R, Afrasiabi, H.B. Kraatz, Rational Design and Application of a Redox-Active, Photoresponsive, Discrete Metallogelator, Chem.-Eur. J. 21 (2015) 7695-7700.

191. R. Afrasiabi, H.B. Kraatz Stimuli-Responsive Supramolecular Gelation in Ferrocene-Peptide Conjugates, Chem.-Eur. J. 19 (2013) 17296-17300.

192. N. Falcone, S. Basak, B. Dong, J. Syed, A. Ferranco, A. Lough, Z. She, H.B. Kraatz, A Ferrocene-Tryptophan Conjugate: The Role of the Indolic Nitrogen in Supramolecular Assembly, ChemPlusChem 82 (2017) 1282-1289.

193. Z.F. Sun, Z.Y. Li, Y.H. He, R.J. Shen, L. Deng, M.H. Yang, Y.Z. Liang, Y. Zhang, Ferrocenoyl Phenylalanine: A New Strategy Toward Supramolecular Hydrogels with Multistimuli Responsive Properties, J. Am. Chem. Soc. 135 (2013) 13379-13386.

194. F.L. Qu, Y. Zhang, A. Rasooly, M.H. Yang, Electrochemical Biosensing Platform Using Hydrogel Prepared from Ferrocene Modified Amino Acid as Highly Efficient Immobilization

Matrix, Anal. Chem. 86 (2014) 973-976.

195. M. Zhou, Z.F. Sun, C.C. Shen, Z.Y. Li, Y. Zhang, M.H. Yang, Application of hydrogel prepared from ferrocene functionalized amino acid in the design of novel electrochemical immunosensing platform, Biosens. Bioelectron. 49 (2013) 243-248.

196. Y. Hou, T. Li, H.Y. Huang, H. Quan, X.Y. Miao, M.H. Yang, Electrochemical immunosensor for the detection of tumor necrosis factor a based on hydrogel prepared from ferrocene modified amino acid, Sens. Actuator B-Chem. 182 (2013) 605-609.

197. Y.X. Huang, Y.Y. Ding, T. Li, M.H. Yang, Redox hydrogel based immunosensing platform for the label-free detection of a cancer biomarker, Anal. Methods 7 (2015) 411-415.

198. Y.F. Wang, R.L. Huang, W. Qi, Z.J. Wu, R.X. Su, Z.M. He, Kinetically controlled self-assembly of redox-active ferrocene-diphenylalanine: from nanospheres to nanofibers, Nanotechnology 24 (2013) 465603.

199. X.J. Yang, Y.F. Wang, W. Qi, R.X. Su, Z.M. He, Bioorganometallic ferrocene-tripeptide nanoemulsions, Nanoscale 9 (2017) 15323-15331.

200. Y.K. Li, C.G. Guo, L. Wang, Y. Xu, C.Y. Liu, C.Q. Wang, A self-healing and multi-responsive hydrogel based on biodegradable ferrocene-modified chitosan, RSC Adv. 4 (2014) 55133-55138.

201. A. Biswas, S. Maiti, D.M. Kalaskar, A.K. Das, Redox-Active Dynamic Self-Supporting Thixotropic 3D-Printable G-Quadruplex Hydrogels, Chem.-Asian J. 13 (2018) 3928–3934.

202. J. Sugai, N. Saito, Y. Takahashi, Y. Kondo, Synthesis and viscoelastic properties of gemini surfactants containing redox-active ferrocenyl groups, Colloid Surf. A-Physicochem. Eng. Asp. 572 (2019) 197-202.

203. L.A. Lyon, Z.Y. Meng, N. Singh, C.D. Sorrell, A.S. John, Thermoresponsive microgel-based materials, Chem. Soc. Rev. 38 (2009) 865-874.

204. Z.F. Li, T. Ngai, Microgel particles at the fluid-fluid interfaces, Nanoscale 5 (2013) 1399-1410.

205. S. Seiffert, Small but Smart: Sensitive Microgel Capsules, Angew. Chem. Int. Ed. 52 (2013), 11462-11468.

206. X.J. Zhang, S. Malhotra, M. Molina, R. Haag, Micro- and nanogels with labile crosslinks - from synthesis to biomedical applications, Chem. Soc. Rev. 44 (2015) 1948-1973.

207. S. Saxena, C.E. Hansen, L.A. Lyon, Microgel Mechanics in Biomaterial Design, Acc. Chem. Res. 47 (2014) 2426-2434.

208. T. Farjami, A. Madadlou, Fabrication methods of biopolymeric microgels and microgel-based hydrogels, Food Hydrocolloids 62 (2017) 262-272.

209. M.S. Ruiz, A. Romerosa, B. Sierra-Martin, A. Fernandez-Barbero, A Water Soluble Diruthenium-Gold Organometallic Microgel, Angew. Chem. Int. Ed. 47 (2008), 8665-8669.

210. Z.F. Li, T. Ming, J.F. Wang, T. Ngai, High Internal Phase Emulsions Stabilized Solely by Microgel Particles, Angew. Chem. Int. Ed. 48 (2009) 8490-8493.

211. M. Antonietti, F. Grohn, J. Hartmann, L. Bronstein, Nonclassical shapes of noble-metal colloids by synthesis in microgel nanoreactors, Angew. Chem. Int. Ed. 36 (1997) 2080-2083.

212. F.A. Plamper, W. Richtering, Functional Microgels and Microgel Systems, Acc. Chem. Res. 50 (2017) 131-140.

213. A. Biffis, N. Orlandi, B. Corain, Microgel-stabilized metal nanoclusters: Size control by microgel nanomorphology, Adv. Mater. 15 (2003), 1551.

214. S. Seiffert, J. Thiele, A.R. Abate, D.A. Weitz, Smart Microgel Capsules from Macromolecular Precursors, J. Am. Chem. Soc. 132 (2010), 6606-6609.

215. I. Berndt, J.S. Pedersen, W. Richtering, Temperature-sensitive core-shell microgel particles with dense shell, Angew. Chem. Int. Ed. 45 (11), 1737-1741.

216. D.K. Hwang, J. Oakey, M. Toner, J.A. Arthur, K.S. Anseth, S. Lee, A. Zeiger, K.J. Van Vliet, P.S. Doyle, Stop-Flow Lithography for the Production of Shape-Evolving Degradable Microgel Particles, J. Am. Chem. Soc. 131 (2009), 4499-4504.

217. X.F. Sui, L.L. Shui, J. Cui, Y.B. Xie, J. Song, A. van den Berg, M.A. Hempenius, G.J. Vancso, Redox-responsive organometallic microgel particles prepared from poly(ferrocenylsilane)s generated using microfluidics, Chem. Commun. 50 (2014), 3058-3060.

218. Q.M. Zhang, D. Berg, J. Duan, S.M. Mugo, M.J. Serpe, Optical Devices Constructed from Ferrocene-Modified Microgels for H2O2 Sensing, ACS Appl. Mater. Interfaces 8 (2016) 27264-27269.

219. K. Marcisz, M. Mackiewicz, J. Romanski, Z. Stojek, M. Karbarz, Significant, reversible change in microgel size using electrochemically induced volume phase transition, Appl. Mater. Today 13 (2018), 182-189.

220. O. Mergel, S. Schneider, R. Tiwari, P.T. Kuhn, D. Keskin, M.C.A. Stuart, S. Schottner, M. de Kanter, M. Noyong, T. Caumanns, J. Mayer, C. Janzen, U. Simon, M. Gallei, D. Woll, P. van Rijn, F.A. Plamper, Cargo shuttling by electrochemical switching of core-shell microgels obtained by a facile one-shot polymerization, Chem. Sci 10 (2019) 1844-1856.

221. L. Peng, A.C. Feng, S.Y. Liu, M. Huo, T. Fang, K. Wang, Y. Wei, X.S. Wang, J.Y. Yuan, Electrochemical Stimulated Pickering Emulsion for Recycling of Enzyme in Biocatalysis, ACS

Appl. Mater. Interfaces 8 (2016) 29203-29207.

222. S.H. Jung, S. Schneider, F. Plamper, A. Pich, Responsive Supramolecular Microgels with Redox-Triggered Cleavable Crosslinks, Macromolecules 53 (2020) 1043-1053.

223. C.G. Hardy, J.Y. Zhang, Y. Yan, L.X. Ren, C.B. Tang, Metallopolymers with transition metals in the side-chain by living and controlled polymerization techniques, Prog. Polym. Sci. 39 (2014) 1742-1796.

224. X. Liu, F.F. Liu, W.T. Liu, H.B. Gu, ROMP and MCP as Versatile and Forceful Tools to Fabricate Dendronized Polymers for Functional Applications, Polym. Rev. (2020). DIO: 10.1080/15583724.2020.1723022.

225. M. Gallei, C. Ruttiger, Recent Trends in Metallopolymer Design: Redox-Controlled Surfaces, Porous Membranes, and Switchable Optical Materials Using Ferrocene-Containing Polymers, Chem.-Eur. J. 24 (2018) 10006-10021.

226. Y.L. Wang, D. Astruc, A.S. Abd-El-Aziz, Metallopolymers for advanced sustainable applications, Chem. Soc. Rev. 48 (2019) 558-636.

227. X. Liu, W. Lin, D. Astruc, H.B. Gu, Syntheses and applications of dendronized polymers, Prog. Polym. Sci. 96 (2019) 43-105.

228. B. Hua, L. Shao, Z.H. Zhang, J.Y. Liu., F.H. Huang, Cooperative Silver Ion-Pair Recognition by Peralkylated Pillar[5]arenes, J. Am. Chem. Soc. 141 (2019) 15008-15012.

229. M.B. Wang, J. Zhou, E.R. Li, Y.J. Zhou, Q. Li, F.H. Huang, Separation of Monochlorotoluene Isomers by Nonporous Adaptive Crystals of Perethylated Pillar[5]arene and Pillar[6]arene, J. Am. Chem. Soc. 141 (2019) 17102-17106.

230. Y.J. Zhou, K.C. Jie, R. Zhao, E. Li, F.H. Huang, Highly Selective Removal of Trace

Isomers by Nonporous Adaptive Pillararene Crystals for Chlorobutane Purification, J. Am. Chem. Soc. 142 (2020) 6957-6961.

231. X.R. Sheng, E. Li, Y.J. Zhou, R. Zhao, W.J. Zhu, F.H. Huang, Separation of 2-Chloropyridine/3-Chloropyridine by Nonporous Adaptive Crystals of Pillararenes with Different Substituents and Cavity Sizes, J. Am. Chem. Soc. 142 (2020) 6360-6364.

232. L. Zhang, A. Macias, T.B. Lu, J.I. Gordon, G.W. Gokel, A.E. Kaifer, Calixarenes as hosts in aqueous media: inclusion complexation of ferrocene derivatives by a water-soluble calix[6]arene, J. Chem. Soc. Chem. Comm. (1993) 1017-1019.

233. P.L. Boulas, M. Gomez-Kaifer, L. Echegoyen, Electrochemistry of supramolecular systems, Angew. Chem. Int. Ed. 37 (1998) 216-247.

234. J.S. Kim, D.T. Quang, Calixarene-derived fluorescent probes, Chem. Rev. 107 (2007) 3780-3799.

235. D.S. Guo, Y. Liu, Calixarene-based supramolecular polymerization in solution, Chem. Soc. Rev. 41 (2012) 5907-5921.

236. C. Wieser, C.B. Dieleman, D. Matt, Calixarene and resorcinarene ligands in transition metal chemistry, Coord. Chem. Rev. 165 (1997) 93-161.

237. L. Baldini, A. Casnati, F. Sansone, R. Ungaro, Calixarene-based multivalent ligands, Chem. Soc. Rev. 36 (2007) 254-266.

238. A, Dondoni, A. Marra, Calixarene and Calixresorcarene Glycosides: Their Synthesis and Biological Applications, Chem. Rev. 110 (2010) 4949-4977.

239. H.J. Kim, W.S. Jeon, Y.H. Ko, K. Kim, Inclusion of methylviologen in cucurbit[7]uril, Proc. Natl. Acad. Sci. U. S. A. 99 (2002) 5007-5011.

240. D. Shetty, J.K. Khedkar, K.M. Park, K. Kim, Can we beat the biotin-avidin pair?: cucurbit[7]uril-based ultrahigh affinity host-guest complexes and their applications, Chem. Soc. Rev. 44 (2015) 8747-8761.

241. A.E. Kaifer, Toward Reversible Control of Cucurbit[n]uril Complexes, Acc. Chem. Res. 47 (2014) 2160-2167.

242. J.W. Lee, S. Samal, N. Selvapalam, H.J. Kim, K. Kim, Cucurbituril homologues and derivatives: New opportunities in supramolecular chemistry, Acc. Chem. Res. 36 (2003) 621-630.

243. S.J. Barrow, S. Kasera, M.J. Rowland, J. del Barrio, O.A. Scherman, Cucurbituril-Based Molecular Recognition, Chem. Rev. 115 (2015) 12320-12406.

244. J. Lu, J.X. Lin, M.N. Cao, R. Cao, Cucurbituril: A promising organic building block for the design of coordination compounds and beyond, Coord. Chem. Rev. 257 (2013) 1334-1356.

245. J.H. Jin, L.L. Cai, Y.G. Jia, S. Liu, Y.H. Chen, L. Ren, Progress in self-healing hydrogels assembled by host-guest interactions: preparation and biomedical applications, J. Mat. Chem. B 7 (2019), 1637-1651.

246. T.X. Xiao, L.X. Xu, L. Zhou, X.Q. Sun, C. Lin, L.Y. Wang, Dynamic hydrogels mediated by macrocyclic host-guest interactions, J. Mat. Chem. B 7 (2019), 1526-1540.

247. M.O.M. Piepenbrock, G.O. Lloyd, N. Clarke, J.W. Steed, Metal- and Anion-Binding Supramolecular Gels, Chem. Rev. 110 (2010) 1960-2004.

248. P. Sutar, T.K. Maji, Coordination polymer gels: soft metal-organic supramolecular materials and versatile applications, Chem. Commun. 52 (2016) 8055-8074.

249. H.Q. Wu, J. Zheng, A.L. Kjoniksen, W. Wang, Y. Zhang, J.M. Ma, Metallogels:

Availability, Applicability, and Advanceability, Adv. Mater. 31 (2019) 1806204.

250. K.C. Bentz, S.M. Cohen, Supramolecular Metallopolymers: From Linear Materials to Infinite Networks, Angew. Chem. Int. Ed. 57 (2018) 14992-15001.

251. Y. Sun, C.Y. Chen, P.J. Stang, Soft Materials with Diverse Suprastructures via the Self-Assembly of Metal-Organic Complexes, Acc. Chem. Res. 52 (2019) 802-817.

252. P. Dastidar, S. Ganguly, K. Sarkar, Metallogels from Coordination Complexes, Organometallic, and Coordination Polymers, Chem.-Asian J. 11 (2016) 2484-2498.

253. L.Y. Shi, P.H. Ding, Y.Z. Wang, Y. Zhang, D. Ossipov, J. Hilborn, Self-Healing Polymeric Hydrogel Formed by Metal-Ligand Coordination Assembly: Design, Fabrication, and Biomedical Applications. Macromol. Rapid Commun. 40 (2019) 1800837.

254. C. Ornelas, Application of ferrocene and its derivatives in cancer research, New J. Chem. 35 (2011) 1973-1985.

ToC figure

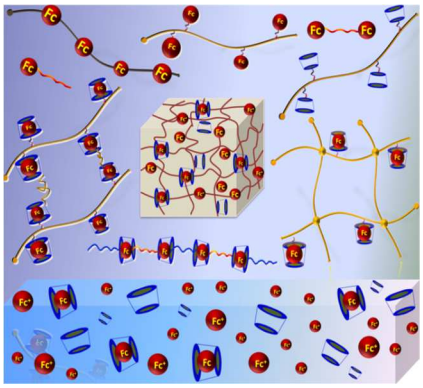

This review focuses on various classes of ferrocene-containing hydrogels via covalently cross-linking and supramolecular strategies and analyzes their gelling mechanisms, characteristic structures, properties, and functional applications.